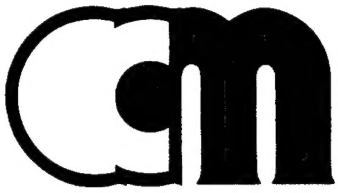

CCM-82-20

TRANSPORT PROPERTIES OF COMPOSITE MATERIALS: I. ELECTRICAL CONDUCTIVITY

ROY L. MC CULLOUGH

JOSEPH J. QUIGLEY, IV

CENTER FOR COMPOSITE MATERIALS

College of Engineering
University of Delaware
Newark, Delaware

3 OF 5

DTIC DOES NOT HAVE THIS ITEM

1 - AD NUMBER: D437156
5 - CORPORATE AUTHOR: DELAWARE UNIV NEWARK CENTER FOR COMPOSITE MATERIALS
6 - UNCLASSIFIED TITLE: TRANSPORT PROPERTIES OF COMPOSITE MATERIALS: I. ELECTRICAL CONDUCTIVITY.
10 - PERSONAL AUTHORS: MCCULLOUGH,R. L. ;QUIGLEY,J. J. ;
11 - REPORT DATE: DEC , 1982
12 - PAGINATION: 167P
14 - REPORT NUMBER: CCM-82-20
15 - CONTRACT NUMBER: N62269-81-C-0255
20 - REPORT CLASSIFICATION: UNCLASSIFIED
22 - LIMITATIONS (ALPHA): APPROVED FOR PUBLIC RELEASE; DISTRIBUTION UNLIMITED. AVAILABILITY: CENTER FOR COMPOSITE MATERIALS, UNIVERSITY OF DELAWARE, NEWARK, DE. 19711.
33 - LIMITATION CODES: 1 24

TRANSPORT PROPERTIES OF COMPOSITE MATERIALS:

I. ELECTRICAL CONDUCTIVITY

Roy L. McCullough

Joseph J. Quigley, IV

Center for Composite Materials
University of Delaware
Newark, Delaware

Sponsored by the

Naval Air Development Center
Warminster, Pennsylvania

Contract Number N62269-81-C-0255

December 1982

ABSTRACT

A new model is reported for the prediction of the electrical conductivity of polymeric materials filled with conducting particles, short fibers, and/or platelets. The model takes into account chain and network formation by contacting filler units which provide continuous conduction paths. The incorporation of this important structural feature shows that sharp transitions in conductivity occur within a narrow range of filler concentrations. The critical concentrations associated with these transitions establish the minimum concentration of conducting filler required to achieve conducting behavior.

Preliminary evaluations of the model indicate that it can be used to rank candidate materials. Predictions of absolute levels of conductivity require knowledge of (i) experimentally determined values for the conductivity of each of the components, (ii) the volume fraction (or weight fraction) of each of the components, (iii) an independent characterization of the average state of orientation of the conducting components, and (iv) an independent characterization of the average aspect ratio associated with the filler

shape. The characteristic parameters of the contact probabilities (determined by the orientation and aspect ratio distributions) are particularly sensitive to processing conditions. Consequently, variations in processing procedures can have a pronounced effect on the electrical properties. This result emphasizes the importance of conducting a microstructural characterization program in concert with electrical characterizations. A procedure is identified for determining the essential microstructural data.

The routine application of the model relationships as a screening tool for candidate material systems requires tedious computations. An interactive computer program was developed to conduct these routine calculations. A user's guide with illustrative examples is given in the appendix.

TABLE OF CONTENTS

ACKNOWLEDGEMENTS

This work was supported through a contract (N62269-81-C-0255) with the Naval Air Development Center, Warminster, Pennsylvania. The authors are indebted to Mr. R. Trabacco and Mr. I. Shaffer of the Naval Air Development Center for graciously providing the data and specimens used to test the model predictions. The authors wish to express their appreciation for the contributions of Dr. S. H. McGee to the development of the model relationships and the interactive computer program to implement the model relationships.

INTRODUCTION

The rapidly evolving electronics industry has prompted the need for light weight, low cost materials that can be formed by existing processing procedures into housings that possess electromagnetic shielding characteristics resembling metals. Considerable interest has developed in the use of corrosion resistant polymeric materials filled with conducting particles, fibers, and/or platelets. The word "metalloplastic" [Davenport, 1981] has been coined to distinguish this class of heterogeneous materials from the emerging class of homgeneous semiconducting and conducting polymeric materials.

One of the key material properties required of metalloplastics in these applications is electrical conductivity approaching the range of metals. The wide range of possible compositions and filler geometries (e.g., fibers, particles, platelets) precludes a total reliance on direct laboratory characterization of the directionally dependent electrical properties of these materials. Accordingly, an objective of this work was to develop models to predict the electrical properties of metalloplastics with the intent of

providing a screening tool for the identification of composite systems which are conducting and exhbit acceptable properties.

It is evident that such a model will contain parameters associated with:

- o the electrical properties of the components;
- o the composition (e.g., volume fraction or weight fraction);
- o the shape of the conducting filler; and
- o the relative orientation and/or packing geometries of the conducting fillers.

It can be anticipated that the computational complexities introduced by the necessity of treating such an extended set of parameters will require computer programs for the implementation of the model. Accordingly, a second objective of this work was to develop interactive computer programs to facilitate the use of the models as a screening tool.

CLASSIFICATION OF TRANSPORT PROPERTIES

Electrical conductivity belongs to the general class of transport properties which include:

- o thermal conductivity
- o dielectric constants
- o magnetic permeability
- o diffusivity

As noted by Wu and McCullough [1977], among others, each of these properties is governed by linear constitutive relationships which connect a response field to an applied field through an appropriate descriptor of the material. These descriptors (e.g., electrical and thermal conductivity) are the key "intrinsic" material parameters that are required for the evaluation of the performance of various designs of fabricated parts of complex shapes. In particular, computer-aided design techniques aimed at achieving such evaluations require these material parameters as input. Such an evaluation would include the processing of position variant fiber distribution and orientation information [Quigley, 1982] into a format for a finite element analysis package such as ADINAT [1982].

Although the underlying physical processes differ for each of the transport properties, the mathematical structure for model relationships that connect the properties and microstructure of the components of these composite systems to the effective (average) bulk descriptors will be similar. Consequently, it can be anticipated that models developed for electrical conductivity will find application in predicting other transport properties (e.g., thermal conductivity and dielectric constants).

The general structure of linear transport relationships is of the matrix form:

$$\begin{bmatrix} F_1 \\ F_2 \\ F_3 \end{bmatrix} = \begin{bmatrix} K_{11} & K_{12} & K_{13} \\ K_{21} & K_{22} & K_{23} \\ K_{31} & K_{32} & K_{33} \end{bmatrix} \begin{bmatrix} G_1 \\ G_2 \\ G_3 \end{bmatrix} \qquad (1)$$

where the G's are components of the applied field (e.g., electrical fields, temperature gradients, chemical potentials) and the F's are components of the corresponding response field. The K_{ij}'s are the appropriate descriptors of the material (e.g., thermal conductivity, electrical conductivity, and diffusivity, respectively). Symmetry requires that $K_{ij} = K_{ji}$. These relationships can be

simplified by restricting attention to the important class of composite materials which exhibit orthotropic symmetry characterized by three mutually perpendicular planes of material symmetry. If the "1", "2", and "3" directions are selected as the principle axes, only the diagonal terms of [K] survive, so that Equation (1) reduces to

$$\begin{bmatrix} F_1 \\ F_2 \\ F_3 \end{bmatrix} = \begin{bmatrix} K_{11} & 0 & 0 \\ 0 & K_{22} & 0 \\ 0 & 0 & K_{33} \end{bmatrix} \begin{bmatrix} G_1 \\ G_2 \\ G_3 \end{bmatrix} \qquad (2)$$

where K_{11}, K_{22}, and K_{33} can be selected to refer to the "longitudinal", "transverse" and "through-the-thickness" properties of a rectangular panel specimen. The behavior of a transversely isotropic material can be obtained as a special case by setting any two of the K's equal (e.g., $K_{22} = K_{33}$); isotropic material symmetry is obtained by equating all K's, viz., $K_{11} = K_{22} = K_{33}$. Behavior in directions other than the principle axes can be obtained by projecting the K's through well known rotational transformations. As a consequence of this reduction, the double index "ji" can be replaced by a single index, i.e., $K_{ji} = K_j$.

Based on this general formulation, models developed for the various K's (representing electrical conductivity) may be extended to the prediction of other transport properties by replacing the appropriate modification of the K's with the transport property of interest.

REVIEW OF TRANSPORT MODELS

The literature is replete with relationships proposed to predict various transport properties. Models for thermal conductivity are reviewed by Progelhof et al [1976]; models for electrical and magnetic properties are reviewed by Hale [1976]. As with thermomechanical properties [McCullough, 1971], the various approaches to model development may be broadly classified as "Mechanics of Materials," "Self-Consistent Field," and "Bounding."

The mechanics of materials approach directs attention to simple geometries and introduces gross approximations to the response fields. For example, the simplest of such models would correspond to continuous conducting fibers all aligned parallel to the "1" direction. The conductivity in the "1" direction is obtained by considering that the conducting fibers are connected in parallel with an "insulating" matrix so that

$$K_1 = v_f K_f + v_m K_m \tag{3a}$$

where the subscripts denote the fiber "f" and matrix "m", respectively; v_f is the volume fraction of the fiber with $v_m = 1 - v_f$.

The conductivity in the "2" (or "3") direction is obtained by considering that, in the transverse direction, the conducting fibers and insulating matrix respond through a series connection so that

$$(1/K_2) = (v_f/K_f) + (v_m/K_m)$$

or

$$\rho_2 = v_f \rho_f + v_m \rho_m \qquad (3b)$$

The "rule of mixtures" expressed by Equations (3) has been verified as an appropriate model for predicting the longitudinal transport properties for the special case of continuous and aligned fibers [Equation (3a)]. However, these simple models fail to predict the transverse properties [Equation (3b)], and are inadequate for particulate and short fiber filler geometries.

In contrast, the self-consistent field approach introduces gross approximations in phase geometry and simplifies the representation of the response field in an attempt to obtain rigorous solutions to boundary value problems. These models generally overestimate transport properties. The bounding approach avoids the difficulties introduced by complex microstructures by directing attention to establishing upper and lower bounds on the transport

properties rather than predicting the properties. The results from these bounding approaches can serve as a practical guide to material behavior only if the upper and lower bounds are sufficiently close so as to bracket the actual behavior within experimental error. In general, the transport properties of filler and polymer differ by several orders of magnitude so that the upper and lower bounds are too far apart to provide useful results.

All of these approaches have their counterpart in developing models to predict the elastic constants of composite materials. Indeed, several workers have noted the similarity between the structure of Equation (2) to the shear modulus "block" of the elastic constant array and have proposed that transport properties can be predicted by replacing the shear modulus in various elastic models by the transport properties [e.g., Aston et al, 1969]. This analogy appears to give reasonable results for continuous fiber composites; it fails to describe the behavior of short fiber and particulate filled materials.

While some models appear adequate for predicting certain transport properties for restricted filler geometries, no model provides the generality demanded for the prediction of the entire class of transport properties

for a variety of filler geometries. As pointed out by Nielsen [1974], among others, the deficiencies of the various models stem from the neglect of important structural features. Noting that the Halpin-Tsai relationship [Aston et al, 1969] was a convenient form for representing upper and lower bound relationships, as well as results from self-consistent field models, Lewis and Nielsen [1970] introduced modifications in the Halpin-Tsai relationship to partially account for the shape and packing geometry of inclusions. These workers argue that the volume fraction of filler cannot exceed a value associated with close packed geometries (as determined by the shape of the filler). Accordingly, the volume fraction of filler was adjusted to account for the limitation on the maximum volume fraction. Estimates of the modification parameters for various collections of spheres and rods are given by these workers. Predicted values for elastic moduli and thermal conductivity obtained from this modification are in better agreement with observed behavior than predictions obtained from models which ignore the influence of the microstructure. McGee and McCullough [1981] have shown that the Lewis-Nielsen modification of the Halpin-Tsai relationship tends to overestimate elastic moduli at high filler concentration. These workers report a new model that gives good agreement between predicted and

observed elastic moduli for particulate filled systems as well as porous materials. Bradbury and Bigg [1980] show that while the thermal conductivity of aluminum and copper filled epoxies are reasonably approximated by the Lewis-Nielsen relationship, the electrical conductivity exhibits a sharp transition that is not accounted for by the Lewis-Nielsen equation, or any other available relationship.

Gurland [1966] proposed that the observed sharp transitions in electrical conductivity of metal filled polymers was a consequence of the formation of chains of contacting fillers which provide continuous paths for conduction. The relative frequency of such continuous paths should be dependent upon the shape of the filler and the volume fraction of filler. The Lewis-Nielsen relationship requires that such chain formation occur only in the vicinity of the maximum packing fraction of filler. Evidently, significant chain formation can occur at considerably lower volume fractions of filler. This effect is amplified when the transport phenomena can be distinguished as volume (e.g., thermal conductivity) versus surface (e.g., electrical conductivity) transport processes.

FORMULATION OF NETWORK MODEL

In view of Gurland's [1966] and other similar proposals, it is reasonable to assume that chain and network formation is the origin of the sharp transitions observed in the electrical conductivity. The qualitative significance of chain and network formation is illustrated in Figure 1 for a particulate filled polymer. The resistivity of the particulate filler is taken as $\rho_f \cong 10^{-6}$ ohm-cm [$K_f \cong 10^{6}$ (ohm-cm)$^{-1}$]; the polymeric binder has a resistivity of $\rho_m = 10^{16}$ ohm-cm [$K_m = 10^{-16}$ (ohm-cm)$^{-1}$]. As illustrated in Figure 1, the resistivity of the composite may range by several orders of magnitude from that of an insulator ($\rho = 10^{+14} - 10^{+16}$ ohm-cm) to that of a conductor ($\rho = 10^{-2} - 10^{-3}$ ohm-cm) as the volume fraction of the conducting filler, v_f is increased. The transition from insulator to conductor can be rationalized by the following structural arguments.

Structural Basis

At low volume fractions, the conducting fillers are isolated by the insulating matrix phase. Consequently, the

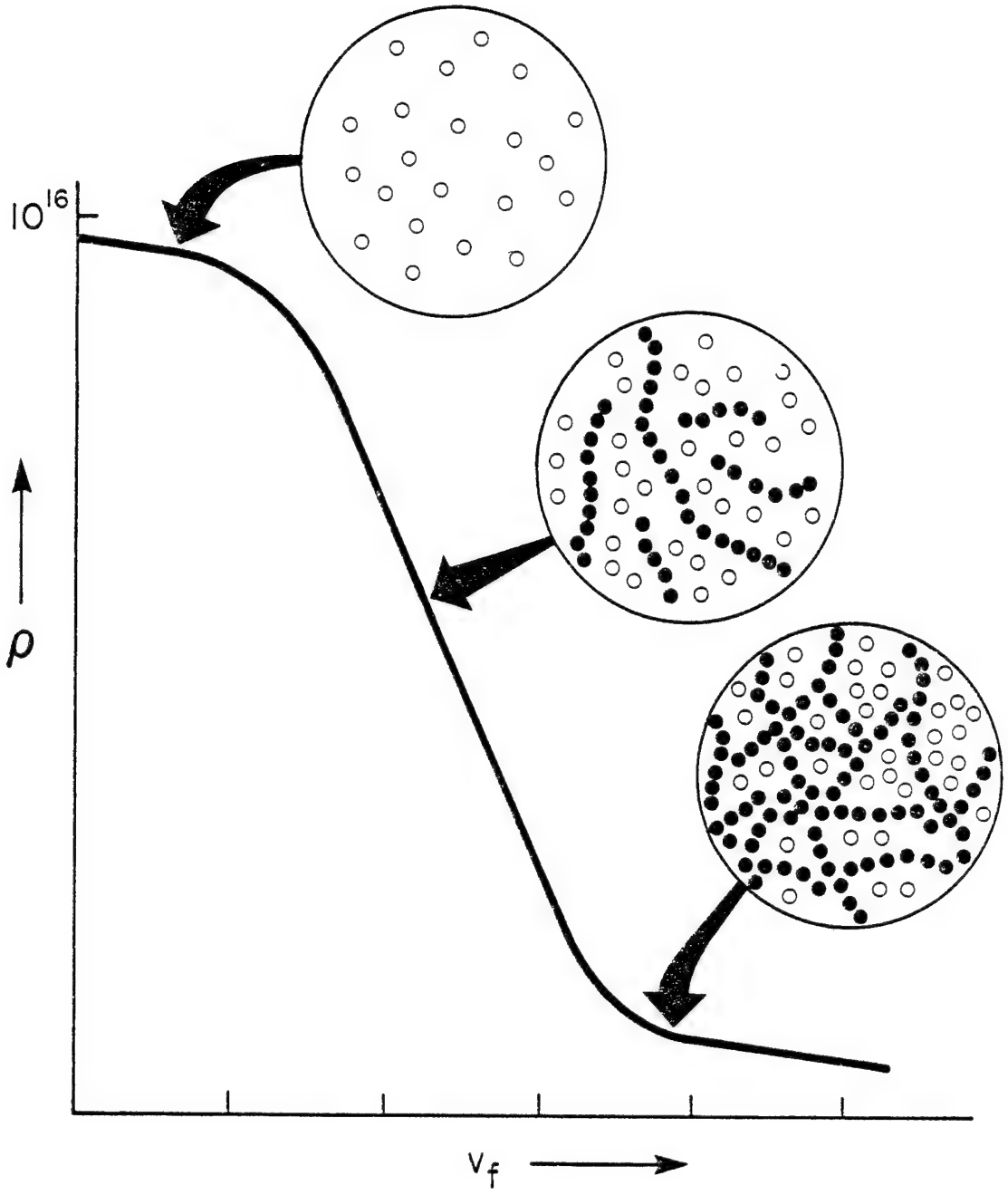

Figure 1. Illustration of the role of chain and network formation in establishing the electrical reisistivity, ρ , of a metal particle filled polymer. The open circles represent isolated metal particles. The closed circles represent contacting particles that form chains and networks of continuous conduction paths as the volume fraction, v_f , of the particles is increased.

composite tends to exhibit the high resistivities of the matrix ($\rho \cong 10^{+16}$ ohm-cm) and behaves as an insulator. In this insulating plateau region, the resistivity slightly decreases with increasing concentration of conducting particles as approximated by Equation (3b). As the concentration of conducting particles is further increased, the probability of particle-particle contact is enhanced. These contacts promote the formation of bead-like chains which provide continuous conduction paths that mimic the behavior of filaments of the the conducting materials. The transition from bead-like to fiber-like behavior occurs at a critical volume fraction, $v_f = \phi_c''$, for which the average number of particle-particle contacts begins to exceed "1". Based on Gurland's observations, this critical concentration is in the vicinity of $v_f \cong 0.3$. Further increases in the volume fraction concentration of the conducting particles causes a progressive increase in the average chain length of contacting particles so that the behavior rapidly tends toward the limiting behavior of a continuous fiber system. The structure associated with the region intermediate between insulating and conducting behavior is illustrated in Figure 1 by the closed circles which represent contacting particles participating in chains of varying conduction path lengths.

A continued increase in the concentration of conducting particles causes an increase in the average number of contacts. Eventually, the average number of contacts will exceed "2" so that chain branching occurs which gives rise to network formation. This second structural transition occurs at the saturation volume fraction $v_f = \phi_c'$ associated with the onset of network formation (i.e., that concentration at which the average number of contacts begins to exceed "2"). From Gurland's observations, the saturation concentration occurs in the vicinity of $v_f \cong 0.4$.

Upon the onset of incipient network formation at $v_f = \phi_c'$, the multitude of continuous conduction paths causes a transition to behavior dominated by the highly conducting (low resistivity) filler material. The structure associated with the conducting plateau is illustrated in Figure 1 by the closed circles which represent contacting particles participating in a continuous network of conducting paths. A further increase in the concentration of conducting particles beyond the saturation concentration simply fills the interstices of the network with additional conducting material so that the conductivity follows the behavior predicted by Equation (3a).

The significance of network formation in establishing high levels of conductivity was demonstrated by

Malliaris and Turner [1971]. These workers tumbled large particles of polymers (polyvinyl chloride; polyethylene) with metal powders (nickel; copper). As illustrated in Figure 2a, the metal powder adhered to the surface of the larger polymer particles. The metal-powder coated polymer particles were subsequently compacted under conditions which limited flow. Photomicrographs of the compacted material revealed metal particle networks shown in an idealized form in Figure 2b. As a consequence of the segregation of metal particles, network formation (and consequently, high levels of conduction) were achieved at a significantly lower saturation concentration ($\phi_c' = 0.06$) than would be required if the particles were dispersed uniformly throughout the polymer phase.

These qualitative considerations indentify features of the microstructure that must be incorporated into quantitative models. The development of such models can be approached in two stages:

- o The development of transport models which account for a distribution of path lengths.
- o The development of statistical models to predict path length distributions in terms of the concentration of filler, and the

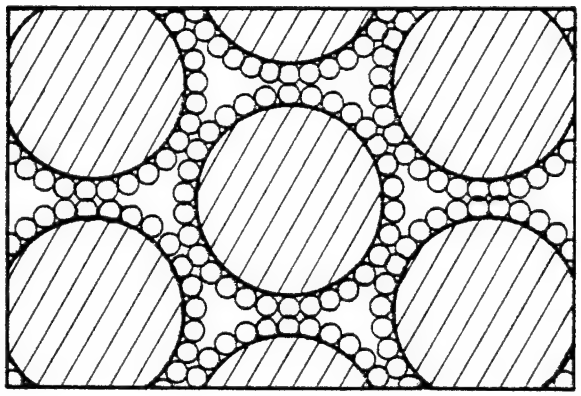

(a)

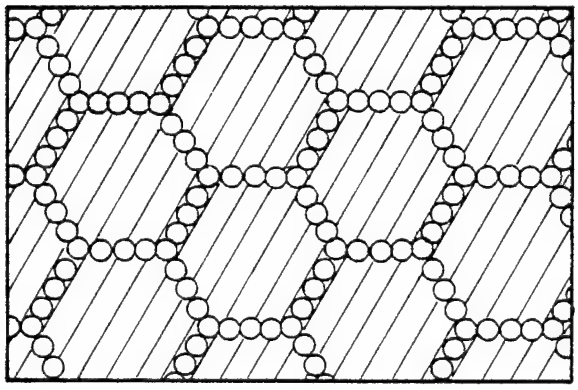

(b)

Figure 2. Illustration of enhancement of conductivity through network formation induced by segregation of conducting particles. The top figure represents an idealized segregated structure for large polymer particles (cross-hatched) coated with metal powder (open circles). The bottom sketch represents an idealized network of contacting metal particles formed by compacting the system. After Malliaris and Turner [1971].

orientation and shape of the conducting filler (e.g., particles, fibers, or platelets).

Approach

Transport Models:

Improved bounds on transport properties were recently reported by Nomura and Chou [1980]. These workers focused attention on a system of aligned fibers of equivalent but arbitrary aspect ratio, "a". The results from this analysis take into account two- and three-point correlation functions through the use of the modified Eshelby tensor developed by Wu and McCullough [1977]. These bounds provide a basis for establishing the theoretical limits for conductivity. However, without further treatment these limits are of little practical value since the upper and lower bounds on electrical conductivity may differ by 14 to 16 orders of magnitude. Wu and McCullough [1977] have shown that behavior intermediate between these wide limits is strongly dependent upon the microstructure developed within the composite material.

The bounding results were extended to account for distributions in fiber lengths. Following the approach of McGee and McCullough [1981], these improved bounds were used

to obtain model relationships to predict intermediate behavior between the limiting bounds as dictated by distributions of contact path lengths for collections of particles, fibers, and platelets. This model provides constitutive relationships for a "Representative Volume Element" (RVE). The predicted properties of the RVE provide subsequent input to an "Aggregate Model" [Jarzebski, McGee and McCullough, 1982], which accounts for orientation distributions.

Statistical Models:

For a given number, N, of filler elements, the path length distributions may be obtained by the application of "random flight statistics" traditionally used to predict dimensions of polymer molecules. The key parameter of the resulting distribution function is the "contact probability". Studies of contact probabilities for particles are available from the chemical engineering literature related to packed bed catalytic reactors; e.g., Suzuki et al [1981]. The results from these studies were used to estimate the concentration dependence of the contact probability and hence the behavior of the path length distributions as a function of particle concentration. These results were extended to fibers through approximate geometrical constructions.

SUMMARY OF MODEL RELATIONSHIPS

The mathematical structure of the network model is summarized in Tables I through III. The K's represent any one of the following transport properties:

- o electrical conductivity
- o thermal conductivity
- o diffusivity
- o dielectric constants (both real and imaginary)
- o magnetic permeability

The distinction between the various transport properties is achieved by specifying certain parameters (described in a subsequent section) related to surface and volume transport mechanisms; however, attention will be restricted to electrical conductivity. The network model accounts for the following important structural features of composite materials:

- o intermediate states of fiber orientation through an orientation parameter, f ;
- o filler shape through the aspect ratio parameter, "a". (For continuous fibers,

TABLE I

Orientation Dependence

$\langle K_i \rangle$ = Bulk transport property

K_i^* = RVE transport property

f_ν = Orientation parameter

Axial Orientation: f_a

$$\langle K_1 \rangle = \frac{1}{3} K_1^* + \frac{2}{3} K_2^* + \frac{2}{3} f_a \, (K_1^* - K_2^*)$$

$$\langle K_2 \rangle = \langle K_3 \rangle = \frac{1}{3} K_1^* + \frac{2}{3} K_2^* - \frac{1}{3} f_a \, (K_1^* - K_2^*)$$

$$f_a = \frac{1}{2} \left[3 \langle \cos^2 \phi \rangle_a - 1 \right]$$

$$\langle \cos^2 \phi \rangle_a = \int_0^{\pi/2} \cos^2 \phi \; n_p(\phi) \; \sin\phi \; d\phi$$

Planar Orientation: f_p

$$\langle K_1 \rangle = \frac{1}{2} K_1^* + \frac{1}{2} K_2^* + \frac{1}{2} f_p \, (K_1^* - K_2^*)$$

$$\langle K_1 \rangle = \frac{1}{2} K_1^* + \frac{1}{2} K_2^* + \frac{1}{2} f_p \, (K_1^* - K_2^*)$$

$$\langle K_3 \rangle = K_2^*$$

$$f_p = 2 \langle \cos^2 \phi \rangle_p - 1$$

$$\langle \cos^2 \phi \rangle_p = \int_0^{\pi/2} \cos^2 \phi \; n_p(\phi) \; \sin\phi \; d\phi$$

TABLE II

Constitutive Properties of RVE

Transport Property	Filler	Matrix
Longitudinal	K_{F_1}	K_m
Transverse	K_{F_2}	K_m
Volume Fraction	v_f	v_m

$$(i = 1,2)$$

$$K_{F_i} > K_m$$

$$K_i^* = \frac{K_{F_i} K_m \{\overline{K}_i + (v_m - v_f)\, \Delta K_i \langle y_i \rangle\}}{K_{F_i} K_m + [v_m^2 K_{F_i} - v_f^2 K_m]\, \Delta K_i \langle y_i \rangle}$$

$$\overline{K} = v_f K_{f_i} + v_m K_m$$

$$\Delta K_i = K_{F_i} - K_m$$

$$\langle y_1 \rangle = Y_o H_1(v_f, a)$$

$$\langle y_2 \rangle = \langle y_3 \rangle = \frac{1}{2} [1 - y_o H(v_f, a)]$$

$$y_o(a) = 1 - h(a)$$

(continued)

(Table II, continued)

$a \to \infty$ $\qquad h(\infty) = 1$

$a > 1$ $\qquad h(a) = \frac{a^2}{a^2-1}\left\{1 - \frac{1}{2}\left[\left(\frac{a^2}{a^2-1}\right)^{1/2} - \left(\frac{a^2-1}{a^2}\right)^{1/2}\right] \ln \times \frac{a+(a^2-1)^{1/2}}{a-(a^2-1)^{1/2}}\right\}$

$a = 1$ $\qquad h(1) = 2/3$

$0<a<1$ $\qquad h(a) = \frac{a^2}{1-a^2}\left\{\left[\left(\frac{1-a^2}{a^2}\right)^{1/2} + \left(\frac{a^2}{1-a^2}\right)^{1/2}\right] \tan^{-1} \times \left(\frac{1-a^2}{a^2}\right)^{1/2} - 1\right\}$

TABLE III

Path Distributions

v_f = filler volume fraction a = filler aspect ratio

Critical Concentrations

$$\phi_c' = \alpha(a)^{-1/3}$$

$$\phi_c'' = \beta(a)^{-1/3}$$

Transport Mechanism

Bulk: $\alpha = 2/3$, $\beta = 1/3$ Surface: $\alpha \simeq 0.4$, $\beta \simeq 0.3$

Distribution Parameters ($i = 1,2$)

Mean: $$\mu_i = \frac{Z_i'\phi_c'' + Z_i''\phi_c'}{Z_i' + Z_i''}$$

Spread: $$\sigma_i = \frac{\phi_c' - \phi_c''}{Z_i' + Z_i''}$$

$$(Z_i')^2 = 2 \ln\left[\frac{y_o\phi_c'(1-\phi_c')R_i^2}{3}\right]$$

$$(Z_i'')^2 = 2\left[\ln \frac{(1-\phi_i'')^2 R_i y_o}{3\{\phi_c''(1-y_o) + (1-\phi_c'')y_o\}^2}\right]$$

$$y_o = 1-h(a) \qquad \text{(Table II)}$$

$$R_i = K_{F_i}/K_m \qquad \text{(Table II)}$$

(continued)

(Table III, continued)

Distribution Functions (i = 1,2)

$v_f \geq \mu_i$

$$H_i(v, a) = 1 - \Phi(X_i)$$

$$X_i = \frac{v_f - \mu_i}{\sigma_i}$$

$v_f < \mu_i$

$$H_i(v_f, a) = \Phi(|X_i|)$$

$$|X_i| = \frac{\mu_i - v_f}{\sigma_i}$$

$$\Phi(X_i) = \frac{1}{\sqrt{2\pi}} \int_{-\infty}^{X_i} e^{-\tau^2/2} \, d\tau$$

$a \to \infty$; for short fibers, $a > 1$; for particles, $a = 1$; and for platelets, $0 < a < 1$.)

These important features are discussed in the following sections.

Orientation Dependence

Under the Aggregate Model [Jarzebski, McGee and McCullough, 1982], the properties of a bulk specimen may be obtained by averaging the properties of a transversely isotropic Representative Volume Element (RVE), characterized by the properties K_1^* and K_2^* , over appropriate orientation distributions. The details of the averaging procedures are given elsewhere [McGee, 1982]. The results for contracted second rank tensors corresponding to transport properties, K, are summarized in Table I for two important types of orientation distributions -- axial and planar. The quantities $\langle K_1 \rangle$, $\langle K_2 \rangle$, and $\langle K_3 \rangle$ are the observed properties of the bulk specimen along the specimen axes (e.g., the longitudinal "1" direction, the transverse or width direction, "2", and the perpendicular or thickness direction, "3"). The quantities K_1^* and K_2^* are the properties of the transversely isotropic RVE predicted by the constitutive relationship given in Table II.

Axial orientation distributions are associated with processing procedures (e.g., injection molding) in which fibers achieve a three-dimensional distribution. The important features of an axial distribution are ilustrated in Figure 3. In this case, the orientation distribution function, $n(\phi)$, gives the fraction of filler elements which lie on a cone making an angle ϕ with respect to the "1" axis of the specimen. The normalized distribution is taken as symmetric around the "1" axis, $n(\phi) = n(-\phi)$, and across the 2-3 plane, $n(\phi) = n(\pi+\phi)$. The statistical characteristics of the axial distribution may be described by a parameter, f_a, scaled to the range $-1/2 < f_a < 1$. This parameter is related to the second moment of the three-dimensional distribution:

$$f_a = (1/2)[3\langle\cos^2\phi\rangle - 1] \qquad \text{(Table I)}$$

with

$$\langle\cos^2\phi\rangle = \int_0^{\pi/2} n(\phi)\cos^2\phi\sin\phi d\phi \quad .$$

A value of $f_a = -1/2$ corresponds to a situation in which all the fibers are confined to lie in the 2-3 plane (i.e., $\langle\cos^2\phi\rangle = 0$); a value of $f_a = 1$ denotes perfect collimation along the "1" axis (i.e., $\langle\cos^2\phi\rangle = 1$). States of partial

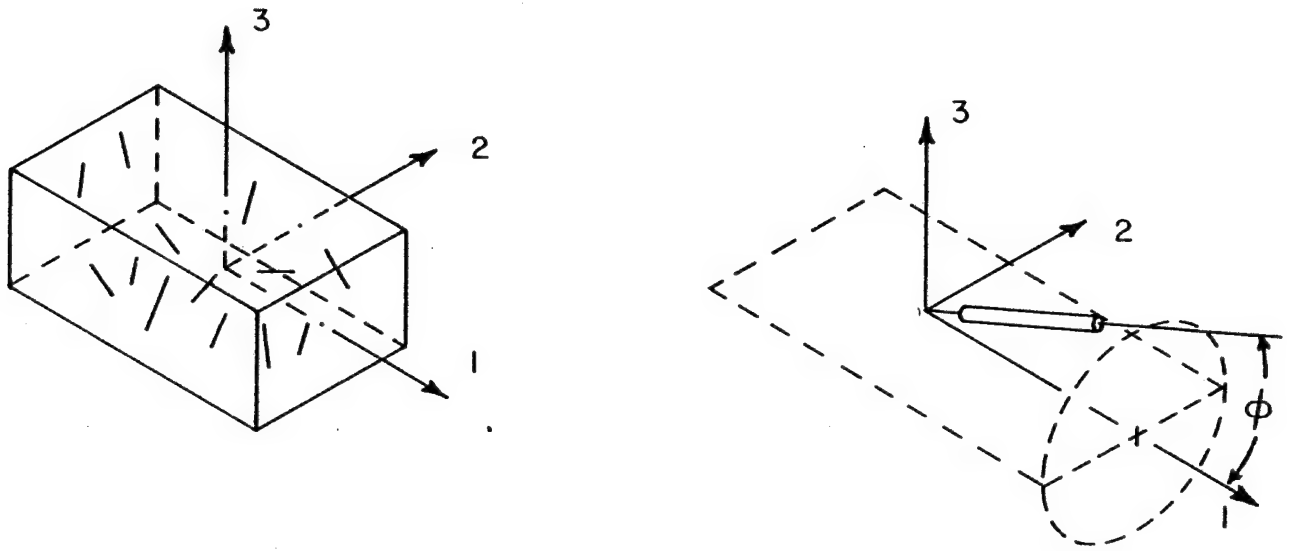

$$n(\phi) = n(-\phi)$$

$$n(\phi) = n(\pi + \phi)$$

$$\int_0^{\pi/2} n(\phi) \sin\phi \, d\phi = 1$$

Figure 3. Schematic definition of the features of a three-dimensional axial orientation distribution.

three-dimensional orientation are indicated by intermediate values of f_a . A three-dimensional random orientation is characterized by $f_a = 0$ (i.e., $\langle \cos^2\phi \rangle = 1/3$). In this event, the bulk specimen is isotropic since $\langle K_1 \rangle = \langle K_2 \rangle = \langle K_3 \rangle$. Alternately, an isotropic bulk specimen is obtained if the RVE is isotropic so that $K_1^* = K_2^*$. In this situation, the term $[K_1^* - K_2^*]$ of Table I vanishes so that the specimen properties are independent of f_a .

Sheet molding materials as well as other systems produced by compression molding can be characterized by a two-dimensional planar orientation in which the fibers are confined to lie in a plane. In some cases, injection and/or transfer molding procedures will give rise to stratified layers that may be locally characterized as planar orientations. The features of this important orientation distribution are illustrated in Figure 4. For this case, the normalized orientation distribution, $n(\phi)$, gives the fraction of fibers, within the 1-2 plane, which makes an angle ϕ with respect to the "1" axis of the specimen. The distribution is taken as symmetric across the 1-3 plane, $n(\phi) = n(-\phi)$, and across the 2-3 plane, $n(\phi) = n(\phi+\pi)$. The statistical characteristics of the planar distribution may be described by a parameter, f_p , scaled to the range $-1 < f_p < 1$. As before, f_p is related to the second moment of the two-dimensional distribution:

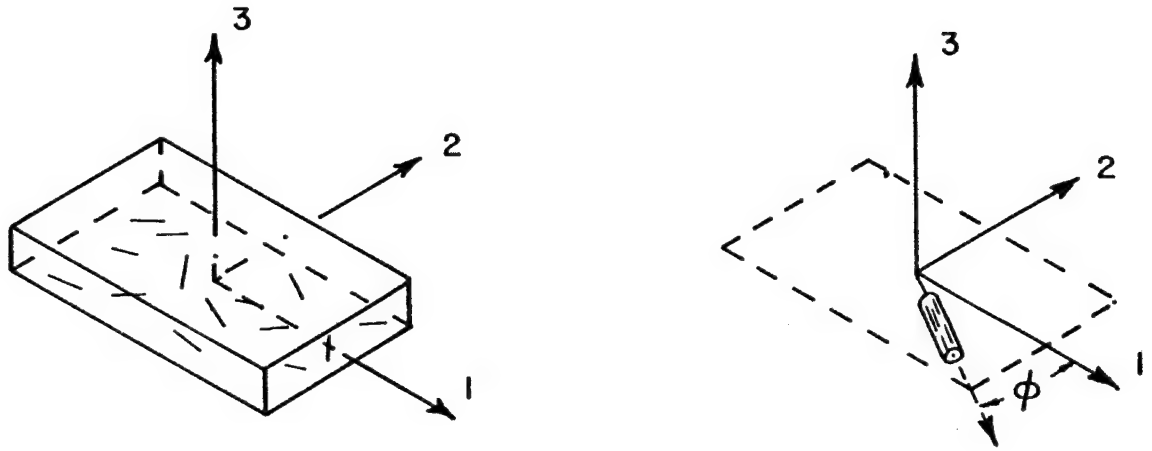

$$n(\phi) = n(-\phi)$$

$$n(\phi) = n(\pi + \phi)$$

$$\int_0^{\pi/2} n(\phi)\, d\phi = 1$$

Figure 4. Schematic definition of the features of a two-dimensional planar orientation distribution.

$$f_p = 2\langle\cos^2\phi\rangle - 1 \qquad \text{(Table I)}$$

with

$$\langle\cos^2\phi\rangle = \int_0^{\pi/2} n(\phi)\cos^2\phi d\phi \ .$$

A value of $f_p = 1$ corresponds to fiber alignment along the "1" axis of the specimen; a value of $f_p = -1$ corresponds to alignment along the "2" axis. Partial states of planar orientation are described by intermediate values of f_p . A value of $f_p = 0$ corresponds to a quasi-isotropic material with $\langle K_1\rangle = \langle K_2\rangle$ but distinct from $\langle K_3\rangle$. In the event that the RVE is isotropic such that $K_1^* = K_2^*$, the bulk specimen exhibits isotropic character with $\langle K_1\rangle = \langle K_2\rangle = \langle K_3\rangle$.

Recently, McGee [1982] generalized the treatment of orientation distributions to account for distributions intermediate between three-dimensional axial and two-dimensional planar. In this extension, the projection of a fiber onto the 1-2 plane is specified by an angle ϕ with an associated orientation parameter, f_p . The orientation with respect to the "3" axis is specified by an angle θ with an associated orientation parameter f_a . Under this revision, the parameter f_a is a measure of the extent to which fibers are tilted out of the 1-2 plane toward the "3" axis. These

generalized orientation descriptors are defined schematically in Figure 5.

The three-dimensional axial and two-dimensional planar distributions are contained as special cases. The two-dimensional planar distribution corresponds to $f_a = -1/2$. The three-dimensional axial distribution is obtained with $f_p = 0$; however, in this revision, the principle axis of axial alignment corresponds to the "3" axis. A three-dimensional random orientation is obtained with both f_a and f_p equal to zero.

The properties of the bulk specimen are given in terms of the generalized distribution by

$$\langle K_1 \rangle = K_o + k[f_p - f_a(1 + f_p)] \tag{4a}$$

$$\langle K_2 \rangle = K_o + k[f_p + f_a(1 - f_p)] \tag{4b}$$

$$\langle K_3 \rangle = K_o + 2kf_a \tag{4c}$$

with

$$K_o = (1/3)[K_1^* + 2K_2^*]$$

$$k = (1/3)[K_1^* - K_2^*]$$

where K_1^* and K_2^* are again the properties of the RVE as predicted by the constitutive relationships of Table II.

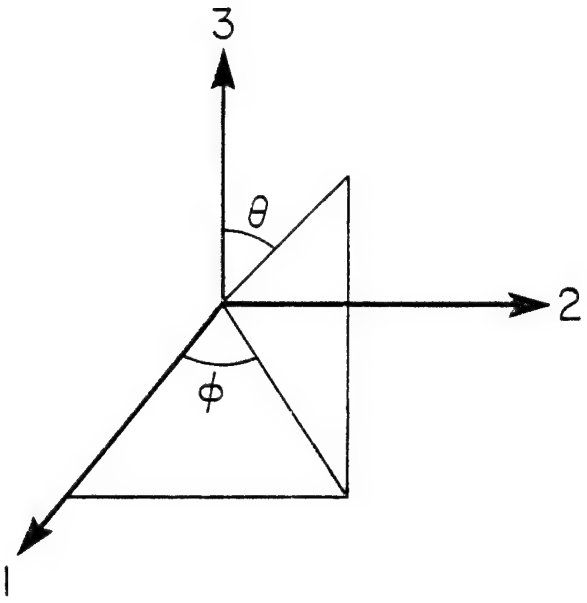

"planar" "axial"

$$f_p = 2\langle \cos^2\phi \rangle - 1 \qquad f_a = \frac{1}{2}\left[3\langle \cos^2\theta \rangle - 1\right]$$

$$g_p = \frac{1}{5}\left[8\langle \cos^4\phi \rangle - 3\right] \qquad g_a = \frac{1}{4}\left[5\langle \cos^4\theta \rangle - 1\right]$$

with

$$\langle \cos^m\phi \rangle = \int_0^{\pi/2} n(\phi)\cos^m\phi\, d\phi$$

$$\langle \cos^n\theta \rangle = \int_0^{\pi} n(\theta)\sin\theta\cos^n\theta\, d\theta$$

Figure 5. Schematic definition of the orientation parameters of the generalized orientation distribution. After McGee [1982].

These important descriptors of fiber orientation must be determined by independent experimental characterizations such as the laser scattering methods described by McGee and McCullough [1982].

Constitutive Relationships

The quantities K_1^* (i = 1,2) of Table I correspond to the properties of a transversely isotropic Representative Volume Element (RVE) of the material system. The relationship of the K* to the properties, concentration, and phase geometry of the components are summarized in Table II.

The quantity K_m refers to the appropriate transport property of an isotropic matrix. The K_{Fi} refer to the effective transport property of a transversely isotropic chain of contacting filler elements with K_{F1} corresponding to the longitudinal property and K_{F2} corresponding to the transverse property. In the event that the filler is isotropic, then $K_{F1} = K_{F2}$.

The quantities v_f and v_m represent the volume fraction of filler and matrix, respectively, with $v_f + v_m = 1$.

The term $\langle y_i \rangle$ is a structure factor which takes into account the shape of the filler, path length distributions,

and the underlying mechanism of transport. The role of these various quantities is further specified in Table III. The quantity y_o is determined by the true aspect ratio, "a", of the filler. The functional dependence of y_o on the aspect ratio is given for three important shapes in Table II; viz., fibers (a > 1), spherical particles (a = 1), and platelets (0 < a < 1) .

The results summarized in Table II can be recast into a form similar to the Halpin-Tsai Relationship [Aston et al, 1969]; viz.,

$$\frac{K_i^*}{K_m} = \frac{1 + \xi_i \chi_i v_f}{1 - \chi_i v_f} \tag{5a}$$

with

$$\chi_i = \frac{K_{Fi} - K_m}{K_{Fi} + \xi_i K_m} \tag{5b}$$

and

$$\xi_i = \psi_i(v_f)\left[\frac{1 - \langle y_i \rangle}{\langle y_i \rangle}\right]$$

where $\psi_i(v_f) = \dfrac{K_{Fi}}{v_f K_m + v_m K_{Fi}}$

As the term $\langle y_i \rangle$ approaches the minimum value of 0, the reinforcing factor ξ_i approaches ∞ so that the constitutive

relationship reduces to the simple form of Equation (3a); viz.,

$$K_i^* = v_f K_{Fi} + v_m K_m \qquad \text{for } \langle y_i \rangle \to 0 \tag{3a}$$

Under these limiting conditions, the highly conducting filler, ($K_{Fi} >> K_m$) dominates the behavior of the composite material.

Alternately, if the term $\langle y_i \rangle$ approaches unity so that the reinforcing factor is given by $\xi_i = 0$, the constitutive relationship takes on the form of Equation (3b):

$$\frac{1}{K_i^*} = \frac{v_6}{K_{Fi}} + \frac{v_m}{K_m}$$

or

$$\rho_i^* = v_f \rho_{Fi} + v_m \rho_m \qquad \text{for } \langle y_i \rangle = 1 \tag{3b}$$

In this limit, the behavior is dominated by the insulating matrix ($\rho_m >> \rho_{Fi}$) .

For the special case of isolated ($H_1 = H_2 = 1$) spherical particles ($y_o = 1/3$), the reinforcing factor is given by

$$\xi_1 = \xi_2 = 2\psi(v_f) \tag{6}$$

The Maxwell relationship [Maxwell, 1892], the Rayleigh equation [Rayleigh, 1892], the Kerner equation [Kerner, 1956], and the composites spheres model [Hashin, 1970], are all equivalent and correspond to $\psi = 1$ (i.e., $\xi = 2$) . The factor $\psi_i(v_f)$ in Equation (6) is a concentration-property dependent correction introduced by the inclusion of higher order correlations.

Path Distribution Statistics

The distribution functions, H_i , account for the transport mechanism and the path length distributions in terms of the filler shape, orientation, and concentration. Tentative descriptions of these functions are proposed in Table III. These functions are dependent upon the "random flight statistics" associated with the distribution of chain lengths for a given collection of conducting filler elements. The key statistical parameter is the contact probability as determined by the shape, orientation, and concentration of the filler elements. An estimate for the contact probability was obtained from studies of packed bed reactors as reported in the chemical engineering literature; e.g., Suzuki et al [1981]. The merged estimates are summarized in Table III.

The parameters α and β in Table III distinguish between surface transport (e.g., electrical conductivity) and volume transport (e.g., thermal conductivity). Accordingly, the proposed model can be used for the entire class of transport properties by the appropriate distinction between surface and volume transport as reflected by these parameters. Tentative estimates for these parameters are given in Table III.

It is evident that the application of the model relationships summarized in Tables I, II, and III requires tedious computations. An interactive computer program has been developed to facilitate the use of these model relationships as a screening tool for ranking candidate conducting composites. A user's guide to the program, with illustrative examples, is given in the Appendix. Interactive computer programs are available for predicting the associated thermoelastic properties. The model development for the thermoelastic properties is described elsewhere [Jarzebski, McGee, and McCullough, 1982].

Models for Three Component Composites

As shown by McCullough and Peterson [1977], combinations of two or more filler materials in a composite

system introduce additional degrees of freedom for tailoring composite materials to multiple design requirements. Accordingly, it is useful to extend the preceding model formulation to include systems comprised of two distinct filler materials that may be differentiated by their (i) properties, (ii) shape, (iii) orientation, and/or any combination of these features.

Unfortunately, rigorous theoretical treatments which take into account higher order correlations between different types of fillers are not currently available. Consequently, approximate formulations are required for an extension to three component material systems.

As a first order approximation, the second filler phase will be viewed as an excluded volume. The exclusion of a filler of type "1" from the volume occupied by the filler phase of type "2" forces the conducting elements of the type "1" into a smaller relative volume and hence enhances chain formation, as illustrated in Figure 2. The apparent volume fraction of type "1" filler in the reduced volume of an intermediate two-component system (System I) is given by

$$v_{F1}^{I} = v_{F1}/(1 - v_{F2}) \qquad (7a)$$

where v_{F1} is the true volume fraction of the type "1" filler and v_{F2} is the true volume fraction of the filler viewed as the excluded volume. The apparent volume fraction of the matrix in System I is taken as

$$v_m^I = 1 - v_{F1}^I \tag{7b}$$

The transport properties $\langle K_i^I \rangle$ (i = 1,2,3) of the intermediate two-component system may be computed by the relationships given in Tables I - III and implemented in the computational algorithm described in the Appendix. In this application, the concentration is taken as the apparent volume fractions, v_{F1}^I and v_m^I , given by Equations (7). The filler properties, aspect ratio, and orientation parameters are specified as those associated with the filler of type "1".

A similar excluded volume argument may be applied for fillers of type "2" segregated by exclusion from the volume occupied by fillers of type "1". The apparent volume fraction of type "2" filler in the reduced volume of the second two-component system (System II) is given by

$$v_{F2}^{II} = v_{F2}/(1 - v_{F1}) \tag{8a}$$

with the matrix volume fraction in System II given by

$$v_m^{II} = 1 - v_{F2}^{II} \tag{8b}$$

As before, the quantities v_{F1} and v_{F2} are the true volume fractions of filler "1" and "2", respectively.

The transport properties, $\langle K_i^{II} \rangle$ (i = 1,2,3), of the second intermediate two-component system may be computed by the relationships given in Tables I - III and implemented in the computer programs described in the Appendix. The concentrations of the filler and matrix components are taken as the apparent volume fractions, v_{F2}^{II} and v_m^{II} determined from Equations (8); the filler properties, aspect ratio, and orientation parameters are specified as those associated with the filler of type "2".

The transport properties, $\langle K_i \rangle$ (i = 1,2,3), of the three component system may be estimated as a combination of the properties of System I and System II weighted by their respective volume fraction contributions to the combined system, viz., $v_I = 1 - v_{F2}$ and $v_{II} = 1 - v_{F1}$. However, the volume and the properties of the matrix phase were utilized in both intermediate systems. Consequently, the combined system must be corrected to account for this dual contribution of the matrix material; viz.,

$$\langle K_i \rangle = (1 - v_{F2}) \langle K_i^I \rangle + (1 - v_{F1}) \langle K_i^{II} \rangle - v_m K_m \tag{9}$$

where i = 1,2,3 for the properties along the 1, 2, and 3 axes of the specimen.

In the event that both filler types are particulate (a = 1) and the concentrations are well above the critical concentration for network formation, Equation (9) simplifies to

$$\langle K \rangle \cong v_{F1} K_{F1} + v_{F2} K_{F2} + v_m K_m \qquad (10)$$

The transport properties computed via Equation (9) provide conservative estimates for thermal and electrical conductivities. The excluded volume argument ignores contracts (and higher order correlations) between the two types of fillers. This limitation may not be particularly serious if the filler types differ by several orders of magnitude in their conductivities (i.e., one filler appears to be an insulator relative to the other). A system comprised of glass (or graphite) fibers and metal fillers (particulate, fiber, or platelet) should approach this condition.

SPECIFICATION OF MODEL PARAMETERS

The implementation of the relationships summarized in Tables I through III requires the following input information:

- the effective properties of the filler (K_F) and the polymer matrix (K_m);
- the volume fraction of the filler (v_F) and resin (v_m);
- the state of orientation as characterized by f_p and/or f_a;
- the filler geometry as characterized by the aspect ratio (a); with $a > 1$ for fibers, $a = 1$ for spherical (or near spherical) particles, and $a < 1$ for platelets.

Methods for assessing these quantities are described in the remainder of this section.

Effective Properties

The electrical resistivity ($\rho = 1/K$) and density of several candidate filler and resin materials are summarized in Table IV. These values correspond to typical handbook listings for the various pure materials. The conductivity of the pure polymeric material serves as the appropriate input parameter (K_m) for the continuous binder phase.

TABLE IV

Typical Properties of the Components of Conducting Composites

Material	Resistivity (ohm-cm)	Density (gm/cm^3)
Aluminum	2.63×10^{-6}	2.77
Copper	1.72×10^{-6}	8.96
Graphite Fiber	1.50×10^{-3}	1.77
Iron	10.0×10^{-6}	7.15
Nickel	7.8×10^{-6}	8.33
Silver	1.47×10^{-6}	10.6
Steel	81.0×10^{-6}	7.78
Bakelite (phenolic)	4×10^{11}	1.43
Nylon 6-10	5×10^{14}	1.08
Polyester	4×10^{16}	1.4
Polyphenylene Sulfide	1×10^{16}	1.34

As noted by Malliaris and Turner [1971], as well as Li et al [1982], the effective conductivity of chains of contacting filler, K_F , may be substantially reduced from that of the pure material, K_F^o ; viz.,

$$K_F = \chi K_F^o \tag{11}$$

where K_F^o is the conductivity of the pure filler material and and χ is a reduction factor attributed to geometrical contact irregularities associated with surface roughness and/or surface coatings (e.g., oxide layers or special sizing agents). Malliaris and Turner [1971] report a reduction factor of $\chi = 10^{-3}$ for contacting chains of nickel particles; Gurland's results for contacting silver particles are consistent with this reduction factor. Li, Streider and Joy [1982] report a reduction factor of $\chi = 3 \times 10^{-3}$ for contacting graphite fibers. These results imply that the reduction factor, χ , may be taken as essentially constant and on the order of $1 - 3 \times 10^{-3}$. The conductivity reduction factor corresponds to an enhancement of the effective resistivity by a factor of $3 - 10 \times 10^{2}$.

Concentration of Components

As a consequence of volume averaging, volume fractions emerge as the natural descriptors of concentration.

However, weight fraction concentrations are commonly employed to specify the composition of composite materials. These measures of concentration are related through the densities of the components; viz.,

$$v_f = \frac{w_f}{w_f + (1 - w_f)r} \tag{12a}$$

where w_f is the weight fraction of filler and "r" is the ratio of the density of filler to the density of resin;

$$r = d_f/d_m \tag{12b}$$

The term v_f is the volume fraction of filler with $v_m = 1 - v_f$.

The relationship of volume fraction to weight fraction of filler for several important material systems is displayed in Figure 6.

Metal coated fibers are of particular interest as candidate fillers for conducting composites. The density of metal coated fibers is dependent upon the thickness of the metal layer. Accordingly, the relationship between volume fraction and weight fraction is dependent upon the relative thickness of the coating on the fiber; viz.,

$$v_f = \frac{w_f d_m}{w_f d_m + (1 - w_f)\left[d_b + (d_c - d_b)\lambda(2 - \lambda)\right]} \tag{13a}$$

$$V_f = \frac{w_f}{w_f + (1 - w_f)r}$$

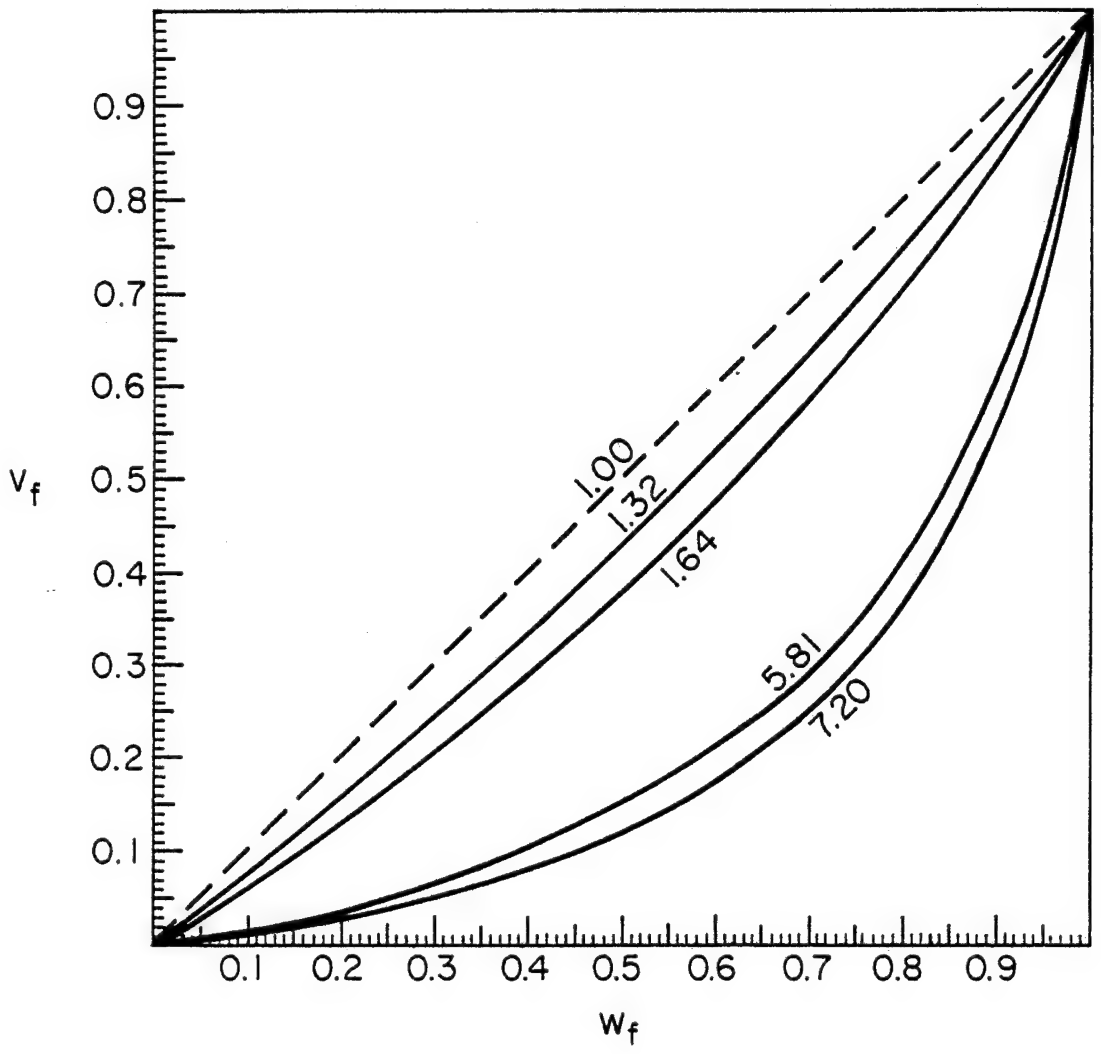

Figure 6. Relationship of volume fraction filler concentration, v_f, to weight fraction, w_f, for several material systems: polyphenylene sulfide/graphite (r = 1.32); Nylon 6-10/graphite (r = 1.64); polyphenylene sulfide/steel (r = 5.81); Nylon 6-10/steel (r = 7.20).

where d_m is the density of the polymer matrix, d_b is the density of the base fiber, and d_c is the density of the metal coating. The parameter "λ" is the ratio of the thickness of the coating , t_c , to the total radius, R , of the coated fiber:

$$\lambda = t_c/R \tag{13b}$$

The relationship of volume fraction to weight fraction for graphite fibers coated with various thicknesses of nickel are displayed in Figure 7 for a Nylon 6-10 matrix and in Figure 8 for a polyphenylene sulfide matrix.

State of Orientation

Information concerning the orientation distribution of fibers can be obtained from photomicrographs of certain sections of the test specimen. Sections taken from a side surface and an end surface are required to characterize the out-of-plane tilting of fibers as measured by f_a . Sections taken from a top surface and a mid-plane surface are required to characterize the uniformity of the in-plane orientation measured by f_p . These sections are schematically defined in Figure 9.

Typical photomicrographs of these four sections are shown in Figure 10 for a test specimen of graphite fibers

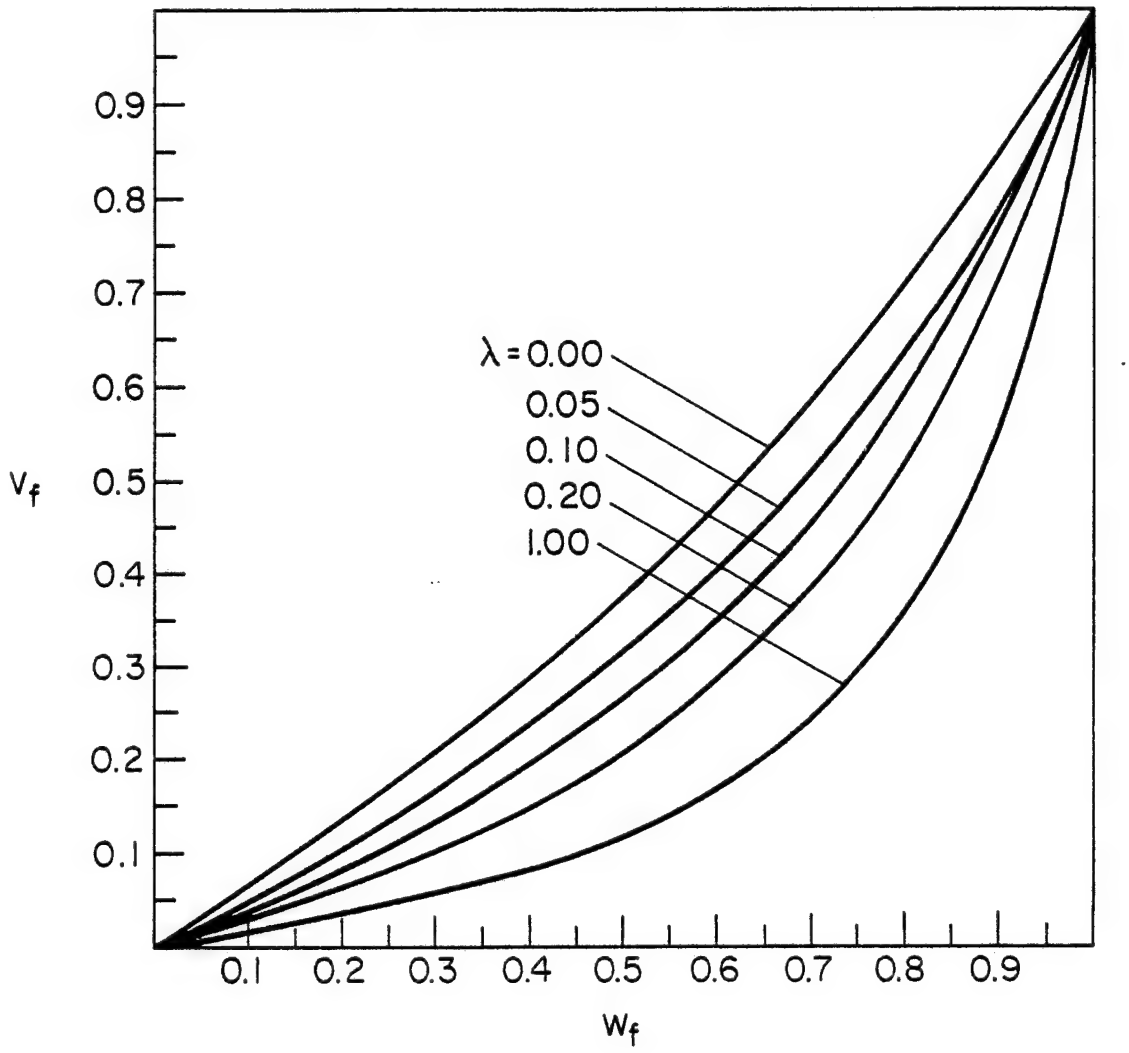

Figure 7. Relationship of volume fraction filler concentration, v_f , to weight fraction, w_f , for graphite fibers coated with various thicknesses of nickel in a Nylon 6-10 matrix. The parameter λ denotes the ratio of the thickness of metal to the total radius of the fiber.

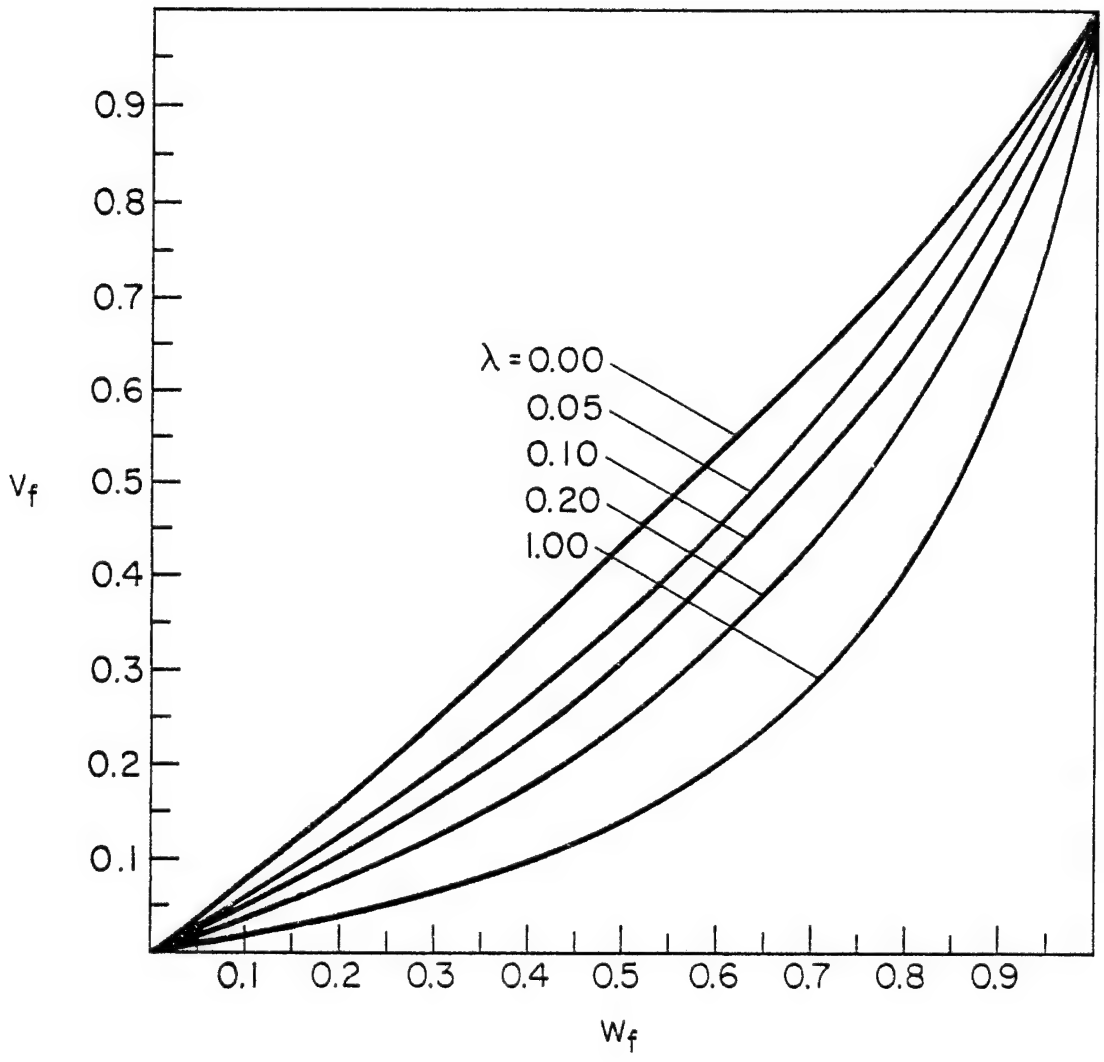

Figure 8. Relationship of volume fraction filler concentration, v_f , to weight fraction, w_f , for graphite fibers coated with various thicknesses of nickel in a polyphenylene sulfide matrix. The parameter λ denotes the ratio of the thickness of metal to the total radius of the fiber.

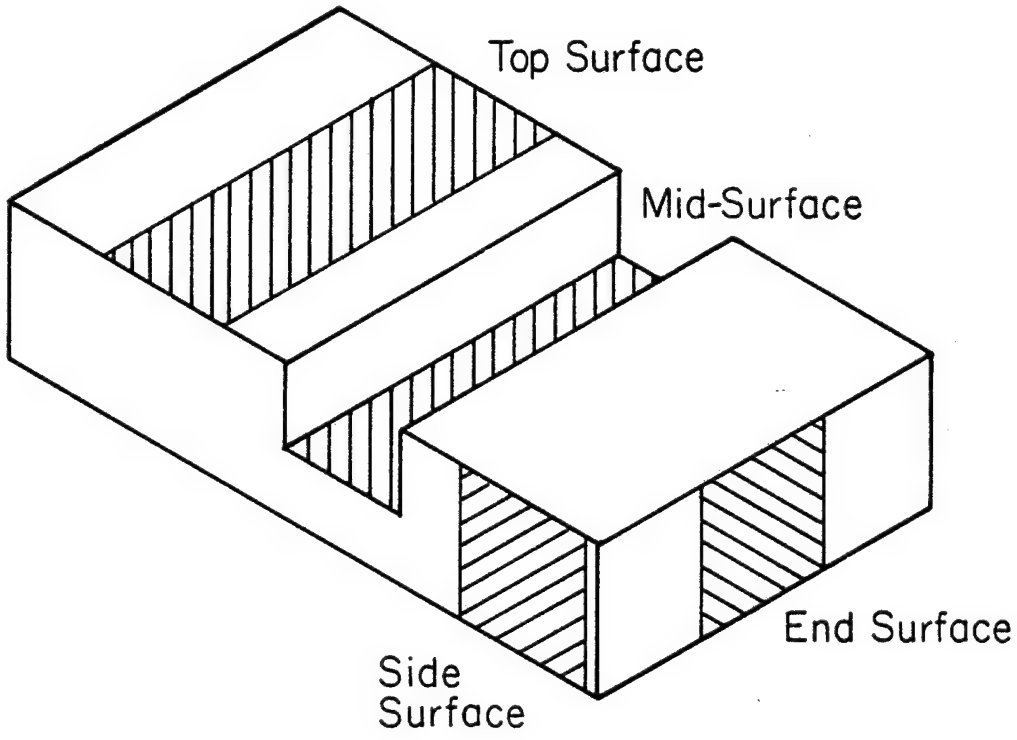

Figure 9. Schematic diagram illustrating various locations from which specimen sections were sampled.

Top Surface

Mid-Surface

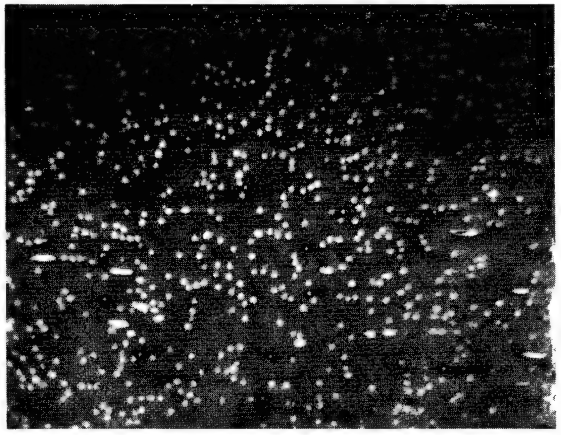

End Surface

Side Surface

Figure 10. Photomicrographs of sections of a 20% (by weight) polyphenylene sulfide/graphite fiber specimen. The top and mid-surface sections were obtained at 10x; end and side sections were obtained at 20x. After McGee [1982].

(20% by weight) in a polyphenylene sulfide matrix. Photomicrographs of four sections taken from a test specimen of nickel coated graphite fibers (30% by weight) in Nylon 6-10 are displayed in Figure 11.

From these direct observations, the number of fibers, $N(\psi)$ which are oriented between $\psi - \Delta\psi$ and $\psi + \Delta\psi(\psi = \phi \text{ or } \theta)$ with respect to the appropriate specimen axis could be counted and a histogram of the orientation distribution constructed. The associated orientation parameters, f_a or f_p, could then be obtained by the numerical integrations prescribed in Table I.

Recently, McGee and McCullough [1982] have shown that photographic negatives of sample sections can be used as diffraction masks in a Fraunhoffer diffractometer to obtain diffraction patterns characteristic of the state of orientation. The components of a Fraunhoffer diffractometer are shown in Figure 12. Diffraction patterns obtained from the photomicrographs shown in Figure 10 are displayed in Figure 13; diffraction patterns from the photomicrographs given in Figure 11 are shown in Figure 14.

McGee and McCullough [1982] have shown that the relative intensity of the diffraction pattern is proportional to the orientation distribution shifted by $\pi/2$; viz.,

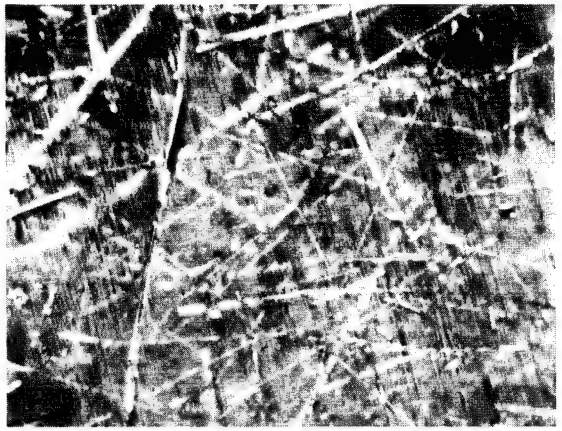

Top Surface

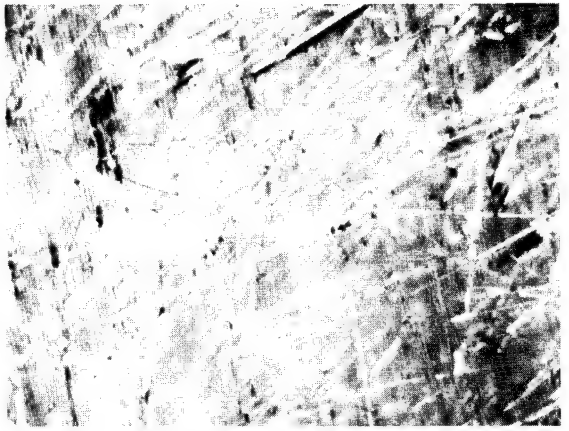

Mid-Surface

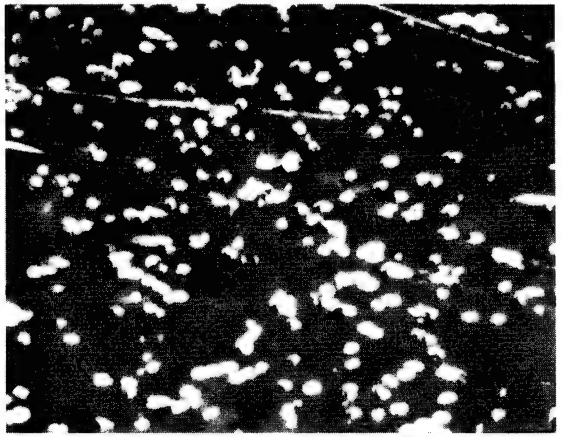

End Surface

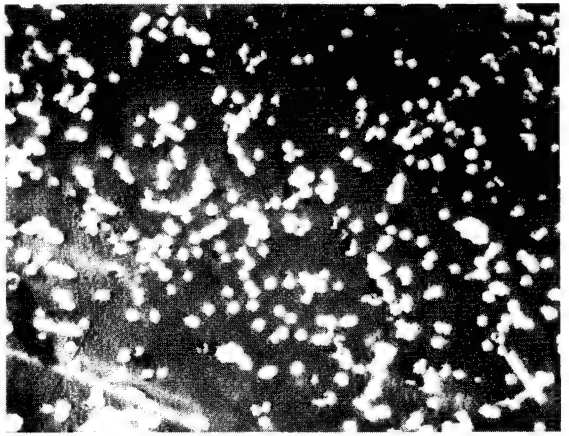

Side Surface

Figure 11. Photomicrographs of sections of a 30% (by weight) Nylon 6-10/nickel coated graphite fiber specimen. The top and mid-surface sections were obtained at 10x; end and side sections were obtained at 20x. After McGee [1982].

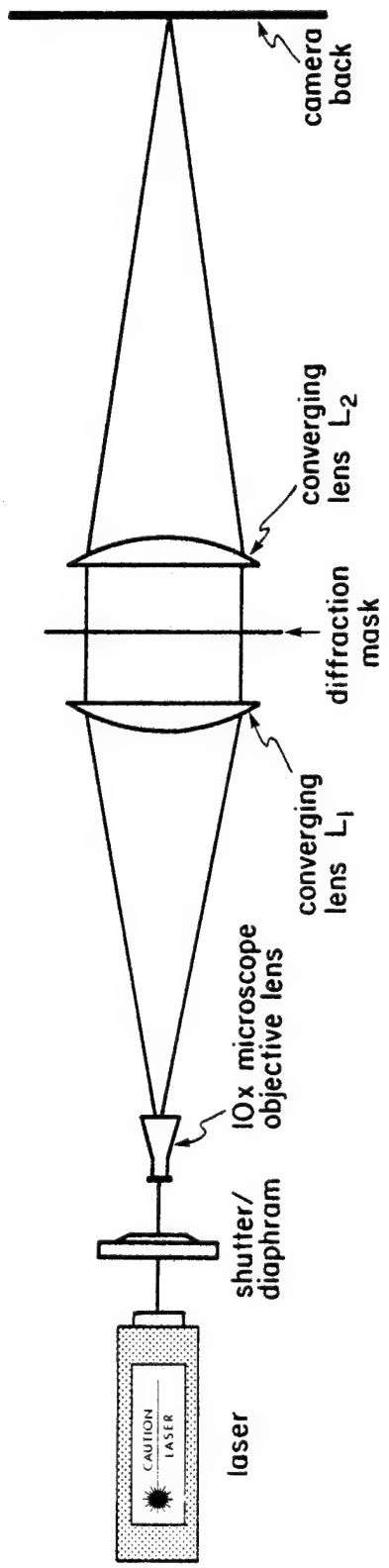

Figure 12. Schematic diagram illustrating the components of a Fraunhoffer diffractometer.

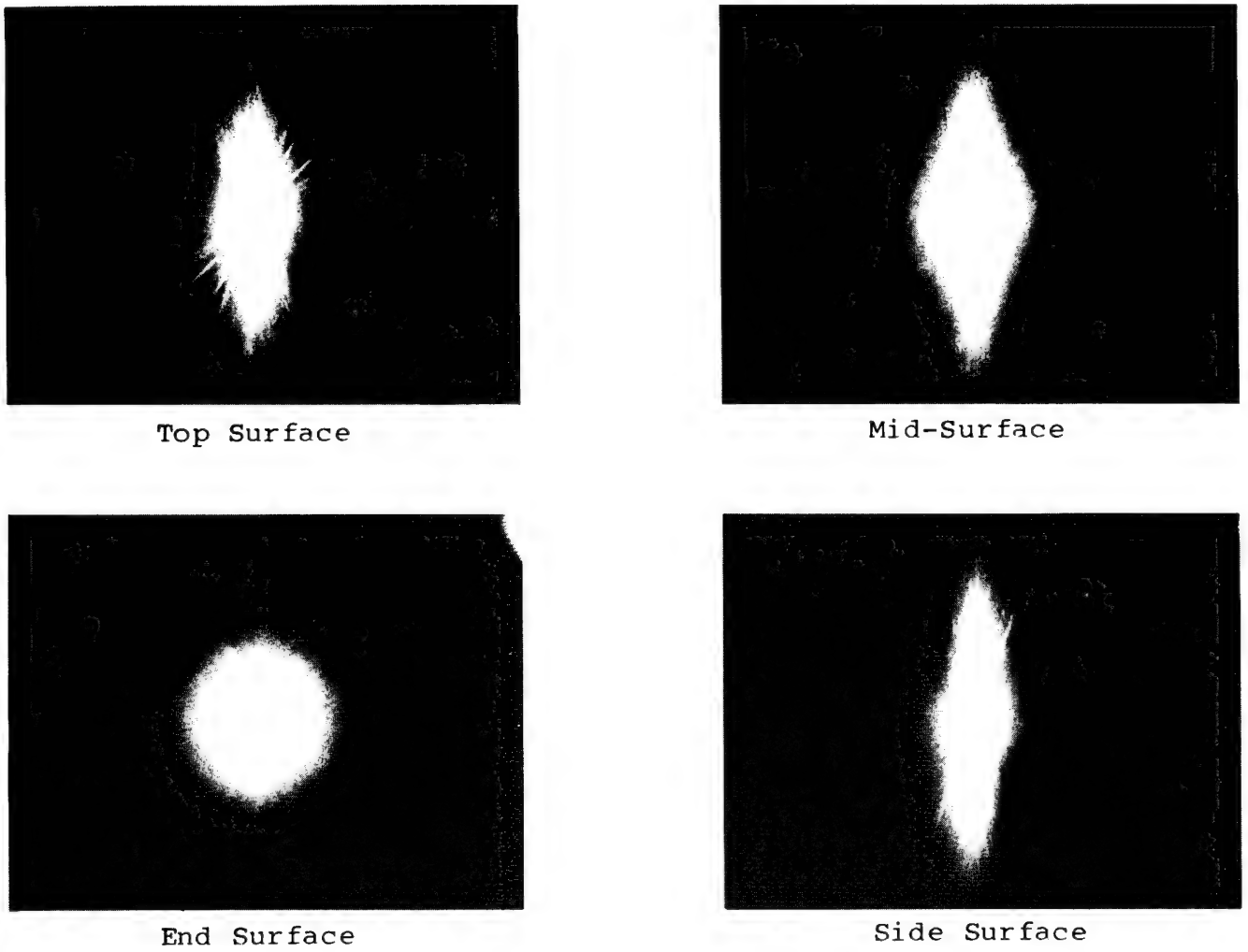

Figure 13. Diffraction patterns obtained from the sample sections of Figure 10 for a 20% (by weight) polyphenylene sulfide/graphite fiber specimen. After McGee [1982].

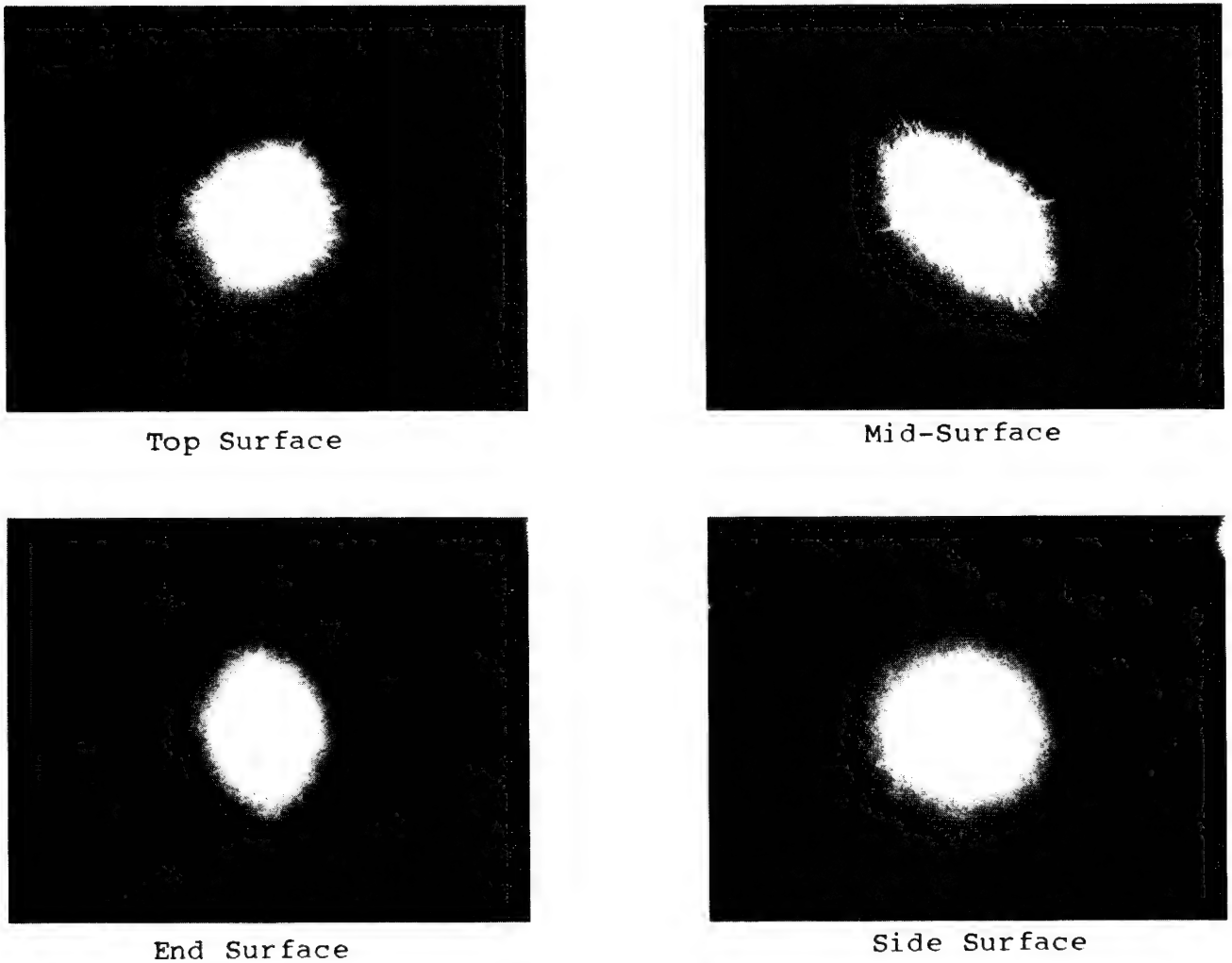

Figure 14. Diffraction patterns obtained from the sample sections of Figure 11 for a 30% (by weight) Nylon 6-10/nickel coated graphite fiber specimen. After McGee [1982].

$$I(r,\psi) = I(r)n(\psi + \pi/2) \qquad (14)$$

where r and ψ are the polar coordinates of the diffraction pattern as measured from the central spot as the origin. Accordingly, an intensity trace over a circle of radius "r" on the diffraction pattern yields the orientation distribution function. Optical densitometer traces of the diffraction patterns shown in Figures 13 and 14 are displayed in Figures 15 and 16. Procedures for extracting orientation parameters from these intensity profiles are given elsewhere [McGee, 1982]. Application of these procedures shows that both the graphite fiber/polyphenylene sulfide and the nickel coated graphite/Nylon 6-10 specimens are in a planar state of orientation ($f_a \cong -1/2$). The graphite fiber/polyphenylene sulfide specimen shown in Figure 10 exhibits a high degree of planar orientation with $f_p \cong 0.7$. In contrast, the nickel coated graphite fiber/Nylon 6-10 specimen shown in Figure 11 exhibits a nearly in-plane random orientation with $f_p = 0.2\text{-}0.3$. It will be shown in the subsequent section that these different states of orientation are reflected in the observed resistivities of the specimens.

Fiber Aspect Ratio

Estimates of the average aspect ratio can be obtained from photomicrographs such as those displayed in Figures 10 and 11. Direct measurements of the ratio of

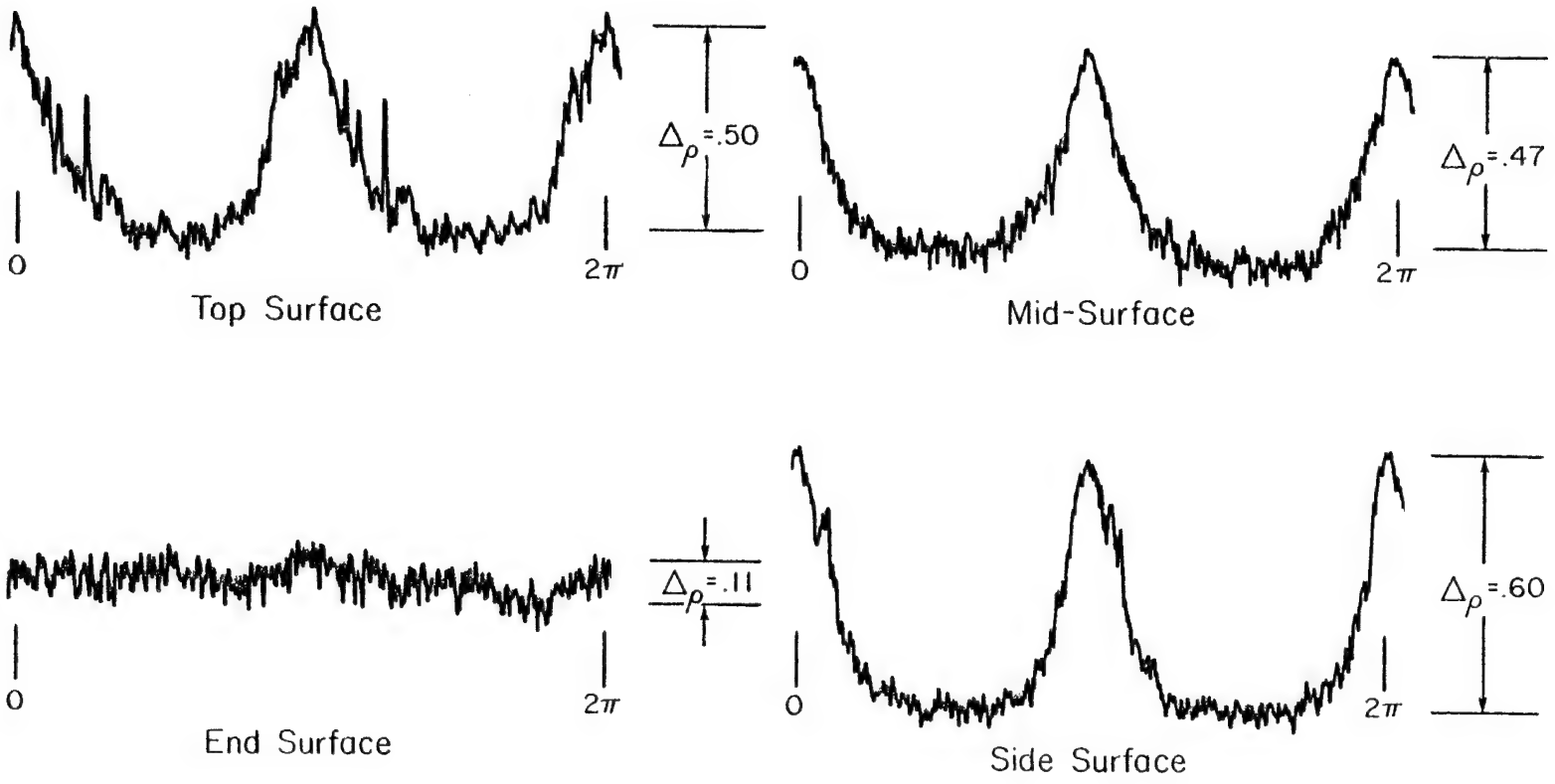

Figure 15. Optical densitometer tracings of the diffraction patterns of Figure 13 obtained from sections of a 20% (by weight) polyphenylene sulfide/graphite fiber specimen. After McGee [1982].

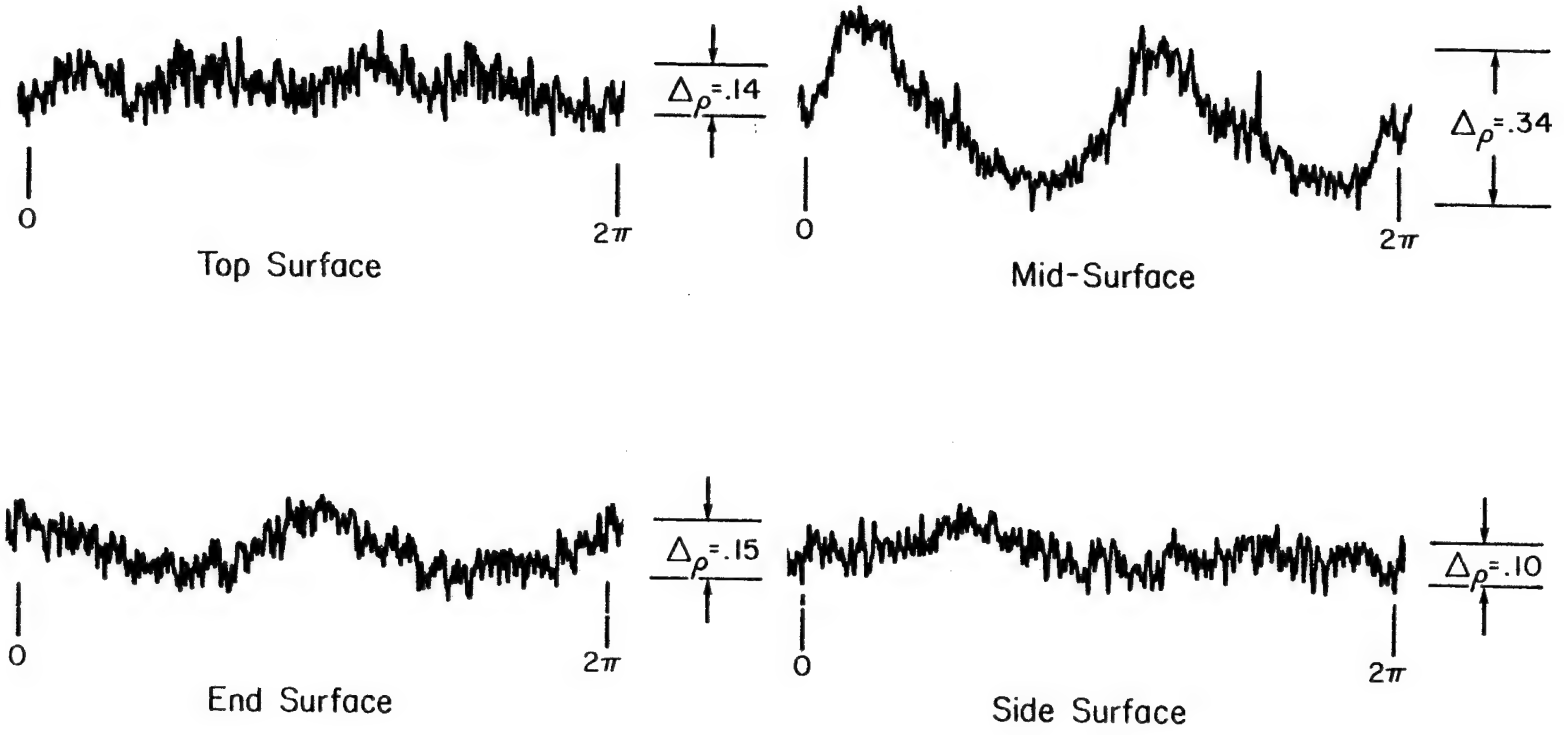

Figure 16. Optical densitometer tracings of the diffraction patterns of Figure 14 obtained from sections of a 30% (by weight) Nylon 6-10/ nickel coated graphite fiber specimen.

fiber lengths to fiber widths yield aspect ratios on the order of 20-30 for the graphite fiber/polyphenylene sulfide specimen (Figure 10) and aspect ratios on the order of 30-50 for the nickel coated graphite fiber/Nylon 6-10 specimen (Figure 11).

Alternately, information concerning the aspect ratio can be obtained from diffraction patterns such as those shown in Figures 13 and 14. Recently, McGee [1982] has reported an analysis of the radial intensity profiles of diffraction patterns that yields the average aspect ratio of the fibers. It is anticipated that future developments in the analyses of such diffraction patterns will yield quantitative information concerning aspect ratio distributions and/or particle size distributions.

COMPARISONS OF PREDICTIONS WITH EXPERIMENTAL DATA

The resort to a modeling approach requires that the suitability of the simplifying abstractions be tested by comparisons between predicted and measured properties. The relationships summarized in Tables I through III point out the necessity for conducting independent experimental characterizations to determine the crucial descriptors of the microstructure: the orientation parameters, f_p and/or f_a , and the aspect ratio. Unfortunately, such structural information is available for only a limited number of systems reported in the literature. Particulate filled systems provide the simplest system for a test of the model relationships. For these isotropic materials, the bulk properties are independent of orientation and the aspect ratio may be taken as unity. Comparison of measured and predicted properties of short-fiber reinforced systems requires estimates of the state of orientation and the aspect ratio.

Particulate Systems

Gurland [1966] reported electrical resistivities of silver particles in a phenolic resin for particulate

concentrations ranging from 10 to 50% (by volume). The silver particles were essentially of the same size. A comparison of the model predictions with Gurland's measurements is shown in Figure 17.

The model predictions are in good agreement with the resistivity-concentration profiles observed by Gurland. In particular, the sharp transition in resistivity is accurately predicted. A comparison of the data reported by Kwan et al [1980] for silver coated glass spheres in polyester showed good correspondence with predicted values. Improved agreement could be achieved by slight modifications of the values for the transport mechanism parameters (e.g., $\alpha = 0.35$, $\beta = 0.25$).

Resistivity data reported by Aharoni [1977] for iron particles in a polyimide-amide matrix could not be reconciled with the model predictions. Aharoni's results indicated a transition from insulating to conducting behavior for volume fractions in the vicinity of $v_f = 0.1$. Nicodemo et al [1978] attribute this anomalously low transition concentration to nonuniformity in the size distribution of the iron particles. These workers propose that a broad distribution of particle size enhances particle-particle contacts. Such enhanced contact probabilities would decrease the con-

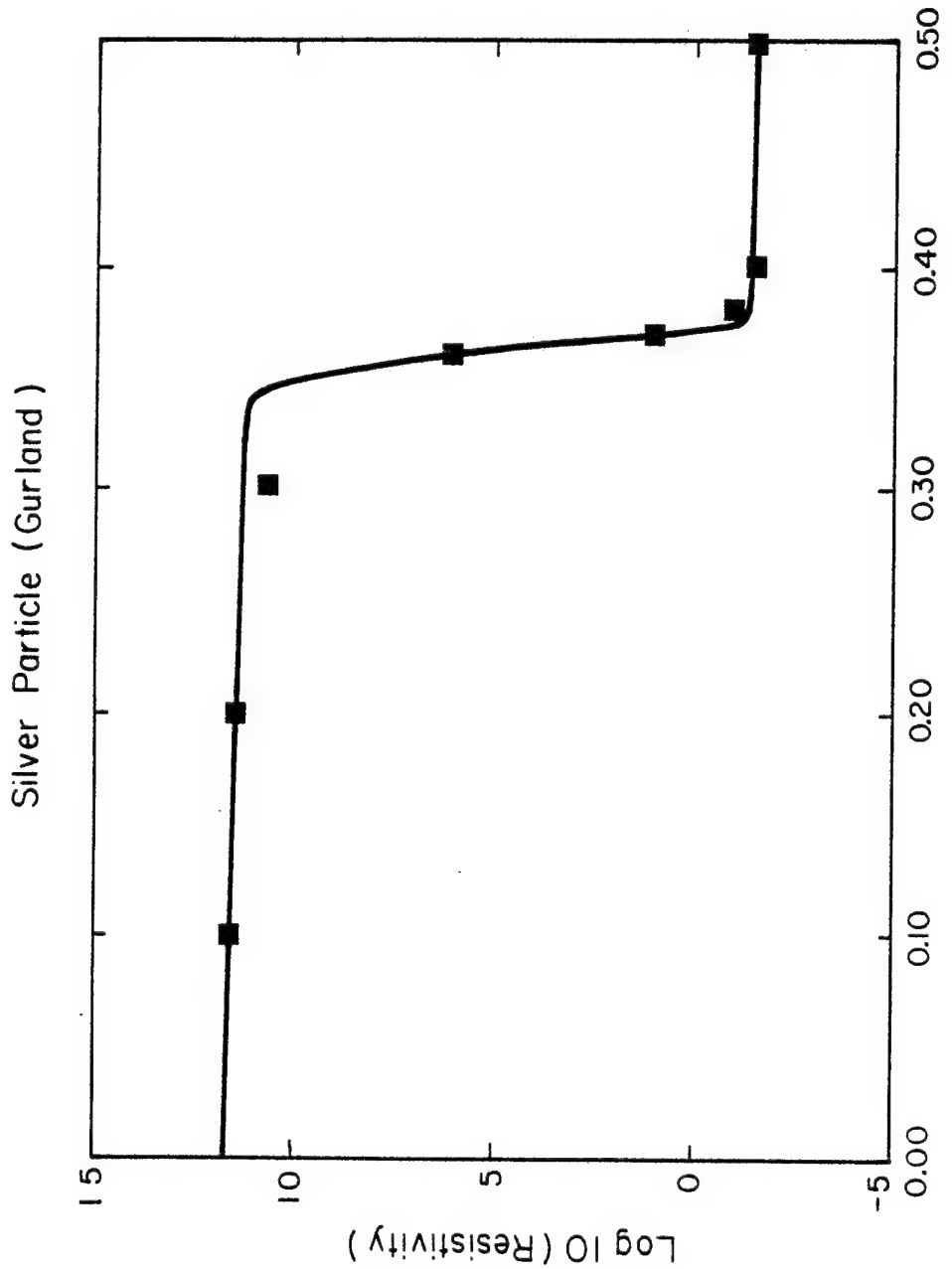

Figure 17. Comparison of model predictions with resistivity data for silver particles in a Bakelite (phenolic) matrix. Predictions are given by the solid line; resistivity data reported by Gurland [1966] is indicated by ■.

centration of particles required for chain and network formation.

Short-Fiber Systems

The influence of fiber aspect ratio on the resistivity-concentration profile is illustrated in Figure 18 for fibers in a three-dimensional random orientation. The profiles are based on silver fibers in a polypropylene matrix. This result predicts that the critical volume fraction with increasing aspect ratio is a consequence of enhanced contact between longer fibers in a random state of orientation.

The decrease in the critical concentration with increasing aspect ratio illustrated in Figure 18 is in good agreement with observations reported by Bradbury and Biggs [1980]. These workers reported limited resistivity-concentration profiles for aluminum fibers (aspect ratio 12.5 and 24) in a polypropylene matrix. The state of orientation of the fibers was not specified. If the state of fiber orientation is assumed to be three-dimensional random, good agreement is achieved between the predicted and observed conductivities.

Unpublished resistivity measurements for several short-fiber systems was provided by Trabacco [1982]. The

molded test specimens were treated by three different methods to achieve contact between the specimens and electrodes: (i) the specimens were painted with a conducting paint, (ii) the specimens were plated with a conducting metal, and (iii) the specimens were plated and dessicated.

Selected specimens were sectioned and subjected to the orientation analyses described in the previous section. These analyses revealed that the state of fiber orientation varied from specimen to specimen. This variation was attributed to processing induced variations in the microstructure. The structural variations, in turn, lead to significant data scatter between specimens. These findings implied that detailed structural analyses should be conducted on each specimen in order to assess the inherent conductivity of the candidate material system. In order to circumvent the necessity for such a detailed characterization program, an alternate data analysis was pursued that permitted the utilization of the existing data.

Inspection of the photomicrographs of Figures 10 and 11 shows that the fiber aspect ratios of these samples are on the order of 20 (or more). The predictions displayed in Figure 18 suggest that short-fiber systems with this aspect ratio are within the conducting plateau for volume fraction

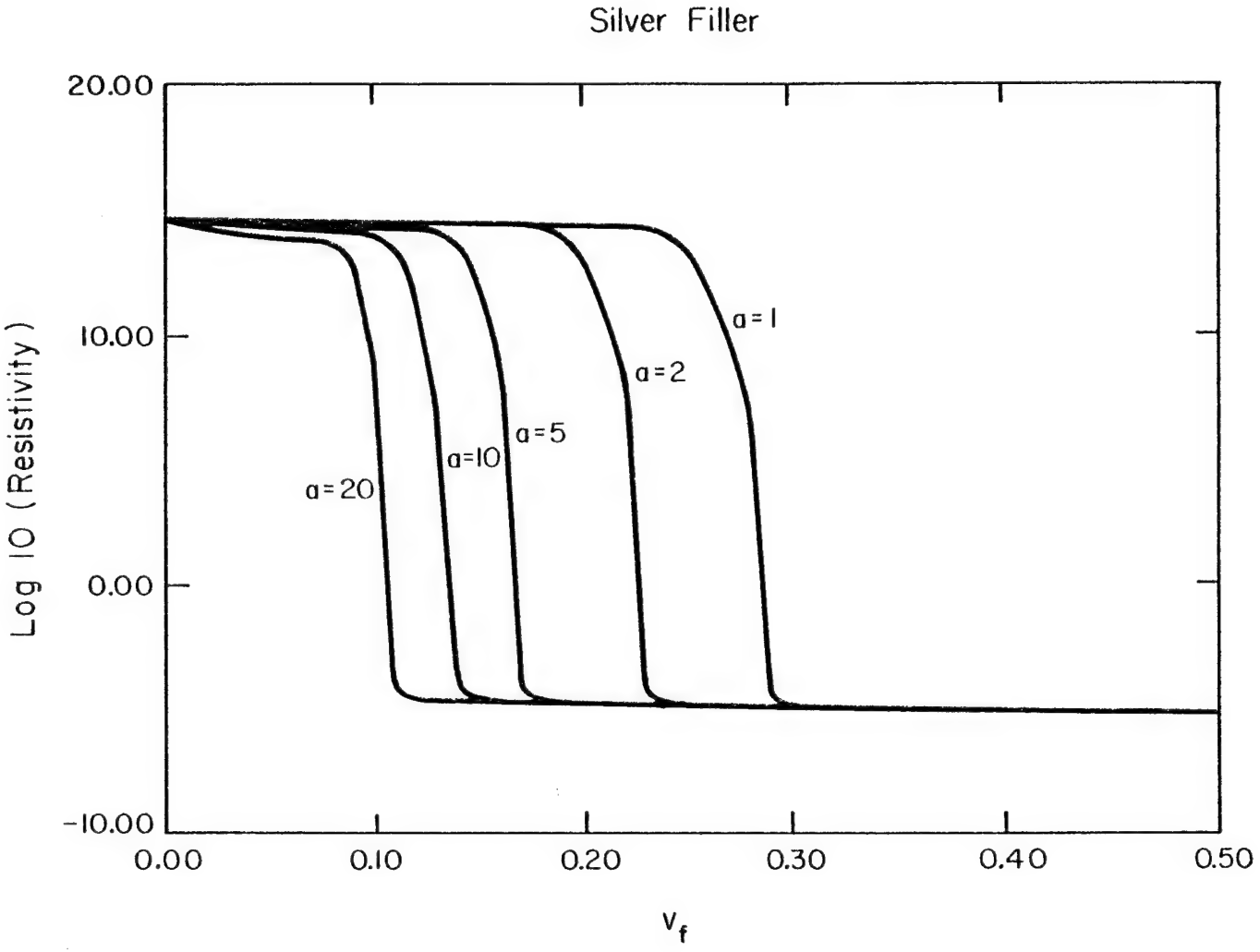

Figure 18. Influence of fiber aspect ratio on resistivity-concentration profiles. Aspect ratios ranging from particulate geometries to filament geometries are indicated by a = 1 through a = 20, respectively. The profiles are based on silver filler in a three-dimensional random state of orientation in a polypropylene matrix.

concentrations in excess of 0.1. In this regime, the behavior is dominated by the conducting filler ($K_F >> K_m$) so that the specimen conductivity can be reasonably approximated by a simplified form of Equations (4);

$$\langle K_1 \rangle = \overline{K}_F(1 + f_p)\ (1 - f_a) \tag{15a}$$

$$\langle K_2 \rangle = \overline{K}_F(1 - f_p)\ (1 - f_a) \tag{15b}$$

$$\langle K_3 \rangle = \overline{K}_F(1 + 2f_a) \tag{15c}$$

with

$$\overline{K}_F = (1/3)v_f K_F \tag{15d}$$

where K_F is the effective conductivity of chains of contacting filler and is related to the conductivity of the pure filler through Equation (11). This formulation takes into account the possibility for out-of-plane tilting of the fibers. The positive deviations of the parameter, f_a , from -0.5 serve as a measure of out-of-plane fiber tilt and, consequently, a measure of the deviation from a state of planar orientation.

These simplified relationships provide three equations with three unknown parameters -- K_F , f_p , and f_a . These parameters can be computed from the measured resistivities by the following relationships:

$$K_F = [\langle K_1 \rangle + \langle K_2 \rangle + \langle K_3 \rangle]/v_f \tag{16a}$$

$$f_p = [\langle K_1 \rangle - \langle K_2 \rangle]/[\langle K_1 \rangle + \langle K_2 \rangle] \tag{16b}$$

$$f_a = \frac{2\langle K_3 \rangle - [\langle K_1 \rangle + \langle K_2 \rangle]}{2[\langle K_1 \rangle + \langle K_2 \rangle + \langle K_3 \rangle]} \tag{16c}$$

with $\langle K_i \rangle = 1/\langle \rho_i \rangle$ where $\langle \rho_1 \rangle$, $\langle \rho_2 \rangle$, and $\langle \rho_3 \rangle$ are the measured resistivities in the longitudinal, width, and thickness directions, respectively.

The parameters computed from the data reductions of Equations (16) provide a means for isolating the inherent characteristics of each test specimen. These inherent characteristics provide a rational basis for identifying the origins of data scatter between various specimens. This analysis was applied to three candidate material systems: polyphenylene sulfide/graphite fiber; Nylon 6-10/nickel coated graphite fiber; and Nylon 6-10/steel fiber.

Polyphenylene sulfide/graphite fiber:

Resistivity data for polyphenylene sulfide filled with graphite fibers [Trabacco, 1982] are summarized in Table V and displayed in Figure 19. The display of the data in Figure 19 shows that the scatter between measurements made on similarly treated samples is essentially equivalent

TABLE V

Resistivity Data for Polyphenylene Sulfide/Graphite Fiber Composites[a]

Fiber Concentration		Resistivity, ohm-cm			
		Longitudinal	Width	Thickness	
w_f	v_f[b]	$\langle\rho_1\rangle$	$\langle\rho_2\rangle$	$\langle\rho_3\rangle$	Sample Treatment
0.20	0.09	4.469	42.69	410.2	Painted
0.20	0.09	3.879	29.66	348.8	Painted
0.20	0.09	6.983	85.38	410.2	Plated
0.20	0.09	14.32	32.77	410.2	Plated and Dried
0.20	0.09	7.890	32.06	348.8	Plated and Dried
0.20	0.09	3.963	49.93	442.5	Plated and Dried
0.30	0.24	4.099	7.108	80.54	Painted
0.30	0.24	4.212	1.738	230.8	Painted
0.30	0.24	6.251	4.764	250.0	Painted
0.30	0.24	3.861	6.461	85.01	Plated
0.30	0.24	4.061	2.336	461.6	Plated
0.30	0.24	3.977	6.566	27.48	Plated and Dried
0.30	0.24	0.664	4.116	47.99	Plated and Dried

[a]Trabacco [1982]

[b]Obtained from Figure 6

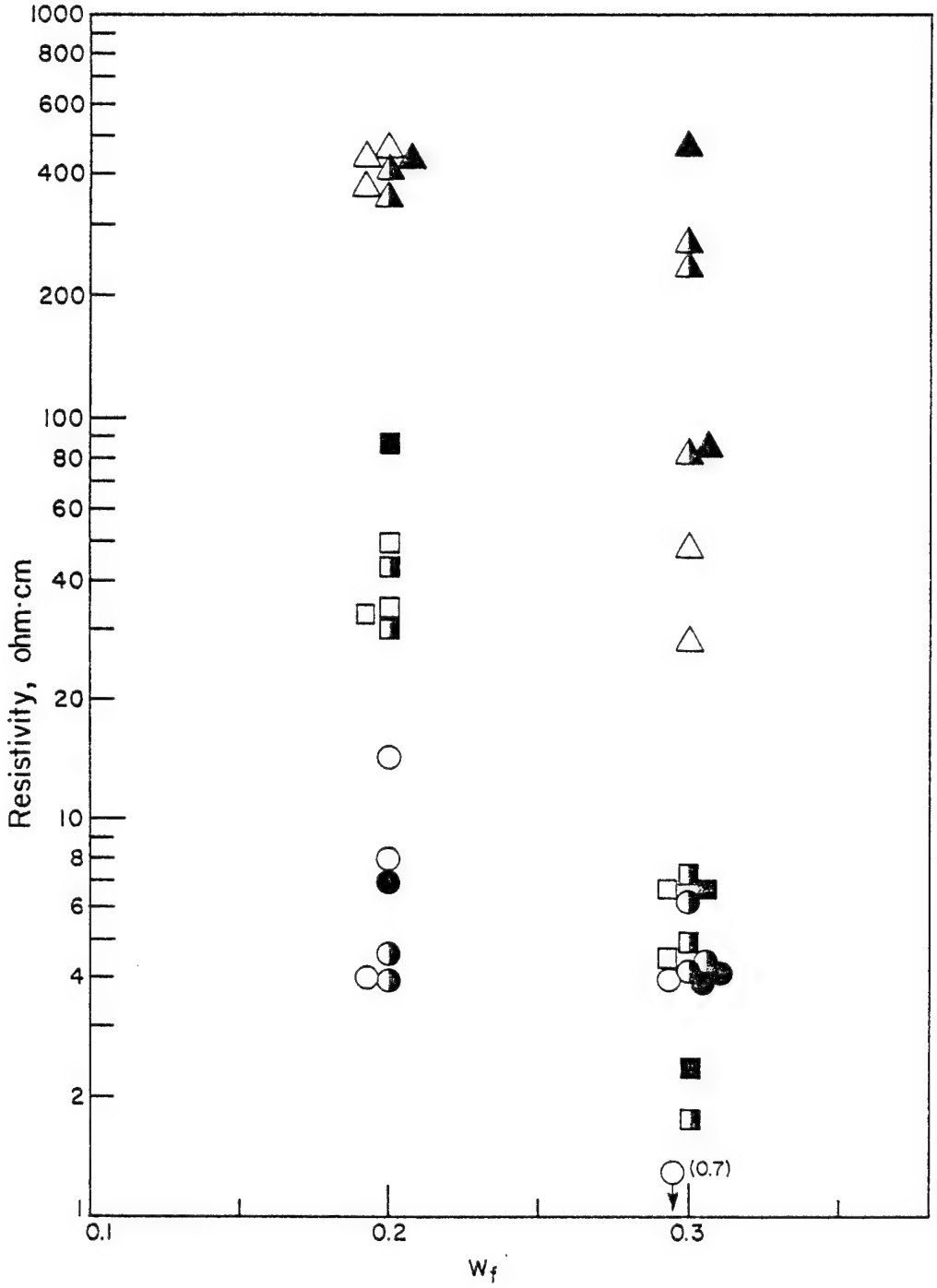

Figure 19. Resistivity data for polyphenylene sulfide/graphite fiber composites [Trabacco, 1982]. Longitudinal resistivities are given by ○ ; transverse (width) resistivities are indicated by □ ; perpendicular (thickness) resistivities are given by △ . Open symbols denote specimens plated and dessicated; closed symbols denote plated specimens; painted specimens are identified by the partial closure of the symbols.

to the variation of the measurements taken on specimens subjected to the different treatments -- (i) painted, (ii) plated, and (iii) plated and dessicated. Accordingly, the data from the various treatments may be pooled. The data display further shows the expected trend for the longitudinal, $\langle\rho_1\rangle$, and width, $\langle\rho_2\rangle$, resistivities to decrease with increasing concentation of the conducting graphite filler.

The inherent parameters computed by Equations (16) are summarized in Table VI. This data reduction shows that all specimens were essentially in a planar state of orientation since all f_a values were very near -0.5. This result is consistent with the direct orientation measurements shown in Figures 10, 13, and 15. Most of the specimens of the 20% (by weight) material tend to achieve a higher state of in-plane orientation (f_p = 0.6-0.8) than the specimens of the 30% (by weight) material. Again, these results are consistent with the direct orientation measurements illustrated in Figures 10, 13 and 15 for a specimen of the 20% (by weight) material. Most of the specimens of the 30% (by weight) material tend toward an in-plane random state of orientation (f_p = 0.2-0.4) so that the longitudinal and width resistivities are essentially equivalent. (The negative sign on some of the f_p values implies an interchange or mislabeling of the "1" and "2" indices used to identify the length and width directions.)

TABLE VI

Computed Parameters for Polyphenylene/Graphite Fiber Composites

Fiber Concentration		Resistivity, ohm-cm[a] Longitudinal	Width	Thickness	Orientation		Effective Properties	
w_f	v_f	$\langle\rho 1\rangle$	$\langle\rho 2\rangle$	$\langle\rho 3\rangle$	f_a	f_p	K_F	P_F
0.20	0.09	4.469	42.69	410.2	-0.49	0.81	2.773	0.361
0.20	0.09	3.879	29.66	348.8	-0.49	0.77	3.271	0.306
0.20	0.09	6.983	85.38	410.2	-0.48	0.85	1.748	0.572
0.20	0.09	14.32	32.77	410.2	-0.47	0.40	1.141	0.876
0.20	0.09	7.89	32.06	348.8	-0.47	0.61	1.787	0.560
0.20	0.09	3.963	49.93	442.5	-0.49	0.85	3.051	0.328
						Avg.	2.30 ±0.85	0.50 ±0.22
0.30	0.24	4.099	7.108	80.54	-0.45	0.27	1.655	0.604
0.30	0.24	4.212	1.738	230.8	-0.49	-0.42	3.405	0.294
0.30	0.24	6.251	4.764	250.0	-0.48	-0.14	1.558	0.642
0.30	0.24	3.861	6.461	85.01	-0.46	0.25	1.773	0.564
0.30	0.24	4.061	2.336	461.6	-0.49	-0.27	2.806	0.356
0.30	0.24	3.977	6.566	27.48	-0.38	0.25	1.834	0.545
0.30	0.24	0.664	4.116	47.99	-0.48	0.72	7.374	0.136
						Avg.	2.90 ±2.1	0.45 ±0.22
						Grand Avg.	2.6 ±2.1	0.47 ±0.2

[a] Trabocco [1982]

The effective chain resistivity, ρ_F, is relatively constant with an average value of 0.47 ohm-cm. This value of the effective resistivity is in good agreement with the resistivity enhancement factor ($1/\chi = 3 \times 10^2$), reported by Li et al [1982], applied to the resistivity of pure graphite fibers ($\rho_F^o = 1.5 \times 10^{-3}$ ohm-cm).

This analysis indicates that the data scatter shown in Figure 19 is a consequence of processing induced variations in the state of fiber orientation rather than measuring errors.

Nylon 6-10/nickel coated graphite fiber:

Resistivity data for Nylon 6-10 filled with nickel coated graphite fibers are summarized in Table VII [Trabacco, 1982] and displayed in Figure 20. Examinations of photomicrographs show that the thickness of the nickel coating corresponds to 10 to 20% of the fiber radius (i.e., $\lambda = 0.10\text{-}0.20$); accordingly, the volume fraction of filler may be obtained from Equations (13) or Figure 7.. The data displayed in Figure 20 shows the remarkable trend for the resistivity to increase as the concentration of the conducting filler is increased.

Data reductions obtained from the application of Equations (16) are summarized in Table VIII. This analysis

TABLE VII

Resistivity Data for Nylon 6-10/Nickel Coated Graphite Fiber Composites[a]

Fiber Concentration		Resistivity, ohm-cm			
		Longitudinal	Width	Thickness	
w_f	v_f [b]	$\langle\rho_1\rangle$	$\langle\rho_2\rangle$	$\langle\rho_3\rangle$	Sample Treatment
0.30	0.10	0.0226	0.0378	1.050	Painted
0.30	0.10	0.0233	0.0745	0.5711	Painted
0.30	0.10	0.020	0.030	1.077	Plated and Dried
0.30	0.10	0.020	0.034	25.61	Plated and Dried
0.30	0.10	0.019	0.033	5.035	Plated and Dried
0.40	0.15	0.0492	0.4328	4.272	Painted
0.40	0.15	0.1165	0.6202	3.049	Painted
0.40	0.15	0.0245	0.3606	1.436	Plated
0.40	0.15	0.0367	0.3101	0.865	Plated
0.40	0.15	0.045	0.290	1.175	Plated and Dried

[a]Trabacco [1982]

[b]Obtained from Figure 7 with $\lambda = 0.10 - 0.20$

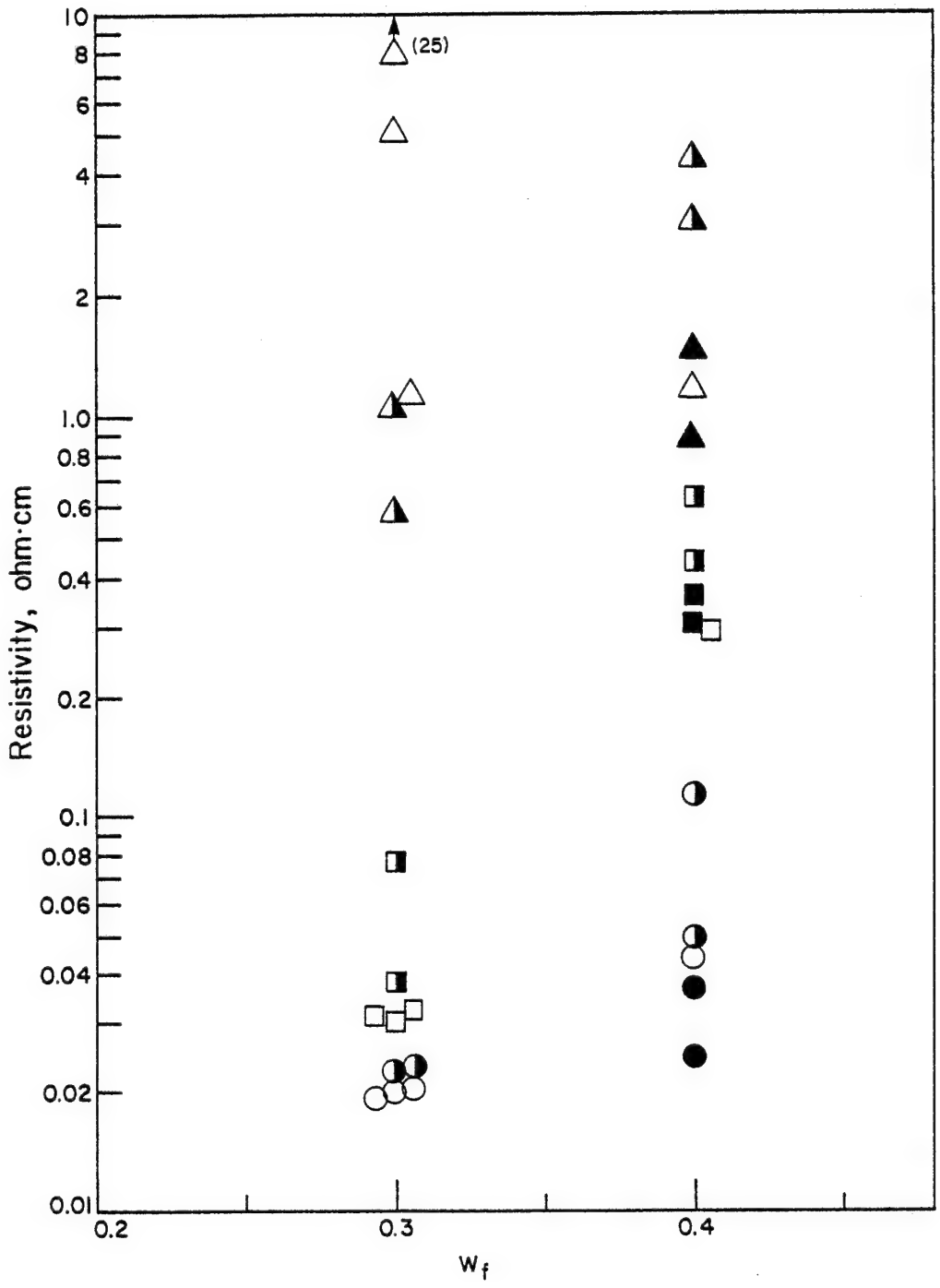

Figure 20. Resistivity data for Nylon 6-10/nickel coated graphite fiber composites [Trabacco, 1982]. Longitudinal resistivities are given by O ; transverse (width) resistivities are indicated by □ ; perpendicular (thickness) resistivities are given by Δ . Open symbols denote specimens plated and dessicated; closed symbols denote plated specimens; painted specimens are identified by the partial closure of the symbols.

TABLE VIII

Computed Parameters for Nickel Coated Graphite Fiber/Nylon 6-10

Fiber Concentration		Resistivity, ohm-cm[a] Longitudinal	Width	Thickness	Orientation		Effective Properties	
w_f	v_f [b]	$\langle\rho_1\rangle$	$\langle\rho_2\rangle$	$\langle\rho_3\rangle$	f_a	f_p	K_F (10^3)	P_F (10^{-4})
0.3	0.10	0.0226	0.0378	1.050	-0.48	0.25	2.15	4.7
0.3	0.10	0.0233	0.0745	0.5711	-0.46	0.52	1.74	5.7
0.3	0.10	0.020	0.030	1.077	-0.48	0.20	2.53	4.0
0.3	0.10	0.020	0.034	25.61	-0.49	0.26	2.39	4.2
0.3	0.10	0.011	0.033	5.035	-0.49	0.27	2.50	4.0
						Avg.	2.26 ± .33	4.8 ±1.44
0.4	0.15	0.0492	0.4328	4.272	-0.48	0.80	0.46	21.9
0.4	0.15	0.1165	0.6202	3.049	-0.45	0.68	0.21	47.5
0.4	0.15	0.0245	0.3606	1.436	-0.48	0.89	0.87	11.3
0.4	0.15	0.0367	0.3101	0.865	-0.45	0.79	0.63	15.8
0.4	0.15	0.045	0.290	1.175	-0.45	0.73	0.53	18.9
						Avg.	0.54 ±0.25	23 ±14

[a] Trabocco [1982]

[b] Obtained from Figure 7 with $\lambda = 0.10 - 0.20$

again shows that all the specimens of the Nylon 6-10/nickel coated graphite fiber materials were in a planar state of orientation since $f_a = -0.5$. This result is consistent with the direct orientation measurements shown in Figures 11, 14 and 16. In contrast to the polyphenylene/graphite fiber material, the lower concentrations (30% by weight, 10% by volume) of the Nylon 6-10/nickel coated graphite fiber materials tended toward a random in-plane orientation ($f_p \cong 0.3$) while the higher concentration specimens (40% by weight; 15% by volume) exhibited a higher degree of in-plane alignment ($f_p = 0.7\text{-}0.8$). Again, these results are consistent with the direct orientation measurements shown in Figures 11, 14, and 16 for a 30% (by weight) specimen.

The effective resistivity of the 30% (by weight) material was essentially constant at 5×10^{-4} ohm-cm. Consistent with the trends of Figure 20, the average effective resistivity of the 40% (by weight) material increased to 25×10^{-4}. This five-fold increase in effective resistivity is due to degradation of the metal coating. A typical photomicrograph of a 40% (by weight) specimen is shown in Figure 21 [Shaffer, 1982]. The fibers were exposed by disolving the Nylon matrix with phenol. This photomicrograph shows that the metal coatings have undergone dedradation. Evidently, sufficient fiber-fiber abrasion occurs at

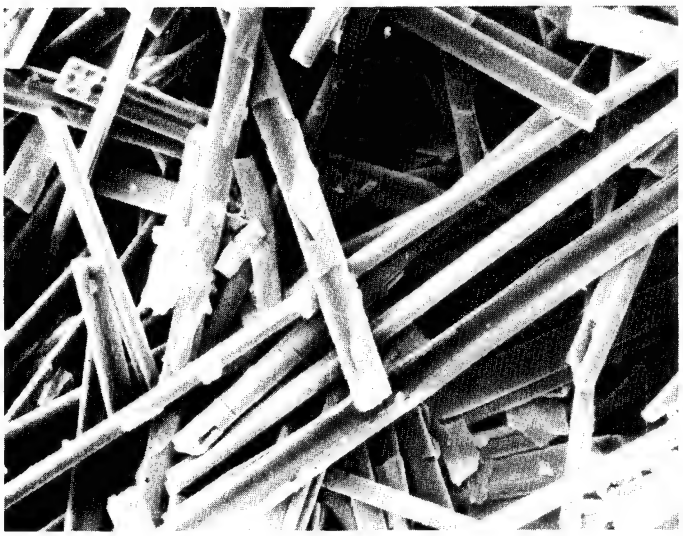

500x

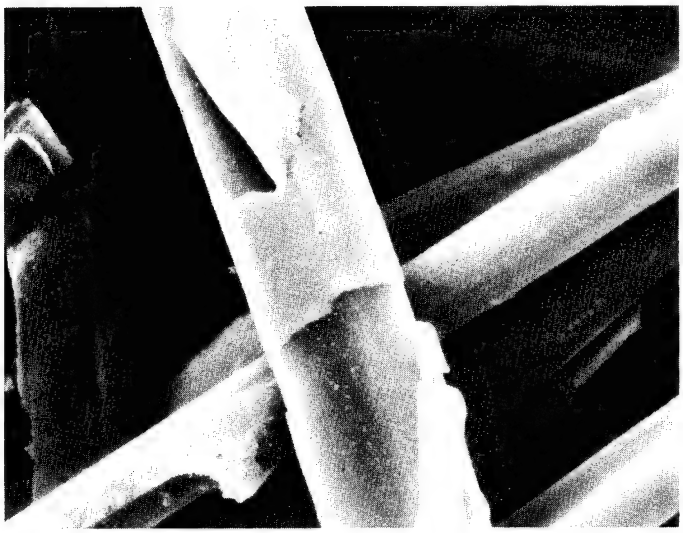

2000x

Figure 21. Scanning electron micrograph of a 40% (by weight) specimen of nickel coated graphite fibers from a Nylon 6-10 matrix at 2000x [Shaffer, 1982]. The Nylon 6-10 matrix was removed with phenol.

these higher volume fraction loadings to damage the fragile metal coatings.

This observation of fiber damage at the higher concentrations coupled with the fact that a 10% increase in weight fraction yields only a 5% increase in volume fraction (see Table VII) strongly suggests that conducting composites comprised of metal coated fibers should be restricted to relatively low concentrations of the coated fibers.

Nylon 6-10/steel fiber:

Resistivity data for Nylon 6-10 filled with stainless steel fibers [Trabacco, 1982] is summarized in Table IX. These specimens correspond to a volume fraction fiber of 0.01. The data reductions obtained through the application of Equations (16) are also summarized in Table IX. As was the case for the preceding specimens, the Nylon 6-10/steel fiber material was in a state of planar orientation with $f_a = -0.49$. This material exhibited a tendency to achieve a moderate state of in-plane orientation with $f_p = 0.4\text{-}0.6$. The effective resistivity was 0.8×10^{-3}. This value is consistent with the standard reduction factor ($1/\chi = 10^{-3}$) applied to the resistivity of steel listed in Table IV.

These results suggest that the long sturdy steel filaments withstood processing degradations to yield

TABLE IX

Computed Parameters for Steel/Nylon 6-10

$w_f = 0.07$

$w_f = 0.01$[a]

Resistivity, ohm-cm[b]

Longitudinal	Width	Thickness	Orientation		Effective Properties	
$\langle\rho_1\rangle$	$\langle\rho_2\rangle$	$\langle\rho_3\rangle$	f_a	f_p	K_F (10^3)	P_F (10^{-3})
0.2857	1.250	41.67	-0.49	0.63	1.297	0.77
0.3466	0.8734	37.67	-0.49	0.43	1.217	0.82

[a]Computed from Figure 6

[b]Trabacco [1982], painted specimens

respectable conductivity ($\langle\rho_1\rangle = 0.3$) at very low volume fractions ($v_F = 0.01$).

Summary

These comparisons of the model predictions with experimental observations on particulate and short-fiber systems shown that the model formulation provides a rational basis for explaining the behavior of conducting composites. The agreement between predicted and measured values lends support to the use of the model relations as a screening tool for selecting candidate materials. Furthermore, the consistency of the computed orientation parameters with direct orientation measurements lends confidence to the use of the modeling relationships to explore the influence of processing induced changes in the state of orientation and aspect ratio on achievable conductivities.

The analyses of the various short-fiber systems emphasizes the important role that processing induced variations in the microstructure play in establishing bulk conductivity. The dependence of bulk conductivity on processing induced variants of the microstructure points out the futility of attempting to compare properties of specimens of unknown microstructure and underscores the

importance of conducting structural characterizations in conjunction with traditional testing programs.

CONCLUSION

The incorporation of the concept of chain and network formation of contacting conductors into a model for electrical transport provides a rational basis for explaining sharp transitions from insulating to conducting behavior in composite materials. An important feature of the resulting model is the indentification of quantitative structural parameters associated with the state of orientation (f_p and/or f_a) and filler shape as specified by the aspect ratio (particulate: $a = 1$; platelet: $a < 1$; fiber: $a > 1$). The incorporation of these important structural features necessarily introduced computational complexitites into the model relationship. An interactive computer program is described in the appendix to facilitate the use of the model relationships as a screening tool for the selection of candidate material systems.

For the important special case of relatively long ($a > 20$) highly conducting ($K_F >> K_m$) fibers at volume fraction concentrations greater than $v_f = .1$, the bulk conductivity can be approximated by the following simplified form of Equations (4):

$$\text{Longitudinal:} \quad \langle K_1 \rangle = (1/3)v_f \chi K_F^o (1 + f_p)(1 - f_a)$$

$$\text{Width:} \quad \langle K_2 \rangle = (1/3)v_f \chi K_F^o (1 - f_p)(1 - f_a)$$

$$\text{Thickness:} \quad \langle K_3 \rangle = (1/3)v_f \chi K_F^o (1 + 2f_a)$$

where K_F^o is the conductivity of the fiber component. The volume fraction concentration, v_f, can be obtained from specified weight fractions, w_f, by Equation (12) or by the calibration curves displayed in Figure 6. The orientation parameters, f_a and f_p, describe the state of orientation of the fibers. Values of f_a in the vicinity of -1/2 indicate that the fibers are in a planar state of orientation with the fibers confined to the 1-2 plane. The parameter, f_p, specifies the extent of orientation within the 1-2 plane. Values of f_p in the vicinity of 1 indicate fiber alignment along the longitudinal ("1") axis; values of f_p near 0 indicate a planar random material. Three-dimensional random fiber distributions are obtained with $f_a = f_p = 0$. The reduction factor, χ, accounts for contact irregularities associated with surface roughness and/or surface coatings and appears to be a constant on the order of $1 - 3 \times 10^{-3}$. The bulk resistivity is obtained as the reciprocal of the conductivity; viz., $\langle \rho_i \rangle = 1/\langle K_i \rangle$ for $i = 1,2,3$.

The satisfactory correlations obtained between predicted and measured resistivities lends confidence to the

application of the model relationships as a screening tool for identifying candidate material systems. The rationalization of data scatter in terms of variations in the state of filler orientation emphasizes the role of microstructure in establishing transport properties. The dependence of the bulk conductivity on microstructural variations induced by fabrication procedures points out the futility of attempting to compare properties of unknown microstructure. This important conclusion underscores the necessity of conducting structural characterizations in conjunction with traditional testing procedures for mechanical and transport properties. The diffraction techniques developed by McGee and McCullough [1982] can be used to obtain the required structural characterizations.

RECOMMENDATIONS

The current model appears to have captured the major features associated with electrical transport in composite materials. Consequently, the model can serve as a preliminary screening tool for candidate materials systems. The relative succcess of these initial attempts to incorporate structural parameters into relationships to predict transport properties suggests the need for more rigorous treatments to extend the model for application to design considerations. Particular attention should be given to developing improved relationships to account for the influence of processing induced variations in microstructure on the transport properties of composite materials.

The contact probability relationships used for uniform spherical filler geometries adequately predict the critical concentrations associated with the insulator-conductor transitions. These relationships should be extended to account for the influence of particle size distributions on the critical concentrations. Literature data suggests that the critical concentrations required to achieve conducting behavior can be significantly reduced with the use of broad distributions of particle size.

Although the approximations used to estimate the concentration dependence of the contact probabilities for fibers and platelets appear to capture the significant trends, the treatment is an oversimplification. Additional work is required to establish precise relationships for this important structural feature of fiber and platelet filler geometries. Particular attention should be devoted to incorporating orientation effects into the expressions for contact probabilities.

The empirical reduction factor, χ , used to estimate the effective network conductance in terms of the filler conductivity represents a significant reduction in achievable conductivities. A study leading to the specification of the factors associated with this reduction could provide insight into surface and/or geometric conditions which could promote higher levels of conductance.

Added confidence in the model predictions could be achieved through comparisons of predictions with an extended data base. In particular, resistivity data for platelet filled and multiple component systems (e.g., two or more types of filler) were not available for test comparisons with model predictions. Consequently, the predictions obtained on such systems must be viewed with some

reservation. It is imperative that structural characterizations be conducted in concert with electrical and mechanical testing programs aimed at establishing an extended data base. The diffraction technique developed by McGee and McCullough [1982] provides a method for the characterization of the state of orientation and the in situ aspect ratio of the filler. In addition, this structural characterization technique can be utilized to correlate processing conditions to the level of conduction through the quantitative determination of these processing sensitive structural parameters. It is reasonable to anticipate that the relationship of processing conditions to material behavior can be established by linking these structure dependent models with analyses designed to trace the development of microstructure with variations in processing conditions.

REFERENCES

1. ADINAT - A Finite Element Program for Automatic Dynamic Incremental Nonlinear Analysis of Temperatures, published by ADINA Engineering, Inc., Watertown, MA, Report AE 81-2 (1981).

2. S. M. Aharoni, J. Appl. Phys., 43, 2463 (1972).

3. J. E. Ashton, J. C. Halpin and P. H. Pettit, Primer on Composite Materials, Technomic Publishing Co. (1969).

4. E. J. Bradbury and D. M. Bigg, American Society of Mechanical Engineers, ASME paper no. 80-DE-4 (1980).

5. L. N. Codemo, L. Nicolais, G. Romeo, and E. Scaford, Polym. Eng. and Sci., 18, 293 (1978).

6. D. E. Davenport, "Metalloplastics: An Answer to Electromagnetic Pollution," Polym. Plast. Technol. Eng., 17 (2), 211 (1981).

7. J. Gurland, Trans. Metall. Soc., AIME, 235, 642 (May 1966).

8. D. K. Hale, J. Materials Sci., 11, 2105 (1976).

9. Z. Hashin, in Mechanics of Composite Materials, Eds.: F. W. Wendt, H. Liebowitz, N. Perrone, Pergamon, 201-242 (1970).

10. G. J. Jarzebski, S. H. McGee and R. L. McCullough, "Constitutive Relationships for Sheet Molding Compounds," published in Proceedings of U.S.A.-Italy Joint Symposium on Composite Materials: The Role of the Polymeric Matrix on Their Processing and Structural Properties, June 15-19, 1981, Capri, Italy. Plenum Publishing Corp., New York.

11. E. H. Kerner, Proc. Phys. Soc. B., 69, 808 (1956).

12. S. H. Kwan, F. G. Shin, and W. L. Tsui, J. Materials Sci., 15, 2978 (1980).

13. T. B. Lewis and L. E. Nielsen, J. Appl. Polym. Sci., 14, 1449 (1970).

14. P. Li, W. Streider, and T. Joy, J. Composite Materials, 16, 53 (1982).

15. A. Malliaris and D. T. Turner, J. Appl. Phys., 42, 614 (1971).

16. J. C. Maxwell, A Treatise on Electricity and Magnetism, Vol. I (3rd Edn.), Clarendon Press, Oxford, 440 (1892).

17. R. L. McCullough, Concepts of Fiber-Resin Composites, Marcel Dekker, Inc., New York (1971).

18. R. L. McCullough and J. M. Peterson, "Property Optimization Analysis for Multicomponent (Hybrid) Composites," Chapter 6, Developments in Composite Materials, G. S. Holister, Ed., Applied Science Publishers (1977).

19. S. H. McGee, The Influence of Microstructure on the Elastic Properties of Composite Materials, Ph.D. Dissertation, Dept. of Chemical Engineering, University of Delaware, Newark, DE 19711 (1982).

20. S. H. McGee and R. L. McCullough, "An Optical Technique for Measuring Fiber Orientation in Short Fiber Composites," published in Proceedings of U.S.A.-Italy Joint Symposium on Composite Materials: The Role of the Polymeric Matrix on Their Processing and Structural Properties, June 15-19, 1981, Capri, Italy. Plenum Publishing Corp., New York.

21. S. H. McGee and R. L. McCullough, "Combining Rules for Predicting the Thermoelastic Properties of Particulate Filled Polymers, Polyblends and Foams," Polymer Composites, 2, 149 (1981).

22. L. E. Nielsen, Ind. Eng. Chem. Fund., 13, 17 (1974).

23. S. Nomura and T. Chou, J. Composite Materials, 14, 120 (1980).

24. R. C. Progelhof, J. L. Throne, and R. R. Ruetsch, Polym. Eng. and Sci., 16 (9), 615 (1976).

25. J. J. Quigley, "Computer-Aided Design of Composite Systems," published in Proceedings of 37th Annual

Conference, Reinforced Plastics/Composites Institute, The Society of the Plastics Industry, Inc., January 11-15, 1982, Washington, D.C.

26. J. N. Rayleigh, Phil. Mag., 34, 481 (1892).

27. I. Shaffer, unpublished results, Naval Air Development Center, Warminster, PA (1982).

28. M. Suzuki, K. Makino, M. Yamada, and K. Linoya, International Chemical Eng., 21 (3), 482 (1981).

29. R. A. Trabacco, unpublished data, Naval Air Development Center, Warminster, PA (1982).

30. C. T. D. Wu and R. L. McCullough, "Constitutive Relationships for Heterogeneous Materials," Chapter 7, Developments in Composite Materials, G. S. Holister, Ed., Applied Science Publishers (1977).

APPENDIX A

USER'S MANUAL FOR MICROMECHANICAL MODELS:

COMPOSITE MATERIALS

ELECTRICAL AND THERMAL

RESISTIVITY AND CONDUCTIVITY

The following user's guide is written to illustrate the operational aspects of the computer program which contains the theoretical models for the prediction of the electrical properties of composite materials. The program is written in ANSI standard FORTRAN-4 with the ability to accept data as free field input. This option allows input to the program to occur anywhere on the input field without reference to column position. A computer graphics capability is implemented in the program for the convenient display of material properties. The graphics FORTRAN call statements are standard CALCOMP® statements and may be implemented for interactive graphics terminals or remote graphics output devices.

Two example executions of the computer program are presented. To indicate the expected input and the programmed flexibilities inherent in the code, detailed descriptions written in italics follow each interaction of the first example. The user input is indicated with an arrow, "→" .

For the first example, we assume a two phase system and calculate the electrical properties for a range of fiber volume fractions. The program execution is given as follows.

```
→run navy/maincd
 #RUNNING 1781
```

The above expression is the expected command for a Burroughs B7700 mainframe. Please respond with an appropriate command for each individual system.

```
 CENTER FOR COMPOSITE MATERIALS
 COMPUTER SOFTWARE SYSTEMS

 MICROMECHANICAL MODEL FOR CALCULATING:
 COMPOSITE MATERIAL ELECTRICAL AND THERMAL
 RESISTIVITIES AND CONDUCTIVITIES

 VERSION: 051182
```

The program responds with the above heading, which indicates the type of transport properties it will calculate and its version number. The version number indicates that this copy of the program was compiled on May 11, 1982.

```
  ENTER> CALCULATION OPTION
         (1) CALCULATE ELECTRICAL PROPERTIES
         (2) CALCULATE THERMAL PROPERTIES
→1
```

The program includes the abilities to calculate material properties for electrical and thermal transport phenomenon. The user selects from the menu and responds. If a number that is not contained in the menu is entered, the above menu list is redisplayed. This is the case for all menu input for this program. The actual transport phenomenon modeled adjusts the calibration constants α *and* β .

```
  ENTER> INPUT OPTION
         (1) INPUT RESISTIVITY DATA
         (2) INPUT CONDUCTIVITY DATA
→1
```

For either case of electrical or thermal transport properties, the program will allow input of either resistivity or conductivity constants.

```
→NO  DO YOU WISH TO INCLUDE A FILLER PHASE?
```

The user responds with either "NO" (or carriage return) or "YES" (or "Y"). When a filler phase is requested, the program constructs a surrogate matrix of resin and filler. At present, the aspect ratio of the filler phase is assumed to be unity.

```
  TWO PHASE SYSTEM ASSUMED: RESIN/FILLER

  ENTER> RESIN RESISTIVITY
→4.5E16

  ENTER> FIBER RESISTIVITIES
         (LONGITUDINAL,TRANSVERSE)
→1.5E-3,1.5E-3
```

The user is prompted to enter the isotropic resin resistivities and orthotropic fiber resistivities. The longitudinal direction corresponds to the axial direction of the fiber, and the transverse corresponds to any direction perpendicular to the fiber axis.

```
  ENTER> FIBER VOLUME FRACTIONS TO SCAN
         START VALUE, END VALUE, INCREMENT
→0.0,1.0,0.1
```

Only for the case of two phase composites will this be displayed. This allows the user to observe the variance of material properties as the amount of fiber loading is varied. For the case of a three phase composite, this report is not given. The user may select one set of values for resin, filler and fiber volume fraction.

```
  ENTER> ASPECT RATIO OF FIBERS
→20.
```

The aspect ratio is defined as the length to diameter ratio of the fiber. For aspect ratios approaching 10^6 the fiber system resembles continuous fiber composites. Aspect ratio equal to one indicates spheres. The significance of aspect ratios less than one controls the program to model platelets. The primary direction of a fiber with aspect ratio greater than one will be the "1"-axis direction. For a platelet phase case, the perpendicular normal to the platelet surface will correspond with the "1" axis direction.

```
  ENTER> TYPE OF AVERAGING
         (1) IN-PLANE: TWO-DIMENSIONAL
         (2) AXIAL SYMMETRIC: THREE-DIMENSIONAL
→1
```

The fibers for the in-plane averaging will remain in the "1-2" plane of the micro-laminate system.

ENTER> HERMANS ORIENTATION PARAMETER
→.4

For the planar type of averaging, the variance of the degree of alignment is controlled by the Herman's orientation parameter with a range of zero to one. The case of "perfectly random" is represented by zero and "perfectly aligned" is represented by one. Most engineering materials will have a value between these ideal numbers.

DEFAULT ELECTRICAL CALIBRATION PARAMETERS

<DATA CHECK>
CALIBRATION PARAMETERS
ALPHA = 0.4100
BETA = 0.2900

→NO DO YOU WISH TO CHANGE THESE VALUES?

These calibration parameters whould not need to be changed. If it is necessary, the program will prompt the user by responding with "YES" (or "Y").

→YES DO YOU WISH A TABLE OF DATA?

→NO DO YOU WISH A COMPUTER PLOT?

These questions allow the user to control the flow of output.

ELECTRICAL
RESISTIVITIES OF COMPOSITE MATERIAL : PLANAR CASE

VF	F	K11	K22	K33
0.1000	0.4000	3.2451E+15	6.7675E+15	3.6401E+16
0.2000	0.4000	1.0714E-02	2.5000E-02	2.8800E+16
0.3000	0.4000	7.1429E-03	1.6667E-02	2.2050E+16
0.4000	0.4000	5.3571E-03	1.2500E-02	1.6200E+16
0.5000	0.4000	4.2857E-03	1.0000E-02	1.1250E+16
0.6000	0.4000	3.5714E-03	8.3333E-02	7.2000E+15
0.7000	0.4000	3.0612E-03	7.1429E-03	4.0500E+15
0.8000	0.4000	2.6786E-03	6.2500E-03	1.8000E+15
0.9000	0.4000	2.3810E-03	5.5556E-03	4.5000E+14
1.0000	0.4000	1.5000E-03	1.5001E-03	1.5001E-03

The electrical resistivities of the composite material are presented in tabular form. The "VF" column signifies the fiber volume fraction of the fiber phase. The "F" is the Herman's orientation parameter which indicates the degress of randomness

in the composite. The "K_{11}", "K_{22}" and "K_{33}" quantities represent the electrical resistivities for the longitudinal, transverse and perpendicular directions, respectively.

```
 ENTER> REPEAT OPTION
        (1) REPEAT SAME PLOT
        (2) ENTER NEW MATERIAL GEOMETRY
        (3) START OVER
        (4) END PROGRAM
```

The user may direct the flow of the program for additional calculations or to end the program execution.

The second example illustrates the calculation of electrical resistivity for an axially symmetric composite. The constitutive properties are assumed to be identical to the properties in the first example. The program execution is given as follows.

```
→run navy/maincd
 #RUNNING 1809

 CENTER FOR COMPOSITE MATERIALS
 COMPUTER SOFTWARE SYSTEMS

 MICROMECHANICAL MODEL FOR CALCULATING:
 COMPOSITE MATERIAL ELECTRICAL AND THERMAL
 RESISTIVITIES AND CONDUCTIVITIES

 VERSION: 051182

  ENTER> CALCULATION OPTION
         (1) CALCULATE ELECTRICAL PROPERTIES
         (2) CALCULATE THERMAL PROPERTIES
→1

  ENTER> INPUT OPTION
         (1) INPUT RESISTIVITY DATA
         (2) INPUT CONDUCTIVITY DATA
→1
```

```
→NO  DO YOU WISH TO INCLUDE A FILLER PHASE?

  TWO PHASE SYSTEM ASSUMED: RESIN/FILLER

  ENTER> RESIN RESISTIVITY
→4.5E16

  ENTER> FIBER RESISTIVITIES
         (LONGITUDINAL,TRANSVERSE)
→1.5E-3,1.5E-3

  ENTER> FIBER VOLUME FRACTIONS TO SCAN
         START VALUE, END VALUE, INCREMENT
→0.0,1.0,0.1

  ENTER> ASPECT RATIO OF FIBERS
→20.

  ENTER> TYPE OF AVERAGING
         (1) IN-PLANE; TWO-DIMENSIONAL
         (2) AXIAL SYMMETRIC; THREE-DIMENSIONAL
→2
```

The user has selected the type of averaging for an axially symmetric composite. The following calculations indicate this type of approximation.

```
  ENTER> HERMANS ORIENTATION PARAMETER
→0.4
```

The interpretation of the Herman's orientation parameter is different for the axially symmetric case than for the planar case. The Herman's orientation parameter may vary from -0.5 to 1.0. The value of 1.0 indicates a perfectly aligned composite. A three-dimensional random composite is modeled with a 0.0 value and a transversely isotropic composite with a -0.5 value.

```
 DEFAULT ELECTRICAL CALIBRATION PARAMETERS

 <DATA CHECK>
 CALIBRATION PARAMETERS
     ALPHA =   0.4100
     BETA  =   0.2900

→NO  DO YOU WISH TO CHANGE THESE VALUES?

→YES DO YOU WISH A TABLE OF DATA?

→NO  DO YOU WISH A COMPUTER PLOT?
```

ELECTRICAL
RESISTIVITIES OF COMPOSITE MATERIAL : AXIAL CASE

VF	F	K11	K22	K33
0.1000	0.4000	3.7305E+15	9.2879E+15	9.2879E+15
0.2000	0.4000	1.2500E-02	3.7500E-02	3.7500E-02
0.3000	0.4000	8.3333E-03	2.5000E-02	2.5000E-02
0.4000	0.4000	6.2500E-03	1.8750E-02	1.8750E-02
0.5000	0.4000	5.0000E-03	1.5000E-02	1.5000E-02
0.6000	0.4000	4.1667E-03	1.2500E-02	1.2500E-02
0.7000	0.4000	3.5714E-03	1.0714E-02	1.0714E-02
0.8000	0.4000	3.1250E-03	9.3750E-03	9.3750E-03
0.9000	0.4000	2.7778E-03	8.3333E-03	8.3333E-03
1.0000	0.4000	1.5001E-03	1.5001E-03	1.5001E-03

The tabular data presented represents an axially symmetric composite. Note that the K_{22} and K_{33} electrical resistivities are equivalent for this material geometry.

```
ENTER> REPEAT OPTION
       (1) REPEAT SAME PLOT
       (2) ENTER NEW MATERIAL GEOMETRY
       (3) START OVER
       (4) END PROGRAM
```

The user may direct the flow of the program for additional calculations or to end the program execution.

APPENDIX B

SAMPLE EXECUTIONS OF MICROMECHANICS MODELLING FOR ELECTRICAL RESISTIVITY

CONTENTS

1) Graphite Fibers and PPS Resin

	Fiber	Resin
Resistivity (ohm-cm)	1.5×10^{-3}	4.5×10^{16}
Volume Fraction	0.20	0.80
Aspect Ratio	50	
Orientation Parameter, f_p , (planar)	0.5	

Electrical Resistivities

$K_1 = 1.00 \times 10^{-2}$

$K_2 = 3.00 \times 10^{-2}$

$K_3 = 2.88 \times 10^{16}$

The sample execution follows in Table 1. Another execution is given in Table 2 for a scan over volume fractions of the fiber. Sample computer plots are given in Figures 1, 2, and 3 for K_1 , K_2 , and K_3 , respectively.

Note: The reduction factor, χ , has been taken as unity. The influence of geometrical irregularities under surface coatings may be taken into account by replacing the fiber resistivity by 0.45 ohm-cm [= (1.5x10-3) x (3x102)].

Table 1.
Sample Execution of Micromechanics
Model for Graphite fibers and PPS Resin.

```
 CENTER FOR COMPOSITE MATERIALS
 COMPUTER SOFTWARE SYSTEMS

 MICROMECHANICAL MODEL FOR CALCULATING:
 COMPOSITE MATERIAL ELECTICAL AND THERMAL
 RESISTIVITIES AND CONDUCTIVITES

 VERSION: 051182


  ENTER> CALCULATION OPTION
         (1) CALCULATE ELECTRICAL PROPERTIES
         (2) CALCULATE THERMAL PROPERTIES
1

  ENTER> INPUT OPTION
         (1) INPUT RESISTIVITY DATA
         (2) INPUT CONDUCTIVITY DATA
1

     DO YOU WISH TO INCLUDE A FILLER PHASE?
N

  TWO PHASE SYSTEM ASSUMED: RESIN/FILLER

  ENTER> RESIN RESISTIVITY
4.5E+16

  ENTER> FIBER RESISTIVITIES
         (LONGITUDINAL,TRANSVERSE)
0.0015, 0.0015

  ENTER> FIBER VOLUME FRACTIONS TO SCAN
         START VALUE, END VALUE, INCREMENT
0.2, 0.2, 1.0

  ENTER> ASPECT RATIO OF FIBERS
50.0

  ENTER> TYPE OF AVERAGING
         (1) IN-PLANE; TWO-DIMENSIONAL
         (2) AXIAL SYMMETRIC; THREE-DIMENSIONAL
1

  ENTER> HERMANS ORIENTATION PARAMETER
0.5

 DEFAULT ELECTRICAL CALIBRATION PARAMETERS

 <DATA CHECK>
 CALIBRATION PARAMETERS
     ALPHA =   0.4100
     BETA  =   0.2900
```

Table 1 (continued)

```
    DO YOU WISH TO CHANGE THESE VALUES?
N

    DO YOU WISH A TABLE OF DATA?
Y

    DO YOU WISH A COMPUTER PLOT?
N

ELECTRICAL
RESITIVITIES OF COMPOSITE MATERIAL : PLANAR CASE
=============================================================
     VF          F          K11           K22           K33
=============================================================
   0.2000      0.5000    1.0000E-02    3.0000E-02    2.8800E+16

  ENTER> REPEAT OPTION
         (1) REPEAT SAME PLOT
         (2) ENTER NEW MATERIAL GEOMETRY
         (3) START OVER
         (4) END PROGRAM
4
```

Table 2.
Sample Execution of Micromechanics
Model for Graphs of Electrical Resistivities
for Graphite Fibers and PPS Resin.

```
 CENTER FOR COMPOSITE MATERIALS
 COMPUTER SOFTWARE SYSTEMS

 MICROMECHANICAL MODEL FOR CALCULATING:
 COMPOSITE MATERIAL ELECTICAL AND THERMAL
 RESISTIVITIES AND CONDUCTIVITES

 VERSION: 051182


  ENTER> CALCULATION OPTION
         (1) CALCULATE ELECTRICAL PROPERTIES
         (2) CALCULATE THERMAL PROPERTIES
1

  ENTER> INPUT OPTION
         (1) INPUT RESISTIVITY DATA
         (2) INPUT CONDUCTIVITY DATA
1

     DO YOU WISH TO INCLUDE A FILLER PHASE?
 N

  TWO PHASE SYSTEM ASSUMED: RESIN/FILLER

  ENTER> RESIN RESISTIVITY
4.5E+16

  ENTER> FIBER RESISTIVITIES
         (LONGITUDINAL,TRANSVERSE)
0.0015, 0.0015

  ENTER> FIBER VOLUME FRACTIONS TO SCAN
         START VALUE, END VALUE, INCREMENT
0.0, 1.0, 0.02

  ENTER> ASPECT RATIO OF FIBERS
50.0

  ENTER> TYPE OF AVERAGING
         (1) IN-PLANE; TWO-DIMENSIONAL
         (2) AXIAL SYMMETRIC; THREE-DIMENSIONAL
1
```

Table 2 (continued)

```
 ENTER> HERMANS ORIENTATION PARAMETER
0.5

DEFLAULT ELECTRICAL CALIBRATION PARAMETERS

<DATA CHECK>
CALIBRATION PARAMETERS
    ALPHA =   0.4100
    BETA  =   0.2900


    DO YOU WISH TO CHANGE THESE VALUES?
N

    DO YOU WISH A TABLE OF DATA?
Y

    DO YOU WISH A COMPUTER PLOT?
Y

 ENTER> GRAPHIC OUTPUT DATA
        SELECT COORDINATE DIRECTION
        (1) K11
        (2) K22
        (3) K33
1
```

Table 2 (continued)

ELECTRICAL RESITIVITIES OF COMPOSITE MATERIAL : PLANAR CASE

VF	F	K11	K22	K33
0.0200	0.5000	3.8027E+15	9.7008E+15	4.3216E+16
0.0400	0.5000	1.9085E+15	5.2428E+15	4.1467E+16
0.0600	0.5000	1.2389E+15	3.4985E+15	3.9755E+16
0.0800	0.5000	8.9701E+14	2.5700E+15	3.8079E+16
0.1000	0.5000	1.3920E+08	4.1759E+08	3.6450E+16
0.1200	0.5000	1.6667E-02	5.0000E-02	3.4848E+16
0.1400	0.5000	1.4286E-02	4.2857E-02	3.3282E+16
0.1600	0.5000	1.2500E-02	3.7500E-02	3.1752E+16
0.1800	0.5000	1.1111E-02	3.3333E-02	3.0258E+16
0.2000	0.5000	1.0000E-02	3.0000E-02	2.8800E+16
0.2200	0.5000	9.0909E-03	2.7273E-02	2.7378E+16
0.2400	0.5000	8.3333E-03	2.5000E-02	2.5992E+16
0.2600	0.5000	7.6923E-03	2.3077E-02	2.4642E+16
0.2800	0.5000	7.1429E-03	2.1429E-02	2.3328E+16
0.3000	0.5000	6.6667E-03	2.0000E-02	2.2050E+16
0.3200	0.5000	6.2500E-03	1.8750E-02	2.0808E+16
0.3400	0.5000	5.8824E-03	1.7647E-02	1.9602E+16
0.3600	0.5000	5.5556E-03	1.6667E-02	1.8432E+16
0.3800	0.5000	5.2632E-03	1.5789E-02	1.7298E+16
0.4000	0.5000	5.0000E-03	1.5000E-02	1.6200E+16
0.4200	0.5000	4.7619E-03	1.4286E-02	1.5138E+16
0.4400	0.5000	4.5455E-03	1.3636E-02	1.4112E+16
0.4600	0.5000	4.3478E-03	1.3043E-02	1.3122E+16
0.4800	0.5000	4.1667E-03	1.2500E-02	1.2168E+16
0.5000	0.5000	4.0000E-03	1.2000E-02	1.1250E+16
0.5200	0.5000	3.8462E-03	1.1538E-02	1.0368E+16
0.5400	0.5000	3.7037E-03	1.1111E-02	9.5220E+15
0.5600	0.5000	3.5714E-03	1.0714E-02	8.7120E+15
0.5800	0.5000	3.4483E-03	1.0345E-02	7.9380E+15
0.6000	0.5000	3.3333E-03	1.0000E-02	7.2000E+15
0.6200	0.5000	3.2258E-03	9.6774E-03	6.4980E+15
0.6400	0.5000	3.1250E-03	9.3750E-03	5.8320E+15
0.6600	0.5000	3.0303E-03	9.0909E-03	5.2020E+15
0.6800	0.5000	2.9412E-03	8.8235E-03	4.6080E+15
0.7000	0.5000	2.8571E-03	8.5714E-03	4.0500E+15
0.7200	0.5000	2.7778E-03	8.3333E-03	3.5280E+15
0.7400	0.5000	2.7027E-03	8.1081E-03	3.0420E+15
0.7600	0.5000	2.6316E-03	7.8947E-03	2.5920E+15
0.7800	0.5000	2.5641E-03	7.6923E-03	2.1780E+15
0.8000	0.5000	2.5000E-03	7.5000E-03	1.8000E+15
0.8200	0.5000	2.4390E-03	7.3171E-03	1.4580E+15
0.8400	0.5000	2.3810E-03	7.1429E-03	1.1520E+15
0.8600	0.5000	2.3256E-03	6.9767E-03	8.8200E+14
0.8800	0.5000	2.2727E-03	6.8182E-03	6.4800E+14
0.9000	0.5000	2.2222E-03	6.6667E-03	4.5000E+14
0.9200	0.5000	2.1739E-03	6.5217E-03	2.8800E+14
0.9400	0.5000	2.1277E-03	6.3830E-03	1.6200E+14
0.9600	0.5000	2.0833E-03	6.2500E-03	7.2000E+13
0.9800	0.5000	2.0408E-03	6.1224E-03	1.8000E+13
1.0000	0.5000	1.5000E-03	1.5001E-03	1.5001E-03

Table 2 (continued)

```
     READY FOR PLOT?
 Y

   ENTER> VERTICLE AXIS MODE
          (1) PLOT LINEAR SCALE FOR LOG10(Kii)
          (2) PLOT LOG CYCLE SCALE FOR LOG10(Kii)
1

   ENTER> GRAPHICS OUTPUT DEVICE
          (1) TERMINAL
          (2) FLATBED PLOTTER
1

   ENTER> REPEAT OPTION
          (1) REPEAT SAME PLOT
          (2) ENTER NEW MATERIAL GEOMETRY
          (3) START OVER
          (4) END PROGRAM
2

   ENTER> FIBER VOLUME FRACTIONS TO SCAN
          START VALUE, END VALUE, INCREMENT
0.0, 1.0, 0.02

   ENTER> ASPECT RATIO OF FIBERS
50.0

   ENTER> TYPE OF AVERAGING
          (1) IN-PLANE; TWO-DIMENSIONAL
          (2) AXIAL SYMMETRIC; THREE-DIMENSIONAL
1

   ENTER> HERMANS ORIENTATION PARAMETER
0.5

 DEFLAULT ELECTRICAL CALIBRATION PARAMETERS

 <DATA CHECK>
 CALIBRATION PARAMETERS
     ALPHA =    0.4100
     BETA  =    0.2900


     DO YOU WISH TO CHANGE THESE VALUES?
 N

     DO YOU WISH A TABLE OF DATA?
 N
```

Table 2 (continued)

```
    DO YOU WISH A COMPUTER PLOT?
Y


 ENTER> GRAPHIC OUTPUT DATA
        SELECT COORDINATE DIRECTION
        (1) K11
        (2) K22
        (3) K33
2

    READY FOR PLOT?
 Y

 ENTER> VERTICLE AXIS MODE
        (1) PLOT LINEAR SCALE FOR LOG10(Kii)
        (2) PLOT LOG CYCLE SCALE FOR LOG10(Kii)
1

 ENTER> GRAPHICS OUTPUT DEVICE
        (1) TERMINAL
        (2) FLATBED PLOTTER
1
 ENTER> REPEAT OPTION
        (1) REPEAT SAME PLOT
        (2) ENTER NEW MATERIAL GEOMETRY
        (3) START OVER
        (4) END PROGRAM
2

 ENTER> FIBER VOLUME FRACTIONS TO SCAN
        START VALUE, END VALUE, INCREMENT
0.0, 1.0, 0.02

 ENTER> ASPECT RATIO OF FIBERS
50.0

 ENTER> TYPE OF AVERAGING
        (1) IN-PLANE; TWO-DIMENSIONAL
        (2) AXIAL SYMMETRIC; THREE-DIMENSIONAL
1

 ENTER> HERMANS ORIENTATION PARAMETER
0.5

 DEFLAULT ELECTRICAL CALIBRATION PARAMETERS

 <DATA CHECK>
 CALIBRATION PARAMETERS
     ALPHA =   0.4100
     BETA  =   0.2900


     DO YOU WISH TO CHANGE THESE VALUES?
 N

     DO YOU WISH A TABLE OF DATA?
 N

     DO YOU WISH A COMPUTER PLOT?
 Y
```

Table 2 (continued)

```
 ENTER> GRAPHIC OUTPUT DATA
        SELECT COORDINATE DIRECTION
        (1) K11
        (2) K22
        (3) K33
3

    READY FOR PLOT?
 Y

 ENTER> VERTICLE AXIS MODE
        (1) PLOT LINEAR SCALE FOR LOG10(Kii)
        (2) PLOT LOG CYCLE SCALE FOR LOG10(Kii)
1

 ENTER> GRAPHICS OUTPUT DEVICE
        (1) TERMINAL
        (2) FLATBED PLOTTER
1

 ENTER> REPEAT OPTION
        (1) REPEAT SAME PLOT
        (2) ENTER NEW MATERIAL GEOMETRY
        (3) START OVER
        (4) END PROGRAM
4
```

Figure 1. Electrical resistivity for graphite/PPS composite, longitudinal direction.

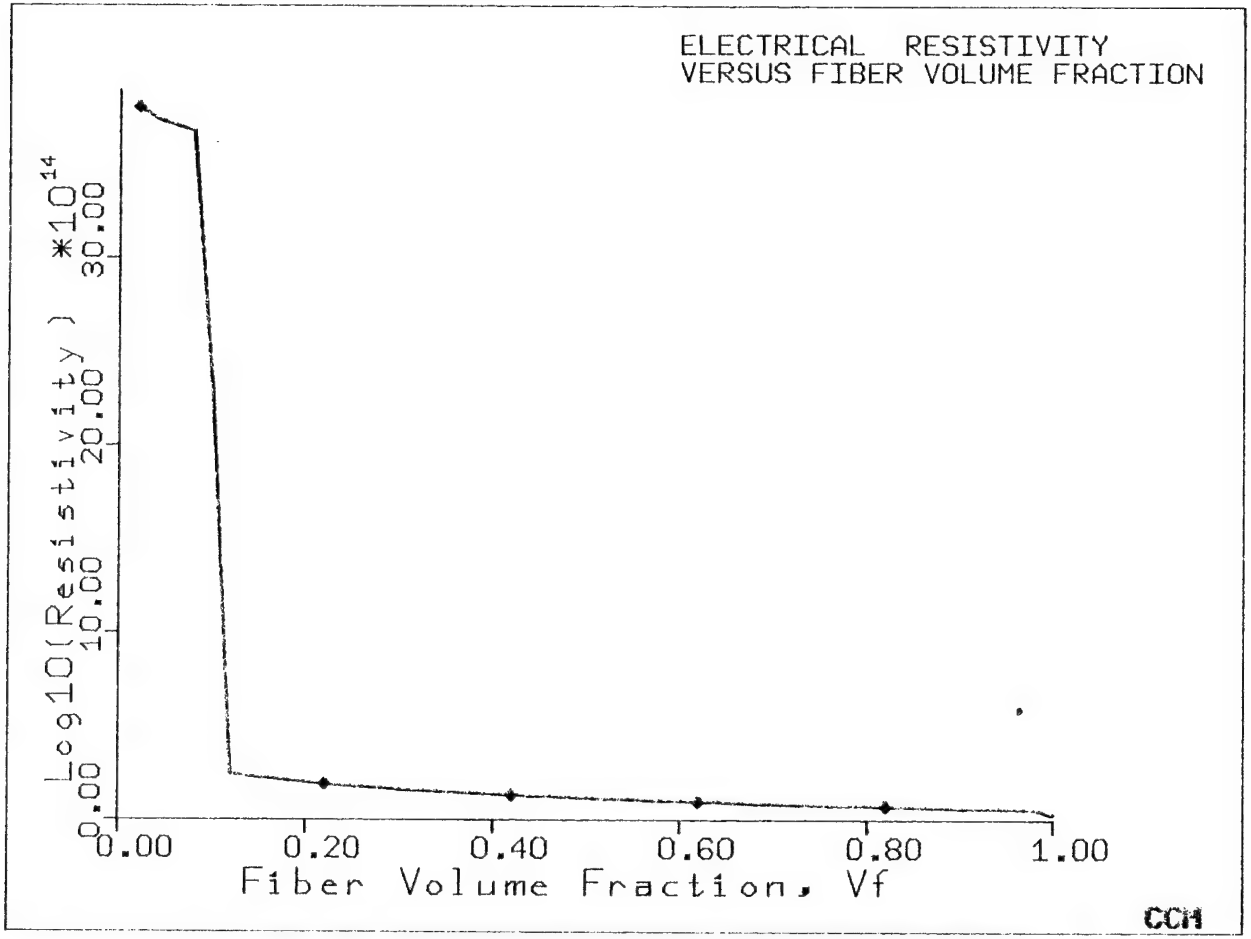

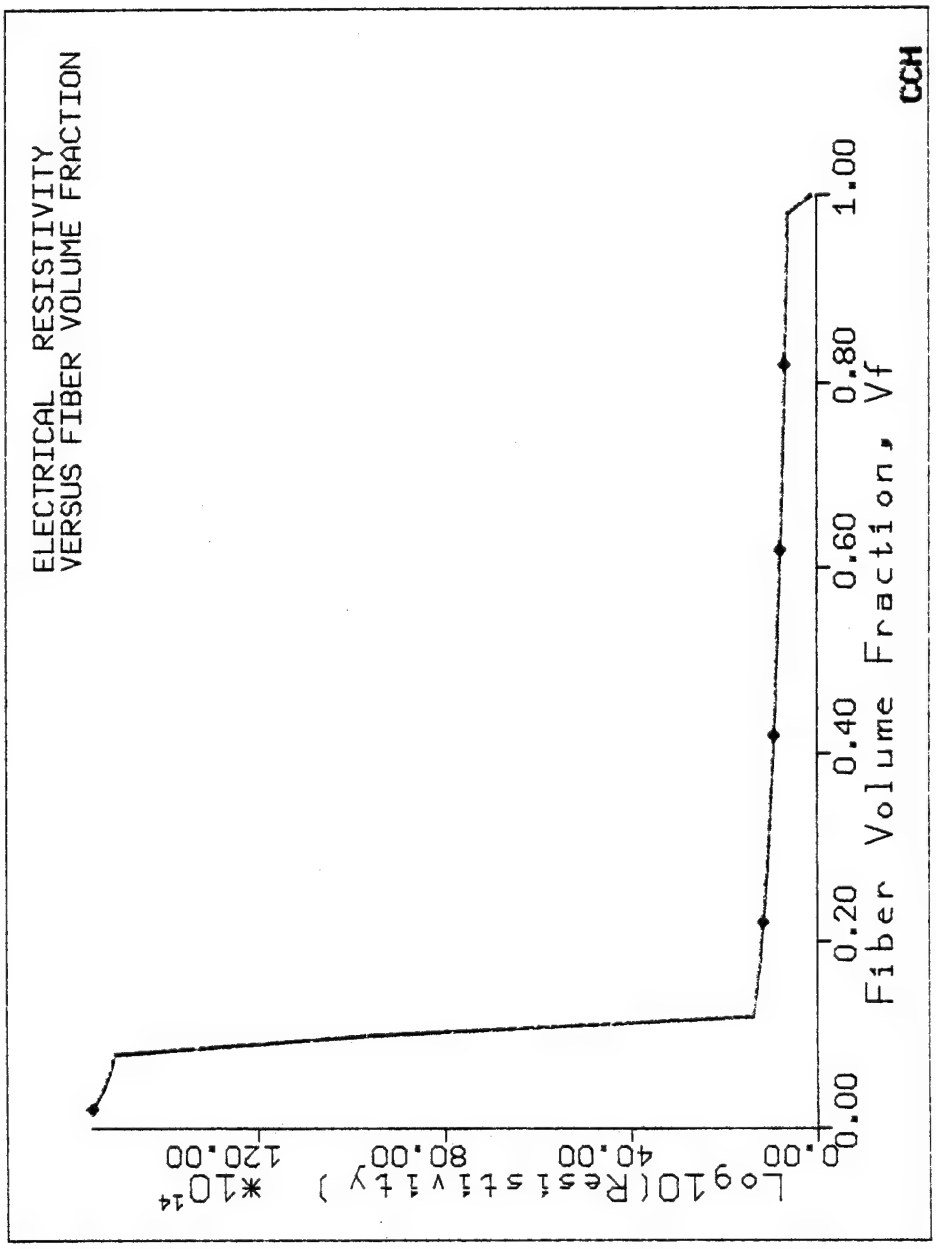

Figure 2. Electrical resistivity for graphite/PPS composite, transverse direction.

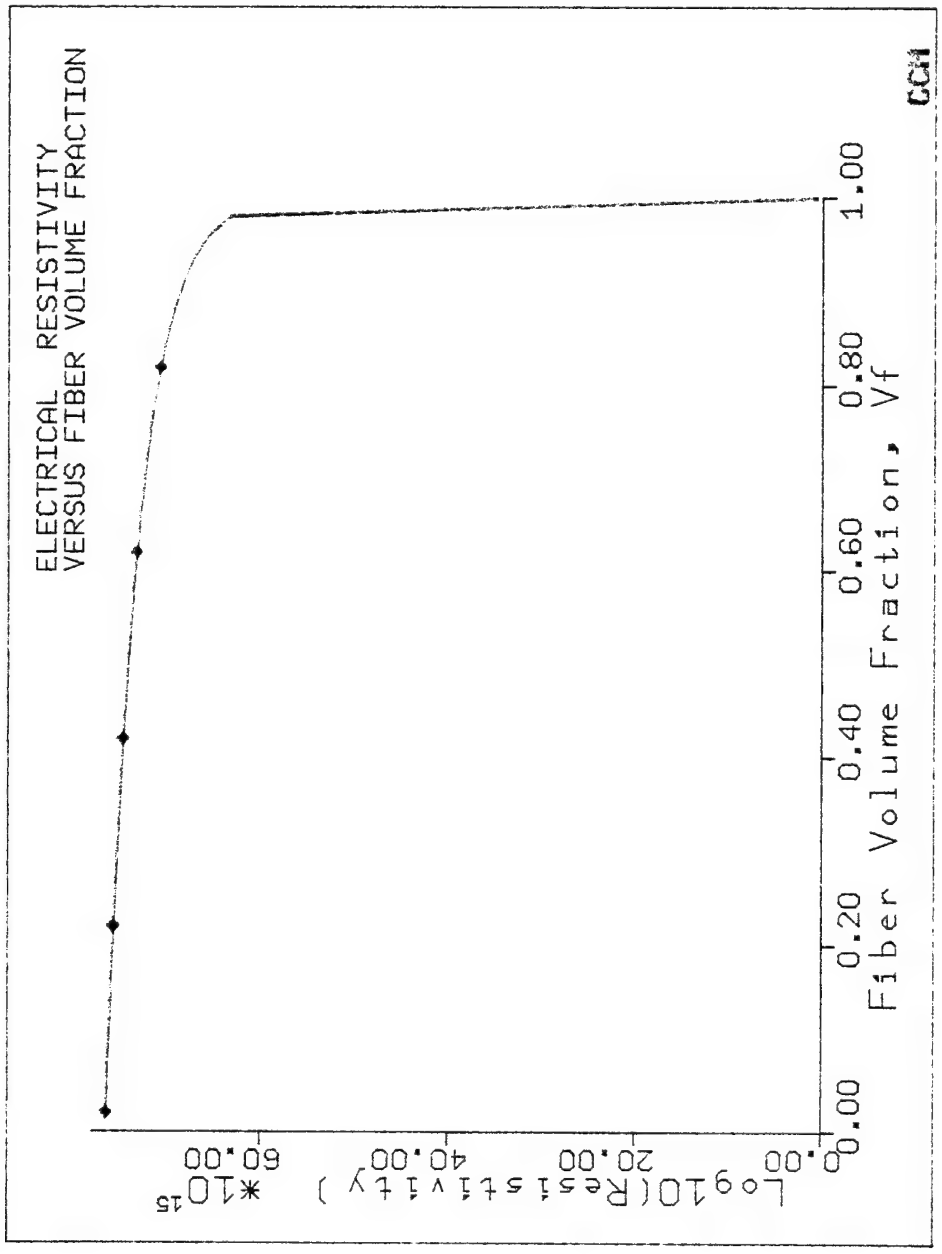

Figure 3. Electrical resistivity for graphite/PPS composite, perpendicular direction.

2) Graphite Fibers - Round Copper Particles and PPS Resin

	F_1 [a] Fiber	F_2 [b] Copper Particles	M Resin
Resistivity (ohm-cm)	1.5×10^{-3}	1.70×10^{-6}	4.5×10^{16}
Volume Fraction	0.30	0.20	0.50
Aspect Ratio	50	1.0	--
Orientation Parameter, f_a , (axial)	0.5	0.0	--

Calculations

Step I: Apparent volume fractions for System I graphite fibers and PPS resin.

$$V'_{f_1} = \frac{V_{f_1}}{1 - V_{f_2}} = \frac{0.30}{1.0 - 0.2} = 0.375$$

$$V'_{f_{m_1}} = \frac{V_{f_m}}{1 - V_{f_2}} = \frac{0.50}{1.0 - 0.2} = 0.625$$

Resistivities for System I (see Table 3)

$$P_I^1 = 6.00\times10^{-3} \text{ ohm-cm}$$

$$P_I^2 = 2.40\times10^{-2} \text{ ohm-cm}$$

$$P_I^3 = 2.40\times10^{-2} \text{ ohm-cm}$$

Note: The influence of geometrical irregularities and/or surface coatings may be taken into account by replacing the filler resistivity by the effective resistivity.

[a] Effective resistivity of graphite fiber ≅ 0.45 ohm-cm.

[b] Effective resistivity of copper particles ≅ 1.7×10^{-3} ohm-cm.

Step II: Apparent volume fractions for System II Round Copper Particles and PPS Resin

$$V'_{f_2} = \frac{V_{f_2}}{1 - V_{f_1}} = \frac{0.20}{1.0 - 0.30} = 0.286$$

$$V'_{f_{m_2}} = \frac{V_{f_m}}{1 - V_{f_1}} = \frac{0.50}{1.0 - 0.30} = 0.714$$

Resistivities for System II (see Table 4)

$$P^1_{II} = 1.784 \times 10^{16} \quad \text{ohm-cm}$$

$$P^2_{II} = 1.784 \times 10^{14} \quad \text{ohm-cm}$$

$$P^3_{II} = 1.784 \times 10^{14} \quad \text{ohm-cm}$$

Step III: Calculate properties of three-phase system

$$p^i = (1 - V'_{f_2})P^i_I + (1 - V'_{f_1})P^i_{II} - V_{f_m} P_m$$

$$1/P^1 = (1 - 0.286)\left(\frac{1}{6.00 \times 10^{-3}}\right) + (1 - 0.375)\left(\frac{1}{1.784 \times 10^{16}}\right) - (0.50)\left(\frac{1}{4.5 \times 10^{16}}\right)$$

$$p^1 = 8.403 \times 10^{-3} \quad \text{ohm-cm}$$

$$1/P^2 = (1 - 0.286)\left(\frac{1}{2.40 \times 10^{-2}}\right) + (1 - 0.375)\left(\frac{1}{1.784 \times 10^{16}}\right) - (0.50)\left(\frac{1}{4.5 \times 10^{16}}\right)$$

$$p^2 = p^3 = 3.36 \times 10^{-2} \quad \text{ohm-cm}$$

Table 3.
Calculations for System I for
Graphite Fibers and PPS Resin

```
 CENTER FOR COMPOSITE MATERIALS
 COMPUTER SOFTWARE SYSTEMS

 MICROMECHANICAL MODEL FOR CALCULATING:
 COMPOSITE MATERIAL ELECTICAL AND THERMAL
 RESISTIVITIES AND CONDUCTIVITES

 VERSION: 051182


  ENTER> CALCULATION OPTION
         (1) CALCULATE ELECTRICAL PROPERTIES
         (2) CALCULATE THERMAL PROPERTIES
1

  ENTER> INPUT OPTION
         (1) INPUT RESISTIVITY DATA
         (2) INPUT CONDUCTIVITY DATA
1

     DO YOU WISH TO INCLUDE A FILLER PHASE?
 N

  TWO PHASE SYSTEM ASSUMED: RESIN/FILLER

  ENTER> RESIN RESISTIVITY
4.5E+16

  ENTER> FIBER RESISTIVITIES
         (LONGITUDINAL,TRANSVERSE)
0.0015, 0.0015

  ENTER> FIBER VOLUME FRACTIONS TO SCAN
         START VALUE, END VALUE, INCREMENT
0.375, 0.375, 1.0

  ENTER> ASPECT RATIO OF FIBERS
50.0

  ENTER> TYPE OF AVERAGING
         (1) IN-PLANE; TWO-DIMENSIONAL
         (2) AXIAL SYMMETRIC; THREE-DIMENSIONAL
2

  ENTER> HERMANS ORIENTATION PARAMETER
0.5

 DEFLAULT ELECTRICAL CALIBRATION PARAMETERS

 <DATA CHECK>
 CALIBRATION PARAMETERS
     ALPHA =    0.4100
     BETA  =    0.2900
```

Table 3 (continued)

```
     DO YOU WISH TO CHANGE THESE VALUES?
N

     DO YOU WISH A TABLE OF DATA?
Y

     DO YOU WISH A COMPUTER PLOT?
N

 ELECTRICAL
 RESITIVITIES OF COMPOSITE MATERIAL : AXIAL CASE
=============================================================
     VF           F          K11            K22          K33
=============================================================
   0.3750      0.5000     6.0000E-03     2.4000E-02     2.4000E-02

  ENTER> REPEAT OPTION
         (1) REPEAT SAME PLOT
         (2) ENTER NEW MATERIAL GEOMETRY
         (3) START OVER
         (4) END PROGRAM
4
```

Table 4.
Calculations for System II for
Round Copper Particles and PPS Resin

```
CENTER FOR COMPOSITE MATERIALS
COMPUTER SOFTWARE SYSTEMS

MICROMECHANICAL MODEL FOR CALCULATING:
COMPOSITE MATERIAL ELECTICAL AND THERMAL
RESISTIVITIES AND CONDUCTIVITES

VERSION: 051182


 ENTER> CALCULATION OPTION
        (1) CALCULATE ELECTRICAL PROPERTIES
        (2) CALCULATE THERMAL PROPERTIES
1

 ENTER> INPUT OPTION
        (1) INPUT RESISTIVITY DATA
        (2) INPUT CONDUCTIVITY DATA
1

    DO YOU WISH TO INCLUDE A FILLER PHASE?
 N

 TWO PHASE SYSTEM ASSUMED: RESIN/FILLER

 ENTER> RESIN RESISTIVITY
4.5E+16

 ENTER> FIBER RESISTIVITIES
        (LONGITUDINAL,TRANSVERSE)
1.7E-6, 1.7E-6

 ENTER> FIBER VOLUME FRACTIONS TO SCAN
        START VALUE, END VALUE, INCREMENT
0.286, 0.286, 1.0

 ENTER> ASPECT RATIO OF FIBERS
1.0

 ENTER> TYPE OF AVERAGING
        (1) IN-PLANE; TWO-DIMENSIONAL
        (2) AXIAL SYMMETRIC; THREE-DIMENSIONAL
2
```

Table 4 (continued)

```
  ENTER> HERMANS ORIENTATION PARAMETER
0.0

 DEFLAULT ELECTRICAL CALIBRATION PARAMETERS

 <DATA CHECK>
 CALIBRATION PARAMETERS
     ALPHA =    0.4100
     BETA  =    0.2900


     DO YOU WISH TO CHANGE THESE VALUES?
 N

     DO YOU WISH A TABLE OF DATA?
 Y

     DO YOU WISH A COMPUTER PLOT?
 N

 ELECTRICAL
 RESITIVITIES OF COMPOSITE MATERIAL : AXIAL CASE
==========================================================
     VF           F          K11             K22             K33
==========================================================
   0.2860      0.0000     1.7839E+16     1.7839E+16     1.7839E+16

  ENTER> REPEAT OPTION
         (1) REPEAT SAME PLOT
         (2) ENTER NEW MATERIAL GEOMETRY
         (3) START OVER
         (4) END PROGRAM
4
```

3) Graphite Fibers - Copper Flakes and PPS Resin

	F_1 [a] Fiber	F_2 [b] Copper Particles	M Resin
Resistivity (ohm-cm)	1.5×10^{-3}	1.70×10^{-6}	4.5×10^{16}
Volume Fraction	0.2	0.5	0.3
Aspect Ratio	50	1.0×10^{-5}	
Orientation Parameter, f_a , (axial)	0.5	0.0	

Calculations

Step I: Apparent volume fractions for System I graphite fibers and PPS resin.

$$V'_{f_1} = \frac{V_{f_1}}{1 - V_{f_2}} = \frac{0.2}{1.0 - 0.5} = 0.4$$

$$V'_{f_{m_1}} = \frac{V_{f_m}}{1 - V_{f_2}} = \frac{0.3}{1.0 - 0.5} = 0.6$$

Resistivities for System I (see Table 5)

$$P_I^1 = 5.616\times10^{-3} \text{ ohm-cm}$$

$$P_I^2 = 2.223\times10^{-2} \text{ ohm-cm}$$

$$P_I^3 = 2.223\times10^{-2} \text{ ohm-cm}$$

Note: The influence of geometrical irregularities and/or surface coatings may be taken into account by replacing the filler resistivity by the effective resistivity.

[a]Effective resistivity of graphite fiber ≅ 0.45 ohm-cm.

[b]Effective resistivity of copper particles ≅ 1.7×10^{-3} ohm-cm.

Step II: Apparent volume fractions for System II Copper Flakes and PPS Resin

$$V'_{f_2} = \frac{V_{f_2}}{1 - V_{f_1}} = \frac{0.5}{1.0 - 0.2} = 0.625$$

$$V'_{f_{m_2}} = \frac{V_{f_m}}{1 - V_{f_1}} = \frac{0.3}{1.0 - 0.2} = 0.375$$

Resistivities for System II (see Table 6)

$$P^1_{II} = 4.080 \times 10^{-6} \text{ ohm-cm}$$

$$P^2_{II} = 4.080 \times 10^{-4} \text{ ohm-cm}$$

$$P^3_{II} = 4.080 \times 10^{-4} \text{ ohm-cm}$$

Step III: Calculate properties of three-phase system

$$1/P^1 = (1 - 0.615)\left(\frac{1}{5.616 \times 10^{-3}}\right) + (1 - 0.4)\left(\frac{1}{4.080 \times 10^{-6}}\right) - (0.3)\left(\frac{1}{4.5 \times 10^{16}}\right)$$

$$p^1 = 6.80 \times 10^{-6} \text{ ohm-cm}$$

$$1/P^2 = (1 - 0.625)\left(\frac{1}{2.223 \times 10^{-2}}\right) + (1 - 0.4)\left(\frac{1}{4.080 \times 10^{-6}}\right) - (0.3)\left(\frac{1}{4.5 \times 10^{16}}\right)$$

$$p^2 = P^3 = 6.80 \times 10^{-6} \text{ ohm-cm}$$

Table 5.
Calculate Resistivities for System I
Graphite Fibers and PPS Resin.

```
 CENTER FOR COMPOSITE MATERIALS
 COMPUTER SOFTWARE SYSTEMS

 MICROMECHANICAL MODEL FOR CALCULATING:
 COMPOSITE MATERIAL ELECTICAL AND THERMAL
 RESISTIVITIES AND CONDUCTIVITES

 VERSION: 051182


  ENTER> CALCULATION OPTION
         (1) CALCULATE ELECTRICAL PROPERTIES
         (2) CALCULATE THERMAL PROPERTIES
1

  ENTER> INPUT OPTION
         (1) INPUT RESISTIVITY DATA
         (2) INPUT CONDUCTIVITY DATA
1

    DO YOU WISH TO INCLUDE A FILLER PHASE?
 n

  TWO PHASE SYSTEM ASSUMED: RESIN/FILLER

  ENTER> RESIN RESISTIVITY
4.5

  ENTER> FIBER RESISTIVITIES
         (LONGITUDINAL,TRANSVERSE)
0.0015, 0.0015

  ENTER> FIBER VOLUME FRACTIONS TO SCAN
         START VALUE, END VALUE, INCREMENT
0.4, 0.4, 1.0

  ENTER> ASPECT RATIO OF FIBERS
50.0

  ENTER> TYPE OF AVERAGING
         (1) IN-PLANE; TWO-DIMENSIONAL
         (2) AXIAL SYMMETRIC; THREE-DIMENSIONAL
2

  ENTER> HERMANS ORIENTATION PARAMETER
0.5

 DEFLAULT ELECTRICAL CALIBRATION PARAMETERS
```

Table 5 (continued)

```
 <DATA CHECK>
 CALIBRATION PARAMETERS
     ALPHA =    0.4100
     BETA  =    0.2900


     DO YOU WISH TO CHANGE THESE VALUES?
 N

     DO YOU WISH A TABLE OF DATA?
 Y

     DO YOU WISH A COMPUTER PLOT?
 N

 ELECTRICAL
 RESITIVITIES OF COMPOSITE MATERIAL : AXIAL CASE
==========================================================================
     VF           F          K11             K22             K33
==========================================================================
   0.4000      0.5000     5.6157E-03     2.2232E-02     2.2232E-02

  ENTER> REPEAT OPTION
         (1) REPEAT SAME PLOT
         (2) ENTER NEW MATERIAL GEOMETRY
         (3) START OVER
         (4) END PROGRAM
4
```

Table 6.
Calculate Resistivities for System II
Copper Flakes and PPS Resin.

```
CENTER FOR COMPOSITE MATERIALS
COMPUTER SOFTWARE SYSTEMS

MICROMECHANICAL MODEL FOR CALCULATING:
COMPOSITE MATERIAL ELECTICAL AND THERMAL
RESISTIVITIES AND CONDUCTIVITES

VERSION: 051182


 ENTER> CALCULATION OPTION
        (1) CALCULATE ELECTRICAL PROPERTIES
        (2) CALCULATE THERMAL PROPERTIES
1

 ENTER> INPUT OPTION
        (1) INPUT RESISTIVITY DATA
        (2) INPUT CONDUCTIVITY DATA
1

N   DO YOU WISH TO INCLUDE A FILLER PHASE?

 TWO PHASE SYSTEM ASSUMED: RESIN/FILLER

 ENTER> RESIN RESISTIVITY
4.5E+16

 ENTER> FIBER RESISTIVITIES
        (LONGITUDINAL,TRANSVERSE)
1.7E-6, 1.7E-6

 ENTER> FIBER VOLUME FRACTIONS TO SCAN
        START VALUE, END VALUE, INCREMENT
0.625,0.625, 1.0

 ENTER> ASPECT RATIO OF FIBERS
1.0E-5

 ENTER> TYPE OF AVERAGING
        (1) IN-PLANE: TWO-DIMENSIONAL
        (2) AXIAL SYMMETRIC: THREE-DIMENSIONAL
2

 ENTER> HERMANS ORIENTATION PARAMETER
0.0

DEFLAULT ELECTRICAL CALIBRATION PARAMETERS
```

Table 6 (continued)

```
<DATA CHECK>
CALIBRATION PARAMETERS
     ALPHA =    0.4100
     BETA  =    0.2900


N    DO YOU WISH TO CHANGE THESE VALUES?

Y    DO YOU WISH A TABLE OF DATA?

N    DO YOU WISH A COMPUTER PLOT?

ELECTRICAL
RESITIVITIES OF COMPOSITE MATERIAL : AXIAL CASE
```

VF	F	K11	K22	K33
0.6250	0.0000	4.0800E-06	4.0800E-06	4.0900E-06

```
 ENTER> REPEAT OPTION
        (1) REPEAT SAME PLOT
        (2) ENTER NEW MATERIAL GEOMETRY
        (3) START OVER
        (4) END PROGRAM
4
```

4) Graphite Fibers - Copper Fibers and PPS Resin

	F_1 [a] Fiber	F_2 [b] Copper Fibers	M Resin
Resistivity (ohm-cm)	1.5×10^{-3}	1.7×10^{-6}	4.5×10^{16}
Volume Fraction	0.2	0.5	0.3
Aspect Ratio	50.0	50.0	--
Orientation Parameter, f_a , (axial)	0.5	0.5	--

Calculations

Step I: Apparent volume fractions for System I graphite fibers and PPS resin.

$$V'_{f_1} = \frac{V_{f_1}}{1 - V_{f_2}} = \frac{0.2}{1.0 - 0.5} = 0.4$$

$$V'_{f_{m_1}} = \frac{V_{f_m}}{1 - V_{f_2}} = \frac{0.3}{1.0 - 0.5} = 0.6$$

Resistivities for System I (see Table 5)

$$P_I^1 = 5.616\times10^{-3} \text{ ohm-cm}$$

$$P_I^2 = 2.223\times10^{-2} \text{ ohm-cm}$$

$$P_I^3 = 2.223\times10^{-2} \text{ ohm-cm}$$

Note: The influence of geometrical irregularities and/or surface coatings may be taken into account by replacing the filler resistivity by the effective resistivity.

[a]Effective resistivity of graphite fiber ≅ 0.45 ohm-cm.

[b]Effective resistivity of copper particles ≅ 1.7×10^{-3} ohm-cm.

Step II: Apparent volume fractions for System II Copper Fibers and PPS Resin

$$V'_{f_2} = \frac{V_{f_2}}{1 - V_{f_1}} = \frac{0.5}{1.0 - 0.2} = 0.625$$

$$V'_{f_{m_2}} = \frac{V_{f_m}}{1 - V_{f_1}} = \frac{0.3}{1.0 - 0.2} = 0.375$$

Resistivities for System II (see Table 7)

$$P^1_{II} = 4.080 \times 10^{-6} \text{ ohm-cm}$$

$$P^2_{II} = 1.632 \times 10^{-5} \text{ ohm-cm}$$

$$P^3_{II} = 1.632 \times 10^{-5} \text{ ohm-cm}$$

Step III: Calculate properties of three-phase system

$$1/P^1 = (1 - 0.625)\left(\frac{1}{5.616 \times 10^{-3}}\right) + (1 - 0.4)\left(\frac{1}{4.080 \times 10^{-6}}\right) - (0.3)\left(\frac{1}{4.5 \times 10^{16}}\right)$$

$$p^1 = 7.00 \times 10^{-6} \text{ ohm-cm}$$

$$1/P^2 = (1 - 0.625)\left(\frac{1}{2.223 \times 10^{-2}}\right) + (1 - 0.4)\left(\frac{1}{1.632 \times 10^{-5}}\right) - (0.3)\left(\frac{1}{4.5 \times 10^{16}}\right)$$

$$p^2 = P^3 = 2.7 \times 10^{-5} \text{ ohm-cm}$$

Table 7.
Calculate Resistivities for System II
Copper Fibers and PPS Resin.

```
 CENTER FOR COMPOSITE MATERIALS
 COMPUTER SOFTWARE SYSTEMS

 MICROMECHANICAL MODEL FOR CALCULATING:
 COMPOSITE MATERIAL ELECTICAL AND THERMAL
 RESISTIVITIES AND CONDUCTIVITES

 VERSION: 051182


  ENTER> CALCULATION OPTION
         (1) CALCULATE ELECTRICAL PROPERTIES
         (2) CALCULATE THERMAL PROPERTIES
1

  ENTER> INPUT OPTION
         (1) INPUT RESISTIVITY DATA
         (2) INPUT CONDUCTIVITY DATA
1

    DO YOU WISH TO INCLUDE A FILLER PHASE?
 N

  TWO PHASE SYSTEM ASSUMED: RESIN/FILLER

  ENTER> RESIN RESISTIVITY
4.5E+16

  ENTER> FIBER RESISTIVITIES
         (LONGITUDINAL,TRANSVERSE)
1.7E-6, 1.7E-6

  ENTER> FIBER VOLUME FRACTIONS TO SCAN
         START VALUE, END VALUE, INCREMENT
0.625, 0.625, 1.0

  ENTER> ASPECT RATIO OF FIBERS
50.0

  ENTER> TYPE OF AVERAGING
         (1) IN-PLANE; TWO-DIMENSIONAL
         (2) AXIAL SYMMETRIC; THREE-DIMENSIONAL
2

  ENTER> HERMANS ORIENTATION PARAMETER
0.5

 DEFLAULT ELECTRICAL CALIBRATION PARAMETERS
```

Table 7 (continued)

```
 <DATA CHECK>
 CALIBRATION PARAMETERS
      ALPHA =    0.4100
      BETA  =    0.2900


      DO YOU WISH TO CHANGE THESE VALUES?
 N

      DO YOU WISH A TABLE OF DATA?
 Y

      DO YOU WISH A COMPUTER PLOT?
 N

 ELECTRICAL
 RESITIVITIES OF COMPOSITE MATERIAL : AXIAL CASE
==========================================================
     VF            F          K11            K22            K33
==========================================================
   0.6250       0.5000     4.0800E-06     1.6320E-05     1.6320E-05

  ENTER> REPEAT OPTION
         (1) REPEAT SAME PLOT
         (2) ENTER NEW MATERIAL GEOMETRY
         (3) START OVER
         (4) END PROGRAM
4
```

5) Nickel Coated Graphite Fibers and PPS Resin

	Nickel Coated Fiber[a]	Resin
Resistivity (ohm-cm)	2.5×10^{-3}	4.5×10^{16}
Volume Fraction	Variable	
Aspect Ratio	50.0	
Orientation Parameter, f_a , (axial)	0.5	

- Executions are given in Table 8 for the computer graphs depicted in Figures 4, 5, and 6 for K_1 , K_2 , and K_3 , respectively.

---

[a]Effective resistivity for damaged coatings (see Table VIII of text).

Table 8.
Calculations for Nickel Coated
Fibers and PPS Resin Composite.

```
 CENTER FOR COMPOSITE MATERIALS
 COMPUTER SOFTWARE SYSTEMS

 MICROMECHANICAL MODEL FOR CALCULATING:
 COMPOSITE MATERIAL ELECTICAL AND THERMAL
 RESISTIVITIES AND CONDUCTIVITES

 VERSION: 051182


  ENTER> CALCULATION OPTION
         (1) CALCULATE ELECTRICAL PROPERTIES
         (2) CALCULATE THERMAL PROPERTIES
1,

  ENTER> INPUT OPTION
         (1) INPUT RESISTIVITY DATA
         (2) INPUT CONDUCTIVITY DATA
1,

+    DO YOU WISH TO INCLUDE A FILLER PHASE?
 N

  TWO PHASE SYSTEM ASSUMED: RESIN/FILLER

  ENTER> RESIN RESISTIVITY
4.5E+16,

  ENTER> FIBER RESISTIVITIES
         (LONGITUDINAL,TRANSVERSE)
0.0025, 0.0025,

  ENTER> FIBER VOLUME FRACTIONS TO SCAN
         START VALUE, END VALUE, INCREMENT
0.0, 1.0, 0.02,

  ENTER> ASPECT RATIO OF FIBERS
50.0,
```

Table 8 (continued)

```
  ENTER> TYPE OF AVERAGING
         (1) IN-PLANE; TWO-DIMENSIONAL
         (2) AXIAL SYMMETRIC; THREE-DIMENSIONAL
1,

  ENTER> HERMANS ORIENTATION PARAMETER
0.5,

 DEFLAULT ELECTRICAL CALIBRATION PARAMETERS

 <DATA CHECK>
 CALIBRATION PARAMETERS
     ALPHA =   0.4100
     BETA  =   0.2900

+    DO YOU WISH TO CHANGE THESE VALUES?
 N

+    DO YOU WISH A TABLE OF DATA?
 Y

+    DO YOU WISH A COMPUTER PLOT?
 Y

  ENTER> GRAPHIC OUTPUT DATA
         SELECT COORDINATE DIRECTION
         (1) K11
         (2) K22
         (3) K33
1,
```

Table 8 (continued)

ELECTRICAL
RESITIVITIES OF COMPOSITE MATERIAL ; PLANAR CASE

VF	F	K11	K22	K33
0.0200	0.5000	3.8027E+15	9.7008E+15	4.3216E+16
0.0400	0.5000	1.9085E+15	5.2428E+15	4.1467E+16
0.0600	0.5000	1.2389E+15	3.4985E+15	3.9755E+16
0.0800	0.5000	8.9701E+14	2.5700E+15	3.8079E+16
0.1000	0.5000	1.6605E+08	4.9814E+08	3.6450E+16
0.1200	0.5000	2.7778E-02	8.3333E-02	3.4848E+16
0.1400	0.5000	2.3810E-02	7.1429E-02	3.3282E+16
0.1600	0.5000	2.0833E-02	6.2500E-02	3.1752E+16
0.1800	0.5000	1.8519E-02	5.5556E-02	3.0258E+16
0.2000	0.5000	1.6667E-02	5.0000E-02	2.8800E+16
0.2200	0.5000	1.5152E-02	4.5455E-02	2.7378E+16
0.2400	0.5000	1.3889E-02	4.1667E-02	2.5992E+16
0.2600	0.5000	1.2821E-02	3.8462E-02	2.4642E+16
0.2800	0.5000	1.1905E-02	3.5714E-02	2.3328E+16
0.3000	0.5000	1.1111E-02	3.3333E-02	2.2050E+16
0.3200	0.5000	1.0417E-02	3.1250E-02	2.0808E+16
0.3400	0.5000	9.8039E-03	2.9412E-02	1.9602E+16
0.3600	0.5000	9.2593E-03	2.7778E-02	1.8432E+16
0.3800	0.5000	8.7719E-03	2.6316E-02	1.7298E+16
0.4000	0.5000	8.3333E-03	2.5000E-02	1.6200E+16
0.4200	0.5000	7.9365E-03	2.3810E-02	1.5138E+16
0.4400	0.5000	7.5758E-03	2.2727E-02	1.4112E+16
0.4600	0.5000	7.2464E-03	2.1739E-02	1.3122E+16
0.4800	0.5000	6.9444E-03	2.0833E-02	1.2168E+16
0.5000	0.5000	6.6667E-03	2.0000E-02	1.1250E+16
0.5200	0.5000	6.4103E-03	1.9231E-02	1.0368E+16
0.5400	0.5000	6.1728E-03	1.8519E-02	9.5220E+15
0.5600	0.5000	5.9524E-03	1.7857E-02	8.7120E+15
0.5800	0.5000	5.7471E-03	1.7241E-02	7.9380E+15
0.6000	0.5000	5.5556E-03	1.6667E-02	7.2000E+15
0.6200	0.5000	5.3763E-03	1.6129E-02	6.4980E+15
0.6400	0.5000	5.2083E-03	1.5625E-02	5.8320E+15
0.6600	0.5000	5.0505E-03	1.5152E-02	5.2020E+15
0.6800	0.5000	4.9020E-03	1.4706E-02	4.6080E+15
0.7000	0.5000	4.7619E-03	1.4286E-02	4.0500E+15
0.7200	0.5000	4.6296E-03	1.3889E-02	3.5280E+15
0.7400	0.5000	4.5045E-03	1.3514E-02	3.0420E+15
0.7600	0.5000	4.3860E-03	1.3158E-02	2.5920E+15
0.7800	0.5000	4.2735E-03	1.2821E-02	2.1780E+15
0.8000	0.5000	4.1667E-03	1.2500E-02	1.8000E+15
0.8200	0.5000	4.0650E-03	1.2195E-02	1.4580E+15
0.8400	0.5000	3.9683E-03	1.1905E-02	1.1520E+15
0.8600	0.5000	3.8760E-03	1.1628E-02	8.8200E+14
0.8800	0.5000	3.7879E-03	1.1364E-02	6.4800E+14
0.9000	0.5000	3.7037E-03	1.1111E-02	4.5000E+14
0.9200	0.5000	3.6232E-03	1.0870E-02	2.8800E+14
0.9400	0.5000	3.5461E-03	1.0638E-02	1.6200E+14
0.9600	0.5000	3.4722E-03	1.0417E-02	7.2000E+13
0.9800	0.5000	3.4014E-03	1.0204E-02	1.8000E+13
1.0000	0.5000	2.5000E-03	2.5001E-03	2.5001E-03

Table 8 (continued)

```
+    READY FOR PLOT?
 Y

  ENTER> VERTICLE AXIS MODE
         (1) PLOT LINEAR SCALE FOR LOG10(Kii)
         (2) PLOT LOG CYCLE SCALE FOR LOG10(Kii)
1,

  ENTER> GRAPHICS OUTPUT DEVICE
         (1) TERMINAL
         (2) FLATBED PLOTTER
2,

  ENTER> REPEAT OPTION
         (1) REPEAT SAME PLOT
         (2) ENTER NEW MATERIAL GEOMETRY
         (3) START OVER
         (4) END PROGRAM
2,

  ENTER> FIBER VOLUME FRACTIONS TO SCAN
         START VALUE, END VALUE, INCREMENT
0.0, 1.0, 0.02,

  ENTER> ASPECT RATIO OF FIBERS
50.0,

  ENTER> TYPE OF AVERAGING
         (1) IN-PLANE; TWO-DIMENSIONAL
         (2) AXIAL SYMMETRIC; THREE-DIMENSIONAL
2,

  ENTER> HERMANS ORIENTATION PARAMETER
0.5,

 DEFLAULT ELECTRICAL CALIBRATION PARAMETERS

 <DATA CHECK>
 CALIBRATION PARAMETERS
     ALPHA =   0.4100
     BETA  =   0.2900


+    DO YOU WISH TO CHANGE THESE VALUES?
 N

+    DO YOU WISH A TABLE OF DATA?
 N

+    DO YOU WISH A COMPUTER PLOT?
 Y

  ENTER> GRAPHIC OUTPUT DATA
         SELECT COORDINATE DIRECTION
         (1) K11
         (2) K22
         (3) K33
2,
```

Table 8 (continued)

```
+    READY FOR PLOT?
 Y

  ENTER> VERTICLE AXIS MODE
         (1) PLOT LINEAR SCALE FOR LOG10(Kii)
         (2) PLOT LOG CYCLE SCALE FOR LOG10(Kii)
1,

  ENTER> GRAPHICS OUTPUT DEVICE
         (1) TERMINAL
         (2) FLATBED PLOTTER
2,

  ENTER> REPEAT OPTION
         (1) REPEAT SAME PLOT
         (2) ENTER NEW MATERIAL GEOMETRY
         (3) START OVER
         (4) END PROGRAM
2,

  ENTER> FIBER VOLUME FRACTIONS TO SCAN
         START VALUE, END VALUE, INCREMENT
0.0, 1.0, 0.02,

  ENTER> ASPECT RATIO OF FIBERS
50.0,

  ENTER> TYPE OF AVERAGING
         (1) IN-PLANE; TWO-DIMENSIONAL
         (2) AXIAL SYMMETRIC; THREE-DIMENSIONAL
2,

  ENTER> HERMANS ORIENTATION PARAMETER
0.5,

 DEFLAULT ELECTRICAL CALIBRATION PARAMETERS

 <DATA CHECK>
 CALIBRATION PARAMETERS
     ALPHA =   0.4100
     BETA  =   0.2900


+    DO YOU WISH TO CHANGE THESE VALUES?
 N

+    DO YOU WISH A TABLE OF DATA?
 N

+    DO YOU WISH A COMPUTER PLOT?
 Y

  ENTER> GRAPHIC OUTPUT DATA
         SELECT COORDINATE DIRECTION
         (1) K11
         (2) K22
         (3) K33
3,
```

Table 8 (continued)

```
+    READY FOR PLOT?
 Y

  ENTER> VERTICLE AXIS MODE
         (1) PLOT LINEAR SCALE FOR LOG10(Kii)
         (2) PLOT LOG CYCLE SCALE FOR LOG10(Kii)
1,

  ENTER> GRAPHICS OUTPUT DEVICE
         (1) TERMINAL
         (2) FLATBED PLOTTER
2,

  ENTER> REPEAT OPTION
         (1) REPEAT SAME PLOT
         (2) ENTER NEW MATERIAL GEOMETRY
         (3) START OVER
         (4) END PROGRAM
4,
```

Figure 4. Electrical resistivity for nickel coated graphite fibers and PPS resin, longitudinal direction.

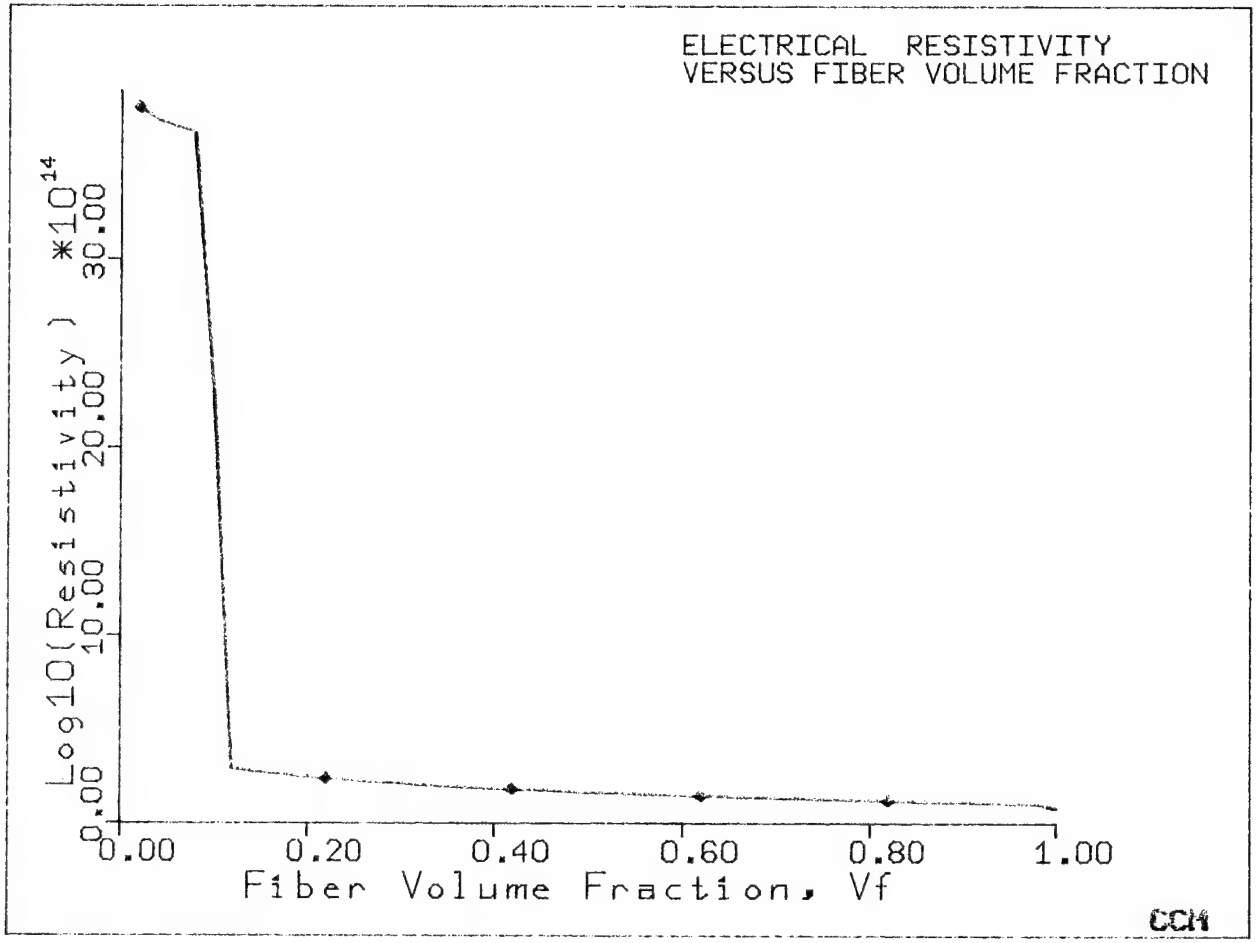

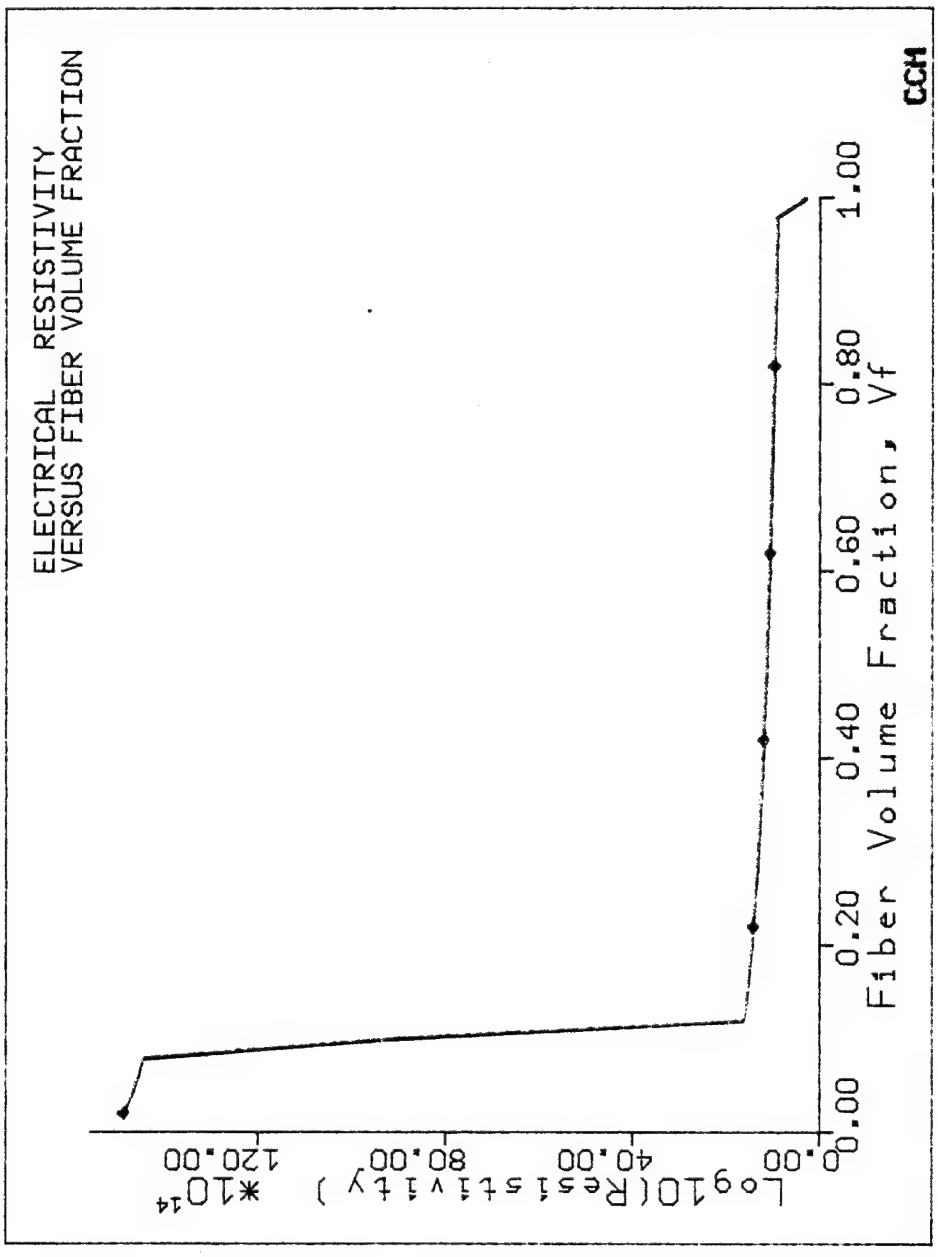

Figure 5. Electrical resistivity for nickel coated graphite fibers and PPS resin, transverse direction.

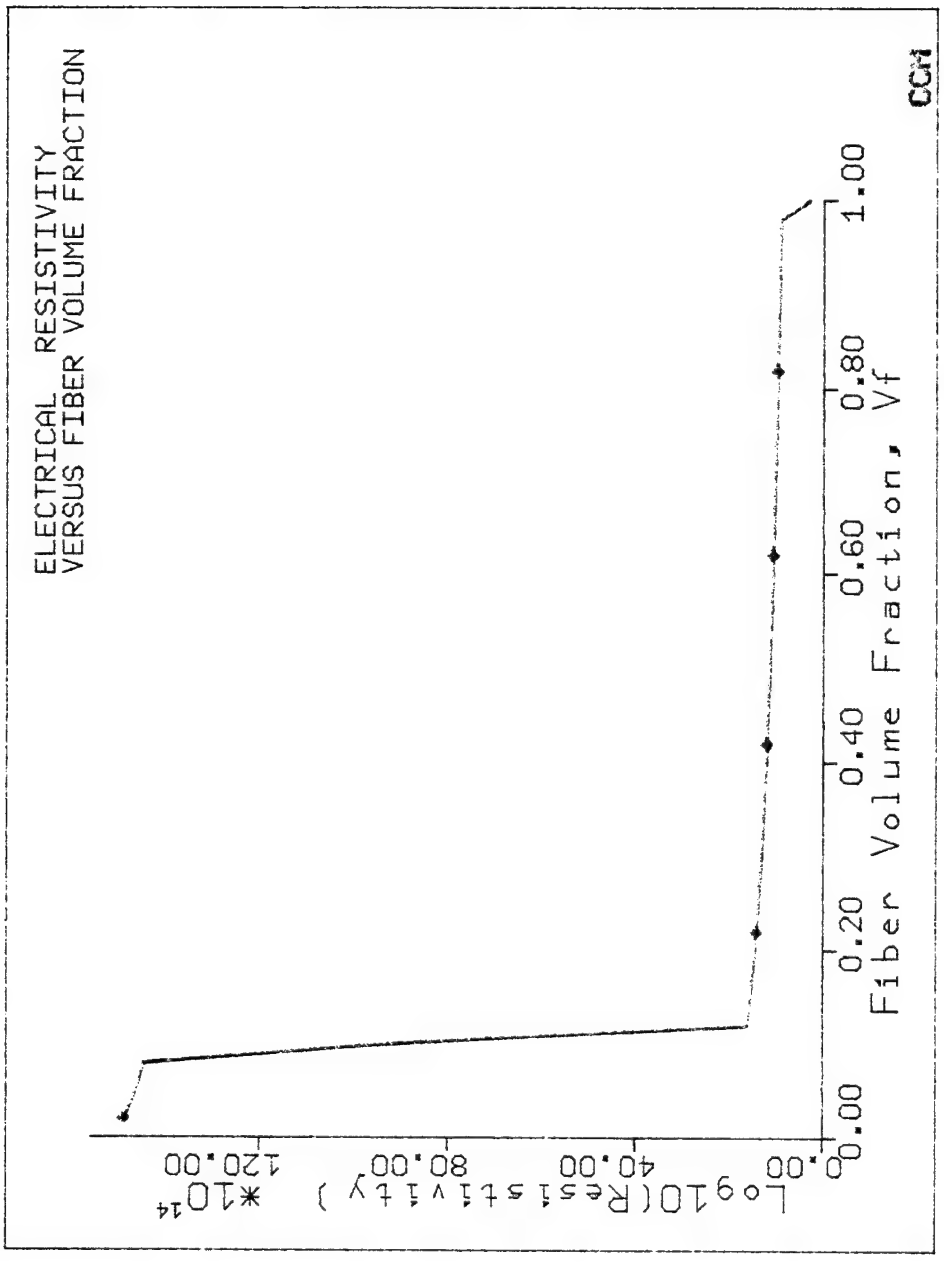

Figure 6. Electrical resistivity for nickel coated graphite fibers and PPS resin, perpendicular direction.

6) Copper Fibers and PPS Resin

	Copper Fibers[a]	Resin
Resistivity (ohm-cm)	1.70×10^{-6}	4.5×10^{16}
Volume Fraction	Variable	
Aspect Ratio	50.0	--
Orientation Parameter, f_a , (axial)	0.5	--

Executions are given in Table 9 for the computer graphs depicted in Figures 7, 8, and 9 for K_1 , K_2 , and K_3 , respectively.

Note: The influence of geometrical irregularities and/or surface coatings may be taken into account for replacing the filler resistivity by the effective resistivity.

[a]Effective resistivity of copper $\cong 1.70 \times 10^{-3}$ ohm-cm.

Table 9.
Calculations for Resistivities
for Copper Fibers and PPS Resin.

```
 CENTER FOR COMPOSITE MATERIALS
 COMPUTER SOFTWARE SYSTEMS

 MICROMECHANICAL MODEL FOR CALCULATING:
 COMPOSITE MATERIAL ELECTICAL AND THERMAL
 RESISTIVITIES AND CONDUCTIVITES

 VERSION: 051182


  ENTER> CALCULATION OPTION
         (1) CALCULATE ELECTRICAL PROPERTIES
         (2) CALCULATE THERMAL PROPERTIES
1,

  ENTER> INPUT OPTION
         (1) INPUT RESISTIVITY DATA
         (2) INPUT CONDUCTIVITY DATA
1,

+    DO YOU WISH TO INCLUDE A FILLER PHASE?
 N

  TWO PHASE SYSTEM ASSUMED: RESIN/FILLER

  ENTER> RESIN RESISTIVITY
4.5E+16,

  ENTER> FIBER RESISTIVITIES
         (LONGITUDINAL,TRANSVERSE)
1.7E-6, 1.7E-6,

  ENTER> FIBER VOLUME FRACTIONS TO SCAN
         START VALUE, END VALUE, INCREMENT
0.0, 1.0, 0.02,

  ENTER> ASPECT RATIO OF FIBERS
50.0,

  ENTER> TYPE OF AVERAGING
         (1) IN-PLANE; TWO-DIMENSIONAL
         (2) AXIAL SYMMETRIC; THREE-DIMENSIONAL
2,

  ENTER> HERMANS ORIENTATION PARAMETER
0.5,
```

Table 9 (continued)

```
 DEFLAULT ELECTRICAL CALIBRATION PARAMETERS

 <DATA CHECK>
 CALIBRATION PARAMETERS
      ALPHA =    0.4100
      BETA  =    0.2900


+     DO YOU WISH TO CHANGE THESE VALUES?
  N

+     DO YOU WISH A TABLE OF DATA?
  Y

+     DO YOU WISH A COMPUTER PLOT?
  Y

   ENTER> GRAPHIC OUTPUT DATA
          SELECT COORDINATE DIRECTION
          (1) K11
          (2) K22
          (3) K33
1,
```

ELECTRICAL
RESITIVITIES OF COMPOSITE MATERIAL : AXIAL CASE

VF	F	K11	K22	K33
0.0200	0.5000	4.2314E+15	1.3083E+16	1.3083E+16
0.0400	0.5000	2.1348E+15	7.3967E+15	7.3967E+15
0.0600	0.5000	1.3883E+15	5.0266E+15	5.0266E+15
0.0800	0.5000	1.0062E+15	3.7291E+15	3.7291E+15
0.1000	0.5000	1.5154E+07	6.0618E+07	6.0618E+07
0.1200	0.5000	2.1250E-05	8.5000E-05	8.5000E-05
0.1400	0.5000	1.8214E-05	7.2857E-05	7.2857E-05
0.1600	0.5000	1.5938E-05	6.3750E-05	6.3750E-05
0.1800	0.5000	1.4167E-05	5.6667E-05	5.6667E-05
0.2000	0.5000	1.2750E-05	5.1000E-05	5.1000E-05
0.2200	0.5000	1.1591E-05	4.6364E-05	4.6364E-05
0.2400	0.5000	1.0625E-05	4.2500E-05	4.2500E-05
0.2600	0.5000	9.8077E-06	3.9231E-05	3.9231E-05
0.2800	0.5000	9.1071E-06	3.6429E-05	3.6429E-05
0.3000	0.5000	8.5000E-06	3.4000E-05	3.4000E-05
0.3200	0.5000	7.9688E-06	3.1875E-05	3.1875E-05
0.3400	0.5000	7.5000E-06	3.0000E-05	3.0000E-05
0.3600	0.5000	7.0833E-06	2.8333E-05	2.8333E-05
0.3800	0.5000	6.7105E-06	2.6842E-05	2.6842E-05
0.4000	0.5000	6.3750E-06	2.5500E-05	2.5500E-05
0.4200	0.5000	6.0714E-06	2.4286E-05	2.4286E-05
0.4400	0.5000	5.7955E-06	2.3182E-05	2.3182E-05
0.4600	0.5000	5.5435E-06	2.2174E-05	2.2174E-05
0.4800	0.5000	5.3125E-06	2.1250E-05	2.1250E-05
0.5000	0.5000	5.1000E-06	2.0400E-05	2.0400E-05
0.5200	0.5000	4.9038E-06	1.9615E-05	1.9615E-05
0.5400	0.5000	4.7222E-06	1.8889E-05	1.8889E-05
0.5600	0.5000	4.5536E-06	1.8214E-05	1.8214E-05
0.5800	0.5000	4.3966E-06	1.7586E-05	1.7586E-05
0.6000	0.5000	4.2500E-06	1.7000E-05	1.7000E-05
0.6200	0.5000	4.1129E-06	1.6452E-05	1.6452E-05
0.6400	0.5000	3.9844E-06	1.5938E-05	1.5938E-05
0.6600	0.5000	3.8636E-06	1.5455E-05	1.5455E-05
0.6800	0.5000	3.7500E-06	1.5000E-05	1.5000E-05
0.7000	0.5000	3.6429E-06	1.4571E-05	1.4571E-05
0.7200	0.5000	3.5417E-06	1.4167E-05	1.4167E-05
0.7400	0.5000	3.4459E-06	1.3784E-05	1.3784E-05
0.7600	0.5000	3.3553E-06	1.3421E-05	1.3421E-05
0.7800	0.5000	3.2692E-06	1.3077E-05	1.3077E-05
0.8000	0.5000	3.1875E-06	1.2750E-05	1.2750E-05
0.8200	0.5000	3.1098E-06	1.2439E-05	1.2439E-05
0.8400	0.5000	3.0357E-06	1.2143E-05	1.2143E-05
0.8600	0.5000	2.9651E-06	1.1860E-05	1.1860E-05
0.8800	0.5000	2.8977E-06	1.1591E-05	1.1591E-05
0.9000	0.5000	2.8333E-06	1.1333E-05	1.1333E-05
0.9200	0.5000	2.7717E-06	1.1087E-05	1.1087E-05
0.9400	0.5000	2.7128E-06	1.0851E-05	1.0851E-05
0.9600	0.5000	2.6563E-06	1.0625E-05	1.0625E-05
0.9800	0.5000	2.6020E-06	1.0408E-05	1.0408E-05
1.0000	0.5000	1.7469E-06	1.8223E-06	1.8223E-06

```
+    READY FOR PLOT?
 Y

  ENTER> VERTICLE AXIS MODE
|        (1) PLOT LINEAR SCALE FOR LOG10(Kii)
         (2) PLOT LOG CYCLE SCALE FOR LOG10(Kii)
1,

  ENTER> GRAPHICS OUTPUT DEVICE
         (1) TERMINAL
         (2) FLATBED PLOTTER
2,

  ENTER> REPEAT OPTION
         (1) REPEAT SAME PLOT
         (2) ENTER NEW MATERIAL GEOMETRY
         (3) START OVER
         (4) END PROGRAM
2,

  ENTER> FIBER VOLUME FRACTIONS TO SCAN
         START VALUE, END VALUE, INCREMENT
0.0, 1.0, 0.02,

  ENTER> ASPECT RATIO OF FIBERS
50.0,

  ENTER> TYPE OF AVERAGING
         (1) IN-PLANE; TWO-DIMENSIONAL
         (2) AXIAL SYMMETRIC; THREE-DIMENSIONAL
2,

  ENTER> HERMANS ORIENTATION PARAMETER
0.5,

 DEFLAULT ELECTRICAL CALIBRATION PARAMETERS

 <DATA CHECK>
 CALIBRATION PARAMETERS
     ALPHA =   0.4100
     BETA  =   0.2900


+    DO YOU WISH TO CHANGE THESE VALUES?
 N

+    DO YOU WISH A TABLE OF DATA?
 N

+    DO YOU WISH A COMPUTER PLOT?
 Y
```

```
  ENTER> GRAPHIC OUTPUT DATA
         SELECT COORDINATE DIRECTION
         (1) K11
         (2) K22
         (3) K33
2,

+    READY FOR PLOT?
 Y

  ENTER> VERTICLE AXIS MODE
         (1) PLOT LINEAR SCALE FOR LOG10(Kii)
         (2) PLOT LOG CYCLE SCALE FOR LOG10(Kii)
1,

  ENTER> GRAPHICS OUTPUT DEVICE
         (1) TERMINAL
         (2) FLATBED PLOTTER
2,

  ENTER> REPEAT OPTION
         (1) REPEAT SAME PLOT
         (2) ENTER NEW MATERIAL GEOMETRY
         (3) START OVER
         (4) END PROGRAM
2,

  ENTER> FIBER VOLUME FRACTIONS TO SCAN
         START VALUE, END VALUE, INCREMENT
0.0, 1.0, 0.02,

  ENTER> ASPECT RATIO OF FIBERS
50.0,

  ENTER> TYPE OF AVERAGING
         (1) IN-PLANE; TWO-DIMENSIONAL
         (2) AXIAL SYMMETRIC; THREE-DIMENSIONAL
2,

  ENTER> HERMANS ORIENTATION PARAMETER
0.5,

 DEFLAULT ELECTRICAL CALIBRATION PARAMETERS

 <DATA CHECK>
 CALIBRATION PARAMETERS
     ALPHA =   0.4100
     BETA  =   0.2900


+    DO YOU WISH TO CHANGE THESE VALUES?
 N

+    DO YOU WISH A TABLE OF DATA?
 N

+    DO YOU WISH A COMPUTER PLOT?
 Y
```

Table 9 (continued)

```
  ENTER> GRAPHIC OUTPUT DATA
         SELECT COORDINATE DIRECTION
         (1) K11
         (2) K22
         (3) K33
3,

+    READY FOR PLOT?
 Y

  ENTER> VERTICLE AXIS MODE
         (1) PLOT LINEAR SCALE FOR LOG10(Kii)
         (2) PLOT LOG CYCLE SCALE FOR LOG10(Kii)
1,

  ENTER> GRAPHICS OUTPUT DEVICE
         (1) TERMINAL
         (2) FLATBED PLOTTER
2,

  ENTER> REPEAT OPTION
         (1) REPEAT SAME PLOT
         (2) ENTER NEW MATERIAL GEOMETRY
         (3) START OVER
         (4) END PROGRAM
4,
```

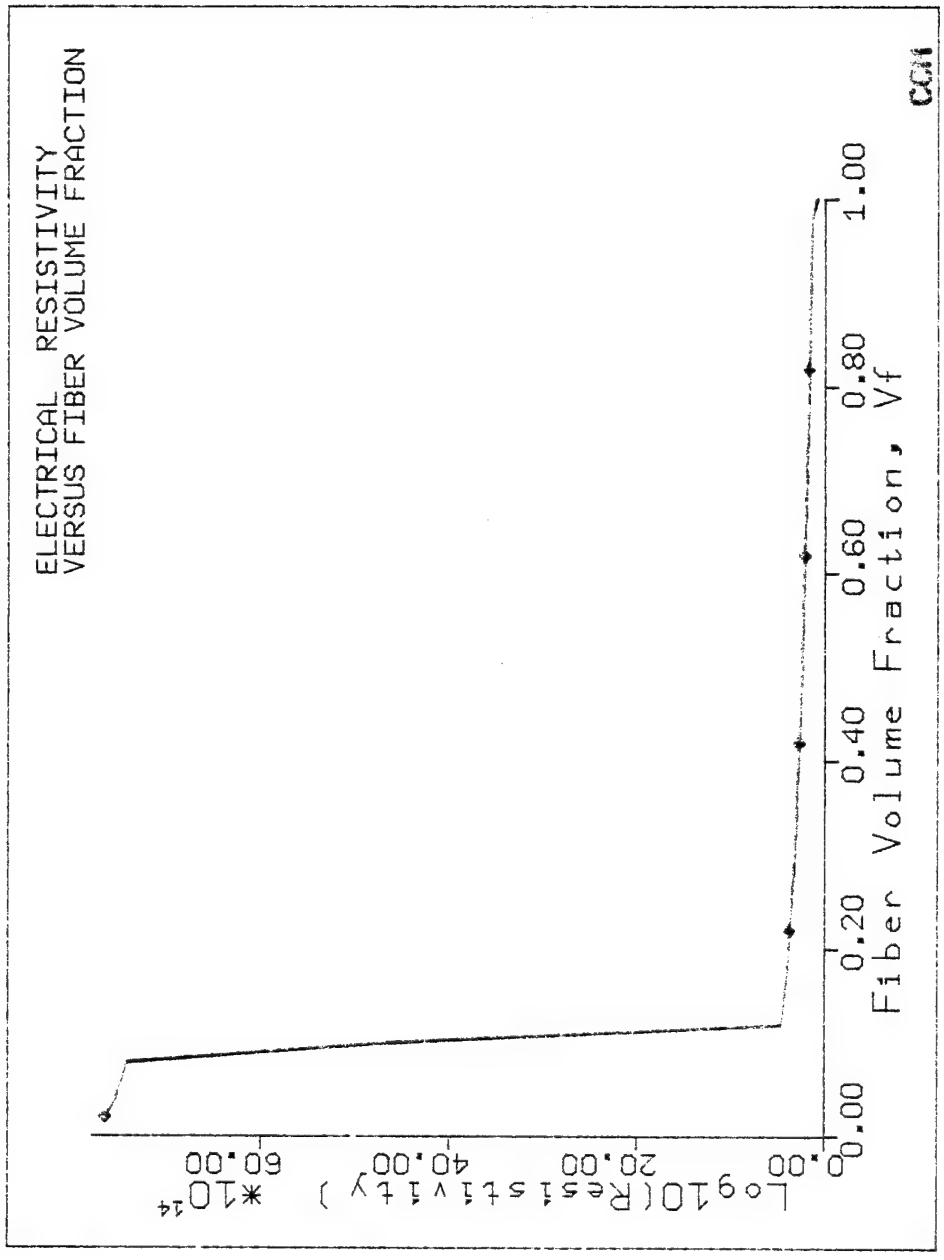

Figure 7. Electrical resistivity for copper fibers and PPS resin, longitudinal direction.

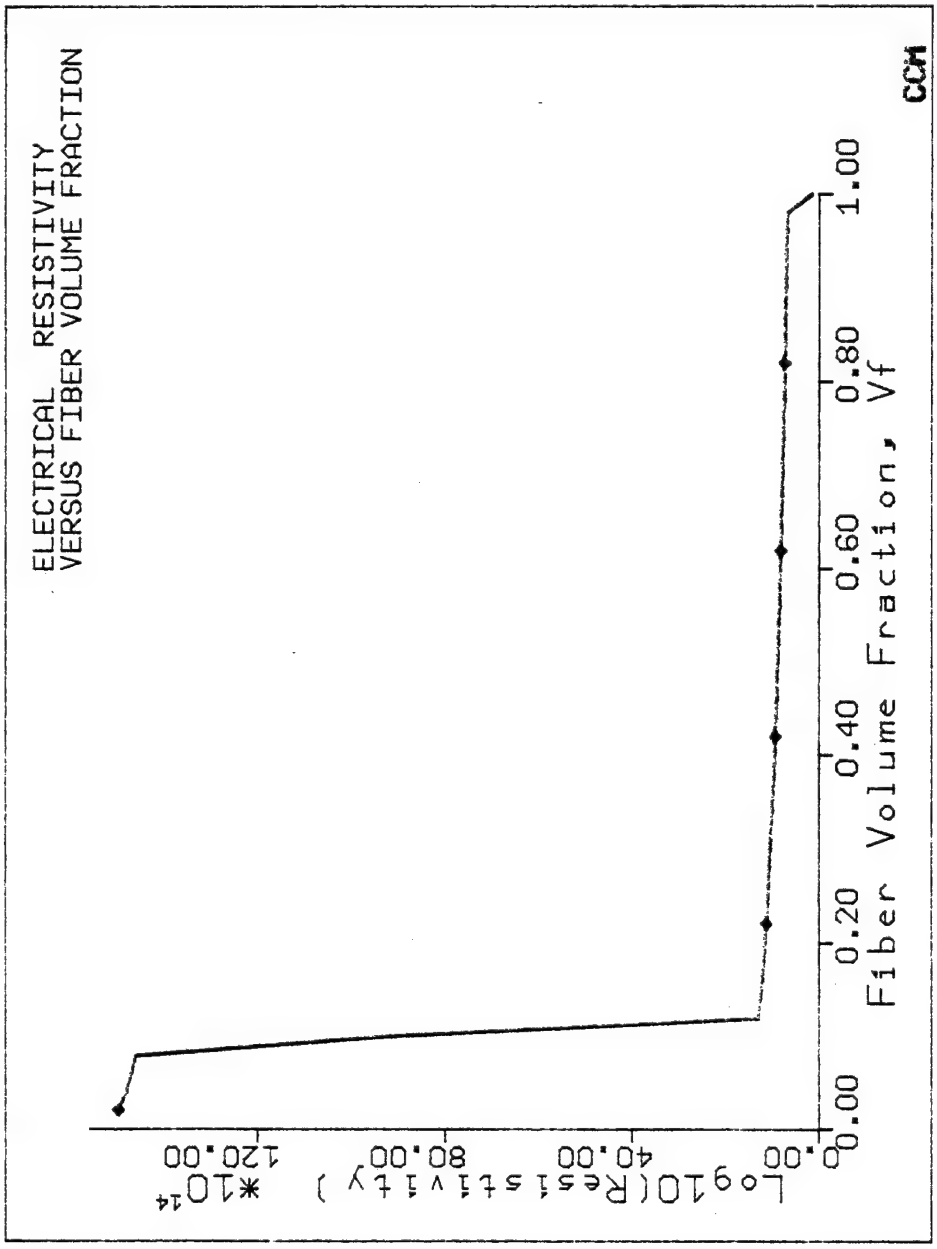

Figure 8. Electrical resistivity for copper fibers and PPS resin, transverse direction.

Figure 9. Electrical resistivity for copper fibers and PPS resin, perpendicular direction.

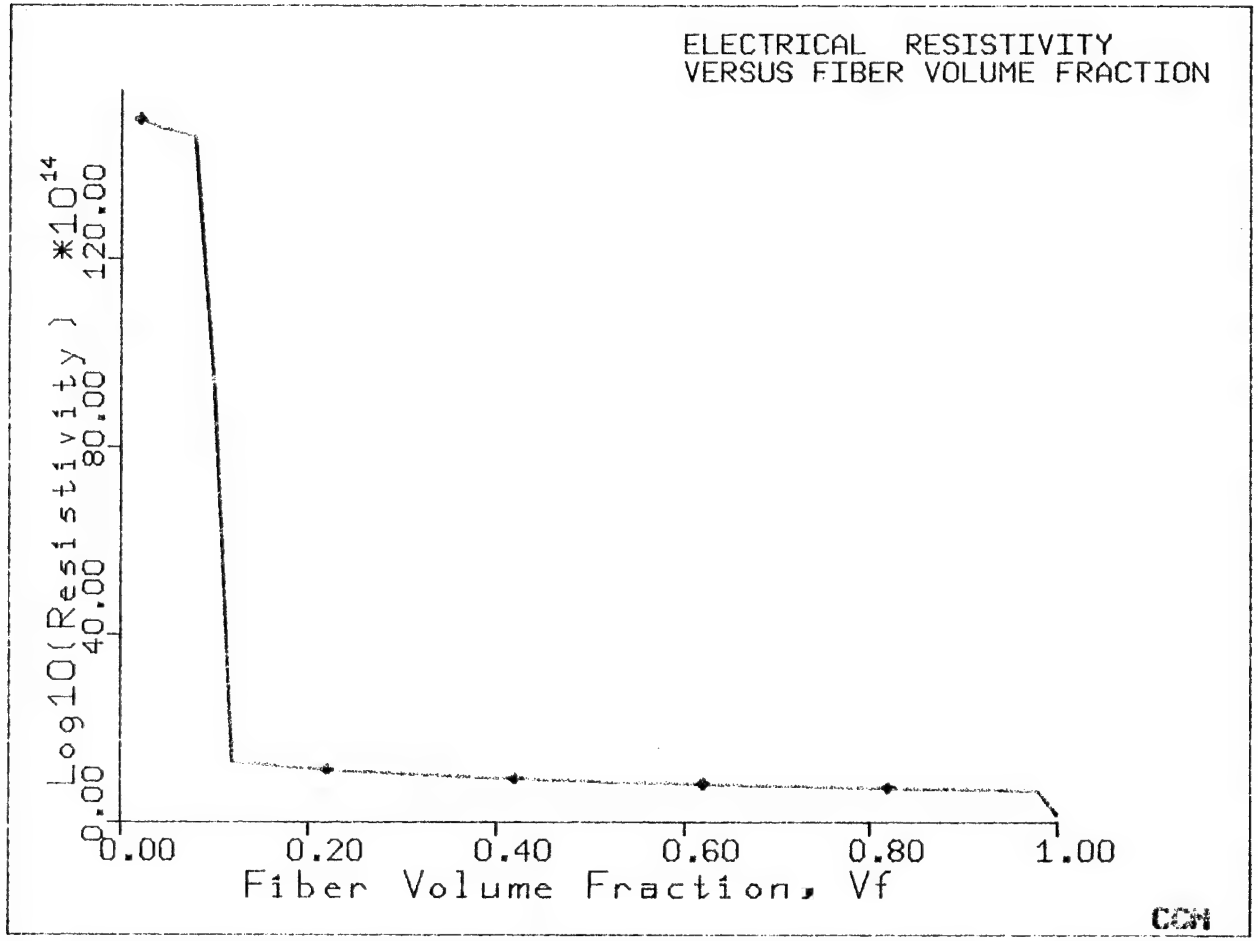

7) Copper Flakes and PPS Resin

	Copper Flakes[a]	Resin
Resistivity (ohm-cm)	1.70×10^{-6}	4.5×10^{16}
Volume Fraction	Variable	
Aspect Ratio	1.0×10^{-5}	--
Orientation Parameter, f_a , (axial)	1.0	--

Executions are given in Table 10 for the computer graphs depicted in Figures 10, 11 and 12 for K_1 , K_2 , and K_3 , respectively.

Note: The influence of geometrical irregularities and/or surface coatings may be taken into account for replacing the filler resistivity by the effective resistivity.

[a]Effective resistivity of copper ≅ 1.70×10^{-3} ohm-cm.

Table 10.
Calculations for Resistivity for
Copper Flakes and PPS Resin.

```
 CENTER FOR COMPOSITE MATERIALS
 COMPUTER SOFTWARE SYSTEMS

 MICROMECHANICAL MODEL FOR CALCULATING:
 COMPOSITE MATERIAL ELECTICAL AND THERMAL
 RESISTIVITIES AND CONDUCTIVITES

 VERSION: 051182


  ENTER> CALCULATION OPTION
         (1) CALCULATE ELECTRICAL PROPERTIES
         (2) CALCULATE THERMAL PROPERTIES
1,

  ENTER> INPUT OPTION
         (1) INPUT RESISTIVITY DATA
         (2) INPUT CONDUCTIVITY DATA
1,

+    DO YOU WISH TO INCLUDE A FILLER PHASE?
 n

  TWO PHASE SYSTEM ASSUMED: RESIN/FILLER

  ENTER> RESIN RESISTIVITY
4.5E+16,

  ENTER> FIBER RESISTIVITIES
         (LONGITUDINAL,TRANSVERSE)
1.7E-6, 1.7E-6,

  ENTER> FIBER VOLUME FRACTIONS TO SCAN
         START VALUE, END VALUE, INCREMENT
0.0, 1.0, 0.02,

  ENTER> ASPECT RATIO OF FIBERS
1.0E-5,

  ENTER> TYPE OF AVERAGING
         (1) IN-PLANE; TWO-DIMENSIONAL
         (2) AXIAL SYMMETRIC; THREE-DIMENSIONAL
2,

  ENTER> HERMANS ORIENTATION PARAMETER
1.0,

 DEFLAULT ELECTRICAL CALIBRATION PARAMETERS

 <DATA CHECK>
 CALIBRATION PARAMETERS
     ALPHA =    0.4100
     BETA  =    0.2900
```

Table 10 (continued)

```
+    DO YOU WISH TO CHANGE THESE VALUES?
 N

+    DO YOU WISH A TABLE OF DATA?
 Y

+    DO YOU WISH A COMPUTER PLOT?
 Y

  ENTER> GRAPHIC OUTPUT DATA
         SELECT COORDINATE DIRECTION
         (1) K11
         (2) K22
         (3) K33
1,
```

Table 10 (continued)

ELECTRICAL
RESITIVITIES OF COMPOSITE MATERIAL : AXIAL CASE

VF	F	K11	K22	K33
0.0200	1.0000	4.4100E+16	1.6965E+13	1.6965E+13
0.0400	1.0000	4.3200E+16	8.1414E+12	8.1414E+12
0.0600	1.0000	4.2300E+16	5.2042E+12	5.2042E+12
0.0800	1.0000	4.1400E+16	3.7389E+12	3.7389E+12
0.1000	1.0000	4.0500E+16	2.8626E+12	2.8626E+12
0.1200	1.0000	3.9600E+16	2.2807E+12	2.2807E+12
0.1400	1.0000	3.8700E+16	1.8670E+12	1.8670E+12
0.1600	1.0000	3.7800E+16	1.5586E+12	1.5586E+12
0.1800	1.0000	3.6900E+16	1.3202E+12	1.3202E+12
0.2000	1.0000	3.6000E+16	1.1309E+12	1.1309E+12
0.2200	1.0000	3.5100E+16	9.7736E+11	9.7736E+11
0.2400	1.0000	3.4200E+16	8.5056E+11	8.5056E+11
0.2600	1.0000	3.3300E+16	7.4436E+11	7.4436E+11
0.2800	1.0000	3.2400E+16	6.5433E+11	6.5433E+11
0.3000	1.0000	3.1500E+16	5.7725E+11	5.7725E+11
0.3200	1.0000	3.0600E+16	5.1069E+11	5.1069E+11
0.3400	1.0000	2.9700E+16	4.5280E+11	4.5280E+11
0.3600	1.0000	2.8800E+16	4.0212E+11	4.0212E+11
0.3800	1.0000	2.7900E+16	3.5748E+11	3.5748E+11
0.4000	1.0000	2.7000E+16	3.1723E+11	3.1723E+11
0.4200	1.0000	2.6100E+16	2.7323E+11	2.7323E+11
0.4400	1.0000	2.5200E+16	2.0181E+11	2.0181E+11
0.4600	1.0000	2.4300E+16	1.0102E+11	1.0102E+11
0.4800	1.0000	2.3400E+16	2.7333E+10	2.7333E+10
0.5000	1.0000	2.2500E+16	3.4660E+09	3.4660E+09
0.5200	1.0000	2.1600E+16	1.9086E+08	1.9086E+08
0.5400	1.0000	2.0700E+16	4.3833E+06	4.3833E+06
0.5600	1.0000	1.9800E+16	4.1042E+04	4.1042E+04
0.5800	1.0000	1.8900E+16	1.5485E+02	1.5485E+02
0.6000	1.0000	1.8000E+16	2.8333E-06	2.8333E-06
0.6200	1.0000	1.7100E+16	2.7419E-06	2.7419E-06
0.6400	1.0000	1.6200E+16	2.6563E-06	2.6563E-06
0.6600	1.0000	1.5300E+16	2.5758E-06	2.5758E-06
0.6800	1.0000	1.4400E+16	2.5000E-06	2.5000E-06
0.7000	1.0000	1.3500E+16	2.4286E-06	2.4286E-06
0.7200	1.0000	1.2599E+16	2.3611E-06	2.3611E-06
0.7400	1.0000	1.1699E+16	2.2973E-06	2.2973E-06
0.7600	1.0000	1.0799E+16	2.2368E-06	2.2368E-06
0.7800	1.0000	9.8994E+15	2.1795E-06	2.1795E-06
0.8000	1.0000	8.9994E+15	2.1250E-06	2.1250E-06
0.8200	1.0000	8.0994E+15	2.0732E-06	2.0732E-06
0.8400	1.0000	7.1994E+15	2.0238E-06	2.0238E-06
0.8600	1.0000	6.2994E+15	1.9767E-06	1.9767E-06
0.8800	1.0000	5.3994E+15	1.9318E-06	1.9318E-06
0.9000	1.0000	4.4994E+15	1.8889E-06	1.8889E-06
0.9200	1.0000	3.5993E+15	1.8478E-06	1.8478E-06
0.9400	1.0000	2.6993E+15	1.8085E-06	1.8085E-06
0.9600	1.0000	1.7993E+15	1.7708E-06	1.7708E-06
0.9800	1.0000	8.9931E+14	1.7347E-06	1.7347E-06
1.0000	1.0000	9.4805E-03	1.7000E-06	1.7000E-06

Table 10 (continued)

```
+    READY FOR PLOT?
 Y

  ENTER> VERTICLE AXIS MODE
         (1) PLOT LINEAR SCALE FOR LOG10(Kii)
         (2) PLOT LOG CYCLE SCALE FOR LOG10(Kii)
1,

  ENTER> GRAPHICS OUTPUT DEVICE
         (1) TERMINAL
         (2) FLATBED PLOTTER
2,

  ENTER> REPEAT OPTION
         (1) REPEAT SAME PLOT
         (2) ENTER NEW MATERIAL GEOMETRY
         (3) START OVER
         (4) END PROGRAM
2,

  ENTER> FIBER VOLUME FRACTIONS TO SCAN
         START VALUE, END VALUE, INCREMENT
0.0, 1.0, 0.02,

  ENTER> ASPECT RATIO OF FIBERS
1.0E-5,

  ENTER> TYPE OF AVERAGING
         (1) IN-PLANE; TWO-DIMENSIONAL
         (2) AXIAL SYMMETRIC; THREE-DIMENSIONAL
2,

  ENTER> HERMANS ORIENTATION PARAMETER
1.0,

 DEFLAULT ELECTRICAL CALIBRATION PARAMETERS

 <DATA CHECK>
 CALIBRATION PARAMETERS
     ALPHA =   0.4100
     BETA  =   0.2900


+    DO YOU WISH TO CHANGE THESE VALUES?
 N

+    DO YOU WISH A TABLE OF DATA?
 N

+    DO YOU WISH A COMPUTER PLOT?
 Y

  ENTER> GRAPHIC OUTPUT DATA
         SELECT COORDINATE DIRECTION
         (1) K11
         (2) K22
         (3) K33
2,
```

Table 10 (continued)

```
+     READY FOR PLOT?
 Y

  ENTER> VERTICLE AXIS MODE
         (1) PLOT LINEAR SCALE FOR LOG10(Kii)
         (2) PLOT LOG CYCLE SCALE FOR LOG10(Kii)
1,

  ENTER> GRAPHICS OUTPUT DEVICE
         (1) TERMINAL
         (2) FLATBED PLOTTER
2,

  ENTER> REPEAT OPTION
         (1) REPEAT SAME PLOT
         (2) ENTER NEW MATERIAL GEOMETRY
         (3) START OVER
         (4) END PROGRAM
2,

  ENTER> FIBER VOLUME FRACTIONS TO SCAN
         START VALUE, END VALUE, INCREMENT
0.0, 1.0, 0.02,

  ENTER> ASPECT RATIO OF FIBERS
1.0E-5,

  ENTER> TYPE OF AVERAGING
         (1) IN-PLANE; TWO-DIMENSIONAL
         (2) AXIAL SYMMETRIC; THREE-DIMENSIONAL
2,

  ENTER> HERMANS ORIENTATION PARAMETER
1.0,

 DEFLAULT ELECTRICAL CALIBRATION PARAMETERS

 <DATA CHECK>
 CALIBRATION PARAMETERS
     ALPHA =   0.4100
     BETA  =   0.2900


+     DO YOU WISH TO CHANGE THESE VALUES?
 N

+     DO YOU WISH A TABLE OF DATA?
 N

+     DO YOU WISH A COMPUTER PLOT?
 Y
```

Table 10 (continued)

```
  ENTER> GRAPHIC OUTPUT DATA
         SELECT COORDINATE DIRECTION
         (1) K11
         (2) K22
         (3) K33
3,

+    READY FOR PLOT?
 Y

  ENTER> VERTICLE AXIS MODE
         (1) PLOT LINEAR SCALE FOR LOG10(Kii)
         (2) PLOT LOG CYCLE SCALE FOR LOG10(Kii)
1,

  ENTER> GRAPHICS OUTPUT DEVICE
         (1) TERMINAL
         (2) FLATBED PLOTTER
2,

  ENTER> REPEAT OPTION
         (1) REPEAT SAME PLOT
         (2) ENTER NEW MATERIAL GEOMETRY
         (3) START OVER
         (4) END PROGRAM
4,
```

Figure 10. Electrical resistivity for copper flakes and PPS resin, longitudinal direction.

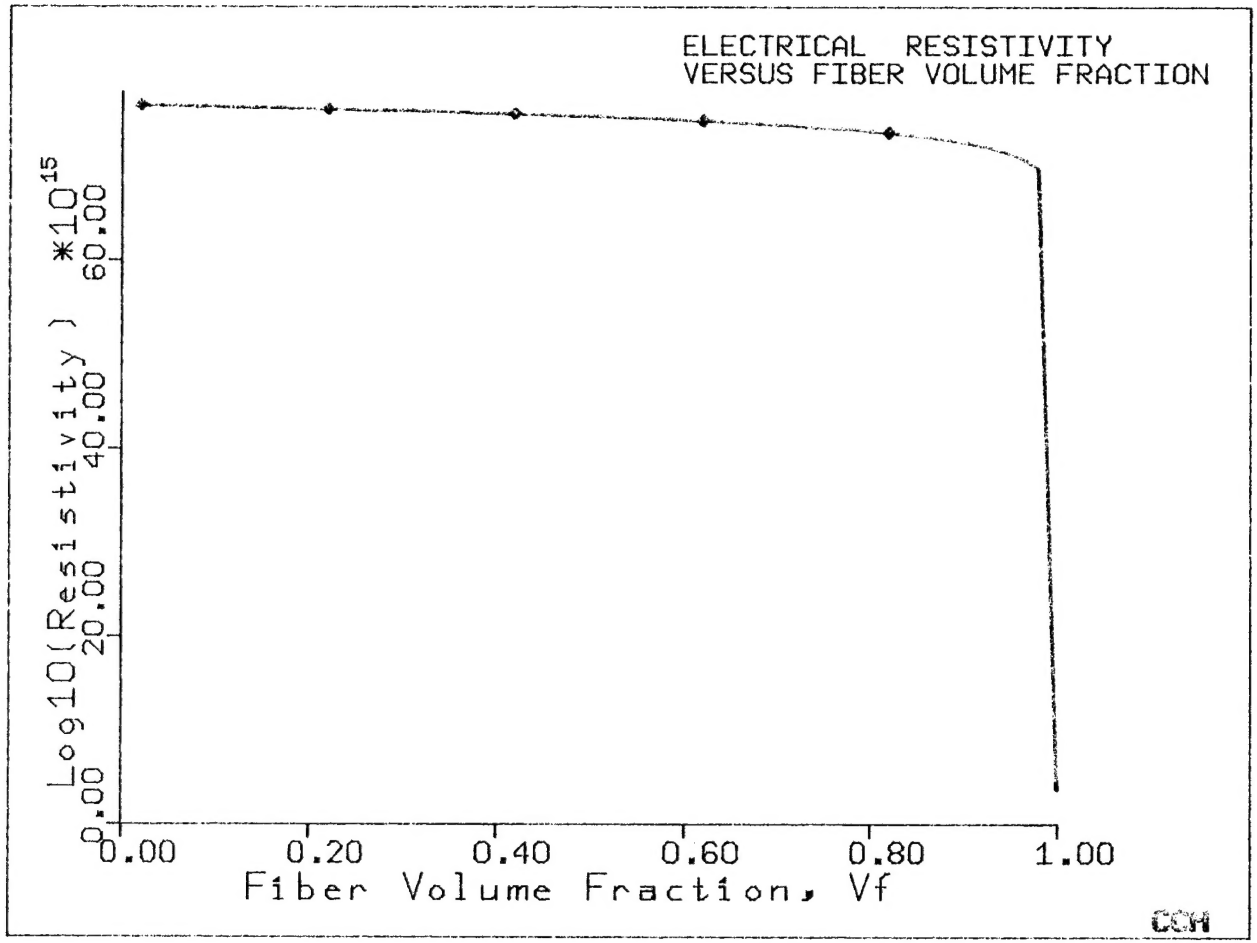

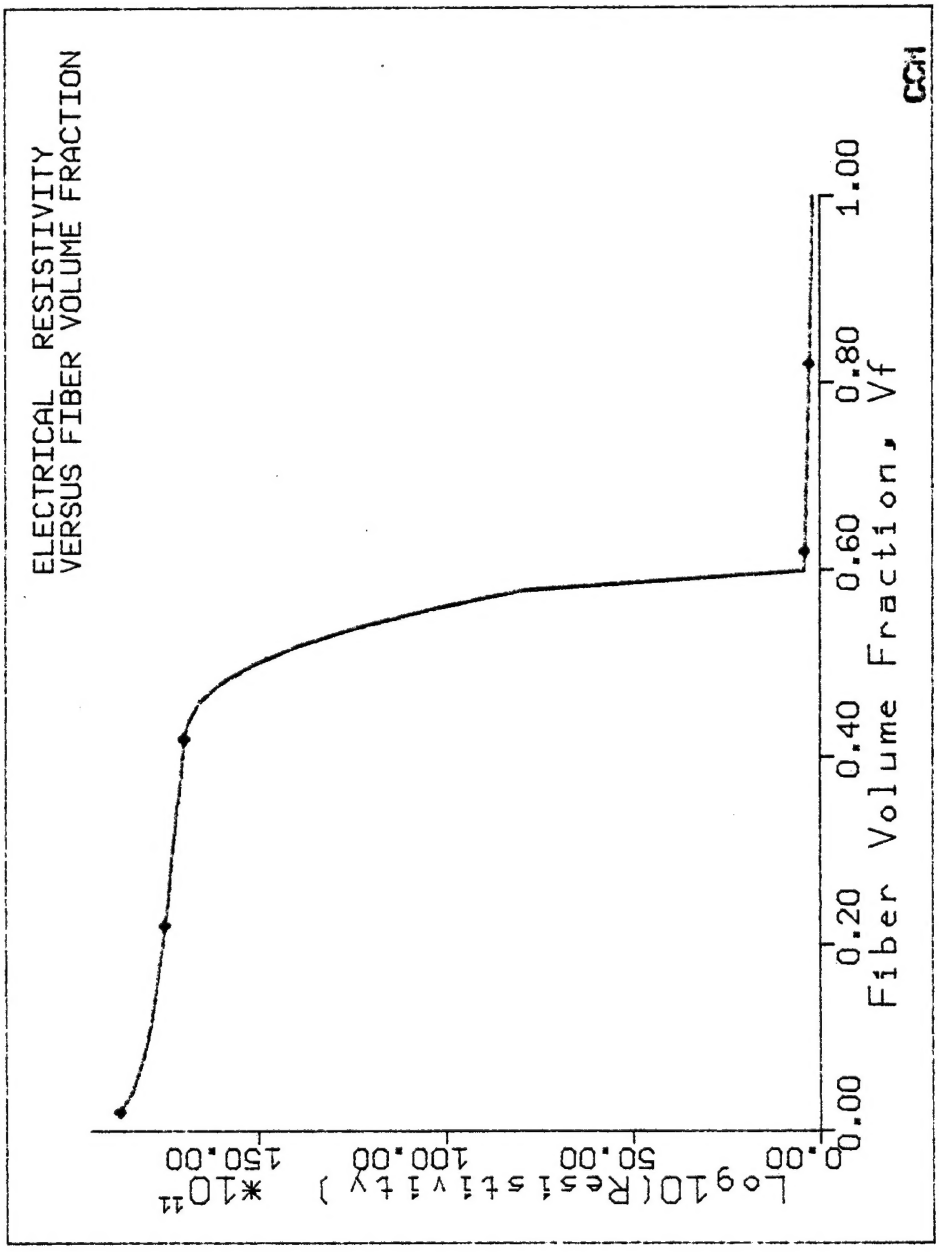

Figure 11. Electrical resistivity for copper flakes and PPS resin, transverse direction.

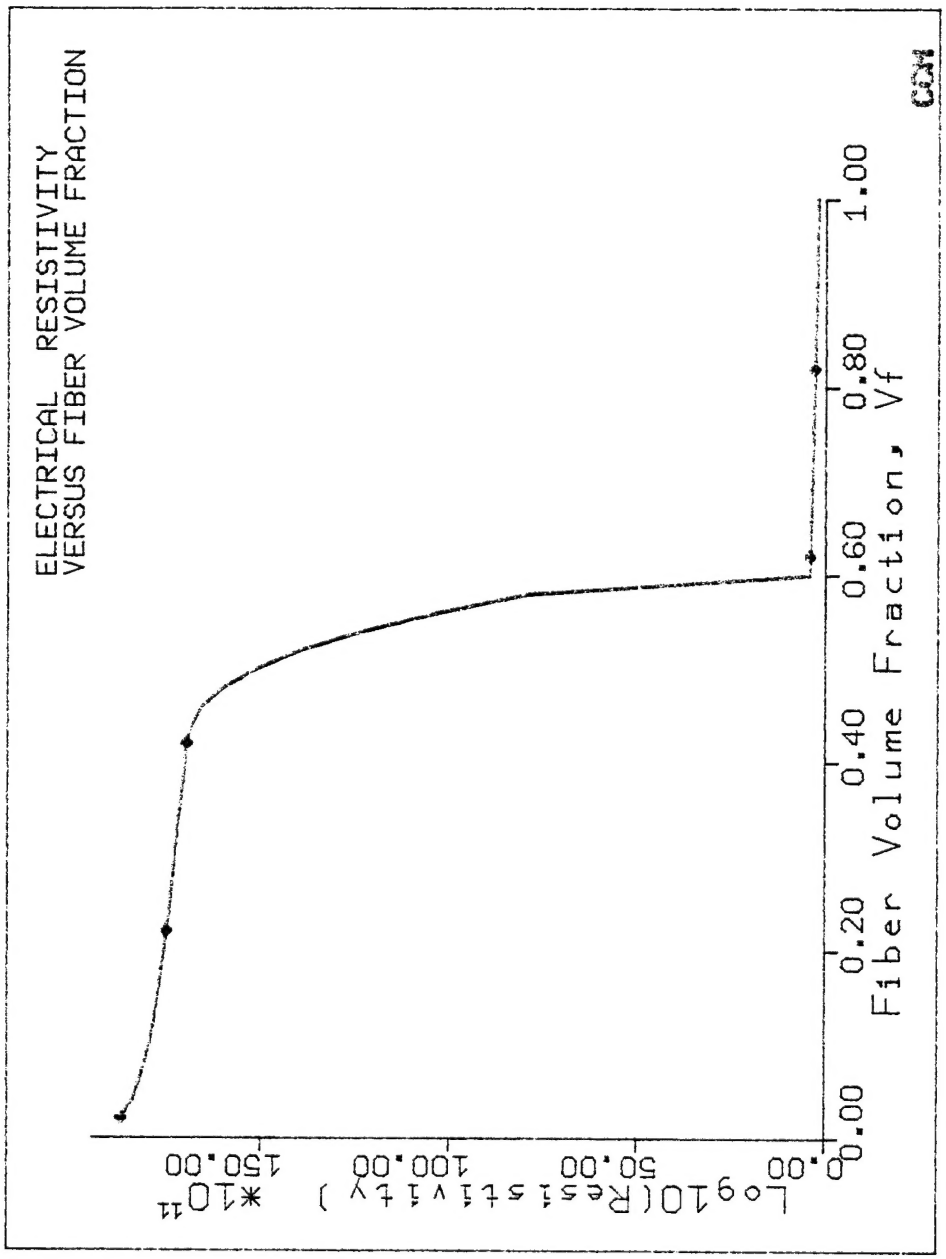

Figure 12. Electrical resistivity for copper flakes and PPS resin, perpendicular direction.